ALTERNATIVE AXIAL DISTANCES FOR SPHERICAL AND CUBOIDAL REGIONS OF CENTRAL COMPOSITE DESIGNS AND THEIR PROPERTIES

BY

ONYISHI, LINUS IFEANYI
MTH/Ph.D/08/001

DEPARTMENT OF STATISTICS
FACULTY OF PHYSICAL SCIENCES
UNIVERSITY OF CALABAR
CALABAR, NIGERIA

SUBMITTED TO

GRADUATE SCHOOL
UNIVERSITY OF CALABAR,
CALABAR,

IN PARTIAL FULFILLMENT OF THE REQUIREMENTS FOR THE AWARD OF DOCTOR OF PHILOSOPHY (Ph.D) DEGREE IN STATISTICS

APRIL, 2019

CHAPTER ONE

INTRODUCTION

1.1 Background of the study

Whenever multiple system variables may influence the outputs, response surface methodology (RSM) could be utilized in assessing the relationship between the dependent (response) and independent (input) variables as well as optimize the relevant processes (Mahsa et al., 2012 and Dyauddeen et al., 2003). Response surface methodology (RSM) is a collection of mathematical and statistical techniques for emperical model building. By careful design of experiments, the objective of RSM is to optimize a response (output variable) of interest which is influenced by several independent variables (input variables), Montgomery (2013). In this context, an experiment is a series of tests called runs in which changes are made to the input variables to understand the reasons for the changes in the output variable. In real life application of response surface methodology, the independent variable can be more than one.

The relationship between a response variable of interest, y, and the k independent variables is usually described by a first-order response surface model,

$$y = \beta_0 + \beta_i \sum_{i=1}^{k} x_i + e, \tag{1}$$

where β_0 and β_i are the coefficients (parameters) of the model, x_i's are the independent variables and e is the random error associated with the response variable such that the random error is normally and independently distributed with zero means and variance, σ_e^2; that is $e \sim NID(0, \sigma_e^2)$. However, if curvature exists, the relationship between the response variable and the independent variables is more appropriately described by a second-order response model,

$$y_{ij} = \beta_0 + \sum_{i=1}^{k} \beta_i x_i + \sum_{i=1}^{k} \beta_{ii} x_i^2 + \sum_{i=1}^{k} \sum_{j=i+1}^{k} \beta_{ij} x_i x_j + e_{ij}, \quad (2)$$

where β_0, β_i, β_{ii} and β_{ij} are coefficients of the response surface model, other components retain their original meanings. Expressed in matrix form, equation (2) becomes

$$\mathbf{y} = \beta_0 + \mathbf{x}'\mathbf{b} + \mathbf{x}'\mathbf{B}\mathbf{x} + e, \quad (3)$$

where $\mathbf{y}$ is the $N \times 1$ vector of responses, β_0 is a constant, $\mathbf{x}$ is a point in the design space spanned by the design, $\mathbf{b}$ is a $k \times 1$ vector of first-order (linear) regression coefficients and N is the number of design runs, $\mathbf{B}$ is a $k \times k$ symmetric matrix whose main diagonal entries are the coefficients of the pure quadratic terms and the off-diagonal entries are coefficients of one-half the mixed quadratic (interaction) terms, and e is the random error term associated with the response. There is a total of $p = (k+1)(k+2)/2$ model parameters to be estimated from the second-order response surface model which includes one constant, k first-order (linear) terms, k quadratic terms and $k(k-1)/2$ interaction terms. The linear terms are the first-order components of the second-order model while the interaction terms are the cross-products of the second-order model.

Designs for fitting second-order response surface models like that of equation (2) are called second-order response surface designs. However, a second-order response surface design is often chosen on the consideration of several criteria. Myers, Montgomery and Anderson-Cook (2009) and Anderson-Cook, Borror and Montgomery (2009) stated that good second-order designs should:

- result in a good fit of the model to the data;
- provide sufficient information to allow for a test for model lack of fit;
- allow models of increasing order to be constructed sequentially;

- provide an estimate of pure experimental error;
- be insensitive (robust) to the presence of outliers in the data;
- be robust to errors in control of design levels;
- be cost effective, that is, do not require too many runs;
- allow experiments to be performed in blocks;
- provide a check on the homogenous variance assumption; and
- provide a good distribution of the variance of the predicted responses throughout the design region.

However Anderson-Cook et al (2009), not all the criteria are required or necessarily important in every RSM application. Some of the criteria listed above also present potential conflict with each other. For instance, one of the criteria suggests small experimental runs for cost effectiveness while another requires good distribution of the prediction variance. Studies have shown that often times, small design runs provide insufficient information for prediction variance evaluation (Li *et al*., 2009).

Second-order models are used primarily for optimization and therefore, a model that performs well in response prediction is vital. This brings about the importance of the prediction variance highlighted in one of the criteria for adequate evaluation of design performance. Characterization of the prediction variance is very important in comparing competing designs. A good design will have minimum prediction variance distributed throughout the entire design space.

At a point, **x**, in the design space, the prediction variance is

$$\mathrm{var}\left[y(\mathbf{x})\right] = \sigma^2 \mathbf{x}'^{\mathrm{m}} \left(\mathbf{X}'\mathbf{X}\right)^{-1} \mathbf{x}^{\mathrm{m}}; \qquad (4)$$

where, $|\boldsymbol{X}'\boldsymbol{X}| \neq 0$, $(\boldsymbol{X}'\boldsymbol{X})^{-1}$ is the inverse of the information matrix of a second-order response surface design whose design matrix is $\boldsymbol{X}$ and

$\mathbf{x}'^{m} = \left(1, x_1, ..., x_k; x_1^2, ..., x_k^2; x_1x_2, ..., x_{k-1}x_k\right)$ is the vector of design points in the design space expanded to model form by classifying the coordinates of the design points into linear, quadratic and mixed (interaction) components of the model. By multiplying equation (4) by N gives the scaled prediction variance (SPV),

$$\frac{N\,\mathrm{var}[y(\mathbf{x})]}{\sigma^2} = N\mathbf{x}'^{m}\left(\mathbf{X}'\mathbf{X}\right)^{-1}\mathbf{x}^{m}. \tag{5}$$

Traditionally, dividing equation (5) by σ^2 eliminates the unknown parameter which makes it impossible to use the equation to access the prediction variance characteristics of a second-order response surface design. However, in the literature, some authors arbitrarily assume $\sigma^2 = 1$ in order to eliminate it (Onukogu, 1997). In industrial settings, some experimenters prefer the standardized or unscaled prediction variance (UPV) for design evaluation. The unscaled prediction variance is given by

$$\frac{\mathrm{var}[y(\mathbf{x})]}{\sigma^2} = \mathbf{x}'^{m}\left(\mathbf{X}'\mathbf{X}\right)^{-1}\mathbf{x}^{m}. \tag{6}$$

The preference for UPV is because it provides the researcher the platform to assess the increase in precision (not influenced by the cost of experimentation, N) obtained from using larger designs by looking at the un-scaled prediction variance. Usually, experimenters determine the cost of experimentation in response surface exploration through the total number of runs, N, of the experiment.

On the other hand, scaled prediction variance allows the practitioner to measure the variance of the predicted responses on a per observation basis, thereby penalizing larger designs over smaller ones (Atkinson & Donev, 1992 and Li *et al.*, 2009). By penalizing larger designs it means the prediction variance of such designs is expected to get bigger when it is scaled (multiplied by N). The rationale for scaling the prediction variance is to account for the cost of the design, represented by N, in comparing designs of various sizes. However, there is increasing awareness for the

use of the UPV in design evaluation. Goos (2009) and Piepel (2009) argue that larger designs often lead to smaller prediction variances and provide the experimenter with more useful information than unscaling the prediction variance.

Among competing designs, the design(s) with the smallest and stable scaled or unscaled prediction variance is/are the most desirable. Stability is in the sense that there is small difference between the minimum and maximum SPV of a design.

Many second-order response surface designs exist of which the central composite design (CCD) is one of them. The central composite design was developed by Box and Wilson (1951) and has remained the most popular and practically useful class of second-order response surface designs. The symmetry and flexibility offered by the structure of the design give substantial advantage in prediction variance characterization and parameter estimation. The CCD exists for $k \geq 2$ in both spherical and cuboidal regions, where k is the number of factors (independent variables of interest). According to Borkowski (1995), Li et al (2009) and Chigbu et al (2009), the structure of the CCD has three components: the factorial (cube) component which is at least a resolution V design, the star (axial) component at distance, α, from the centre of the design along each axis, and the centre point located at the centre of the design space. A resolution V design is a design in which two-factor interactions are aliased with three-factor interactions but no main effect or two-factor interaction is aliased with another main effect or two-factor interaction. That is, main effects and the two-factor interactions do not have other main effects and two-factor interactions as their aliases. Hence, for a resolution V design, the shortest word in the defining relation must have five letters.

The cube or factorial component of the CCD has $f = 2^{k-q}$ full ($q = 0$) or fractional ($q > 0$) factorial number of runs, where q is an integer. The number of runs

of the star component is $2k$ which is augmented with n_0 centre points (the centre component). In other words, the CCD uses a total of $N = f + 2k + n_0$ number of runs to estimate the $p=(k+1)(k+2)/2$ number of model parameters. The cube (factorial) component has coordinates of the form, $(x_1, x_2, \ldots, x_k)=(\pm 1, \pm 1, \ldots, \pm 1)$; the star component has coordinates of the form, $(x_1, \ldots, x_k)=(\pm\alpha, 0, 0, \ldots, 0), \ldots, (0, 0, \ldots, \pm\alpha)$ while the centre is of the form, $(x_1, \ldots, x_k)=(0, 0, \ldots, 0)$. The structure of a three-factor CCD with one centre point is presented in Figure 1 for specific illustration.

x_1	x_2	x_3	
1	1	1	
1	1	−1	
1	−1	1	
1	−1	−1	*factorial component*
−1	1	1	
−1	1	−1	
−1	−1	1	
−1	−1	−1	
$\pm\alpha$	0	0	
0	$\pm\alpha$	0	*star component*
0	0	$\pm\alpha$	
0	0	0	*centre point*

FIG.1: Illustration of Three-Factor CCD with $n_0 = 1$

The three components of the CCD play important but different roles in model parameter estimation. The at least resolution V full or fractional factorial component (the cube) contributes substantially to the estimation of the k linear terms and the $k(k-1)/2$ two-factor interaction terms of the second-order model. Only the factorial point contributes to the estimation of the interaction terms. The star component contributes to the estimation of the k quadratic terms of the second-order model. Without the star component, only the sum of the first-order terms can be estimated.

According to Montgomery (2013), this variation of the CCD is used sometimes because it requires only three levels of each factor and it is difficult in practice to change factor levels. Figure 3 depicts the structure of a three-factor face-centered central composite design.

2.2 Rotatability and prediction variance of designs

Box and Hunter (1957) introduced the concept of rotatability for second-order response surface designs. This is to ensure provision of good predictions throughout the entire design space. For the prediction to be good, it requires that the second-order response surface model should have a reasonably consistent and stable predicted responses at points of interest, **x**, in the design region (Montgomery, 2013). Rotatability is a spherical property. The central composite design is made rotatable by choosing the axial distance to be $\alpha = \sqrt[4]{f}$, where $f = 2^{k-1}$ is the factorial run of the CCD. Therefore, the rotatable axial distance of the CCD depends on the number of points in the factorial component of the design. This axial distance ensures that the prediction variance, $Var[\hat{y}(\mathbf{x})]$, is constant at all points that fall on the surface of a hypersphere centered at the origin, if the design is rotatable. According to Khuri and Mukhopadhyay (2010), the advantage of this property is that the prediction variance remains unchanged under any rotation of the coordinate axes at the centre, (0, 0, . . ., 0). If optimization of $\hat{y}(\mathbf{x})$ is desired on concentric hyperspheres (often called concentric balls), like the case in the application of ridge analysis, then it would be desirable for the design to be rotatable. This makes it easier to compare the values of $\hat{y}(\mathbf{x})$ on a given hypersphere as all such values have the same variance.

Dykstra (1960) extended the rotatable axial distance to accommodate the replication of the cube and star components of the CCD. He gave the rotatable alpha

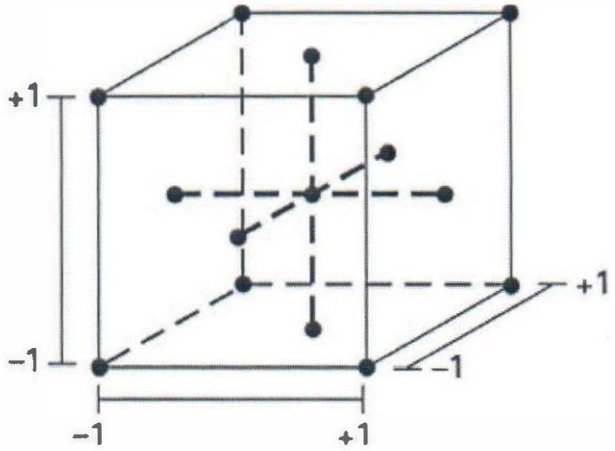

FIG. 3: Structural Illustration of a Three-Factor Face-Centered CCD
Montgomery (2013)

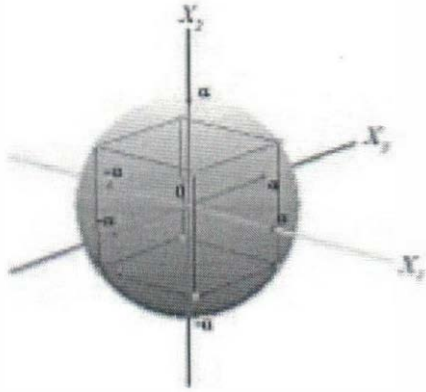

FIG. 2: Structural Illustration of Three-Factor Spherical CCD
Montgomery (2013)

CHAPTER TWO

LITERATURE REVIEW

2.1 Structural form of central composite design

The distinct structures of the central composite designs are characterized by the choice of the axial distance. According to Li *et al.* (2009), the axial distance defines the placement of the star points in response surface exploration using the CCD which consequently have substantial influence on the distribution of the design's prediction variance in the design region. Different axial distances have been proposed for different experimental purposes involving the CCD and each axial distance has specific effect on the structure and property of the CCD.

The works of Box and Wilson (1951) brought to fore the concepts of spherical and cuboidal α for the CCD. The spherical alpha locates the star points at a distance of $\sqrt{k}$ from the centre of the spherical design space, where k is a positive integer and represents the number of experimental factors. This places the star points and the factorial points on the surface of a sphere of radius, $\sqrt{k}$. The structural form of the resulting designs is presented in Figure 2. The spherical axial distance of the star points usually provide values that are not feasible for large number of experimental factors. For k = 20, for instance, $\alpha = 4.4721$ which is an impractical value considering the fact that the extreme values of the design are placed at –1 and +1.

When the region of interest is cuboidal rather than spherical, Box and Wilson (1957) proposed that the axial distance should be $\alpha = 1$. This locates the star points at the centres of the faces of the cubes. Therefore, the CCD with this axial distance is popularly called the Face-centered central composite design or the Face-centered cube.

c. To compare the alternative axial distances with the existing axial distances using D- and G- efficiency criteria and graphical methods.

d. To evaluate the alternative sets of axial distances with the partial replication of the CCD and the inscribed CCD.

1.5 Significance of the study

The axial distances, which are developed in this study account for moderate placement of the star points in the design region and provide stable prediction variance characteristics of the central composite designs in both the cuboidal and spherical design regions. With the alternative axial distances, the prediction variances of the central composite designs were able to discriminate, through graphical procedures, points in the design space that predict better than others and those that predict very poorly.

In general, the alternative axial distances and the consequent design evaluations of the CCD provided more viable alternatives to the characterization of the prediction capabilities of the central composite designs in spherical and cuboidal regions. Most importantly, the outcomes are expected to be highly beneficial to researchers and industrialists who are seeking better alternatives for improving their industrial outputs.

1.6 Scope of the study

This study covers the second-order response surface design known as the central composite design. The study of the central composite design is restricted to assessing the prediction variance properties and prediction capabilities of the CCD with respect to the axial distances. The evaluations of the CCD are considered in the cuboidal and spherical regions only.

impracticable axial distances. For instance, if k = 10, then $\sqrt{10} = 3.1623$and $\sqrt[4]{2^{10}} = 5.6569$, respectively, for the spherical and rotatable axial distances, which are not feasible values when compared relative to −1 and +1, extreme values of the cube. Anderson and Whitcomb (2005) proposed the practical alpha, $\alpha = \sqrt[4]{k}$, as a compromise between the spherical alpha and cuboidal alpha. The practical alpha, which is less extreme when compared to the spherical and rotatable alpha values, also offers reasonable variance inflation factor (VIF) as k increases (Li *et al.*, 2009). Another advantage of the practical α is that it exists for both the spherical and cuboidal design regions, unlike the spherical and rotatable axial distances that exist only in the spherical design region. However, often times, the practical α tends to locate the star points very close to the centre of the design region that it is difficult to determine the true precision of the designs' prediction capabilities. For instance, in the study by Li *et al.* (2009), despite the advantages posed by the practical axial distance, the CCD with spherical α consistently gave smaller and more stable prediction variance throughout the design region than the practical CCD by using fraction of design space plots.

1.3 Aim of the study

The aim of the study is to construct alternative axial distances for the spherical and cuboidal design regions of the central composite designs which are less extreme but provides more stable prediction precision for the design.

1.4 Objectives of the study

Specifically, the objectives of the study include:

a. To construct a set of alternative axial distances for the CCD in spherical region.

b. To construct a set of alternative axial distances for the CCD in cuboidal region.

The star component does not contribute to the estimation of the interaction terms. The centre component contributes to the estimation of pure error and estimation of quadratic terms (Wong, 1993).

Hence, the role of the star component of the CCD is very vital in response surface exploration using the central composite design. It is the introduction of the star component that gives the CCD the second-order design status since the factorial component must be a first-order design. Therefore, the location of the star points on the design region strongly influences the performance of the CCD. Usually, the star points are located at distance, α, from the centre of the design region. This distance, α, from the centre along the axes of the CCD is called the axial distance. Some axial distances exist which leads to the classification of the CCD according to the type of axial distance. For $\alpha = \sqrt{k}$, we have the spherical CCD, $\alpha = \sqrt[4]{f}$ gives the rotatable CCD, $\alpha = \sqrt[4]{k}$ gives the practical CCD and $\alpha = 1$ gives the Face-centered CCD.

In this study, we will develop a set of alternative axial distances for the central composite designs in both the spherical and cuboidal design regions. The alternative sets of axial distances will be evaluated and compared with the existing axial distances in both the spherical and cuboidal design regions using graphical methods and some popular design evaluation criteria. The graphical methods to be utilized in this study will put into consideration the scaled prediction variances for the adequate characterization of the prediction properties of the CCD. Furthermore, evaluation of the alternative axial distances will be extended to the cases involving replications of the star component of the CCD as well as the inscribed CCD.

1.2 Statement of the problem

The problem with the spherical and rotatable alpha, as identified by Li et al (2009), is that as the number of factors increases, these alpha values could give

as $\alpha = \sqrt[4]{\frac{n_1 f}{n_2}}$, where n_1 and n_2 are respectively, the number of replications of the cube and star components of the CCD. The rotatable alpha has been used extensively in the evaluation of the CCD for experimental purposes, Dykstra (1960), Draper (1982), Myers *et al.* (2009) and Ukaegbu and Chigbu (2015a). Though the rotatable axial distance may give desirable prediction variance properties, the level may be impractical for the factors of interest. For industrial experiments requiring large number of factors, say $k = 20$ factors, the star points will have rotatable axial distance of 4.471 (Li *et al.*, 2009). This value may not be feasible considering the fact that the remaining factors in the experiment are set at the levels of -1 and $+1$. This may degenerate further with the replication of the cube or both the cube and star components.

The drawback of the spherical and rotatable axial distances with respect to high alpha values when there are high number of factors led to the recommendation of the practical axial distance by Anderson and Whitcomb (2005). The practical axial distance defines the practical CCD and is given by $\alpha = \sqrt[4]{k}$. This axial distance is a compromise between the cuboidal and spherical axial distances, $\alpha = 1$ and $\alpha = \sqrt{k}$, respectively. According to the authors, the practical axial distance offers small and stable prediction variance with acceptable variance inflation factors. However, recent studies have shown that despite the obvious advantages of the practical axial distance, it does not necessarily provide consistently small prediction variances throughout the entire design region. In a study by Li *et al.* (2009), the CCD with spherical α is consistently superior to that of the practical α in the spherical regions. Ukaegbu (2017) has also shown that the CCD with practical axial distance did not compete favourably with the CCD with cuboidal α in a baking experiment requiring the

choice of appropriate axial distance for the CCD to optimize the experiment. The practical axial distance is applicable in the spherical and cuboidal regions.

2.3 Orthogonality and blocking of CCD

Orthogonality is one of the major and useful properties of the central composite response surface designs. The CCD is made orthogonal by the choice of the axial distance which was recommended by Box and Hunter (1957) to be $\alpha = \sqrt{\left[(Nf)^{1/2} - f\right]/2}$. This gives the orthogonal CCD. The orthogonal α for the CCD was extended by Nwobi *et al.* (2001) to accommodate the replications of the cube and star components of the design. They recommended the axial distance to be $\alpha = \sqrt[4]{n_1 f\left[N^{1/2} - (n_1 f)^{1/2}\right]^2 / 4n_2^2}$, where n_1 and n_2 retained their original meanings (Ukaegbu and Chigbu, 2015b). Orthogonality is a spherical property.

Furthermore, blocking of second-order response surface designs may be required to eliminate nuisance variables. Orthogonal blocking of a response surface design is possible if the design can be divided into blocks such that block effects do not affect the parameter estimates of the response surface model. The CCD is orthogonally blocked by the choice of axial distance that ensures orthogonal blocking. According to Box and Hunter (1957) the axial distance that ensures orthogonal blocking of the CCD is $\alpha = \sqrt{\frac{f(2k + n_a)}{2(f + n_f)}}$, where n_a and n_f are the number of centre points in the axial and factorial blocks, respectively (Montgomery, 2013). Dykstra (1960) extended the α for orthogonal blocking to the case where the axial component of the CCD is replicated twice, $n_2 = 2$ while Ukaegbu and Chigbu (2017) generalized the α for the replication of the cube and star components of the CCD.

The general form given by Ukaegbu and Chigbu (2017) is $\alpha=\sqrt{\frac{F(N-F-n_f)}{2n_2(F+n_f)}}$,

where $F=n_1 f$ and $N=F+2n_2 k+n_a+n_f$.

CHAPTER THREE

METHODOLOGY

3.1 Development of alternative axial distances

Two sets of axial distances are developed for the CCD. The first set is developed for the spherical region and the second set for the cuboidal region. Each set is developed under the three classical Pythagorean means, the arithmetic mean, harmonic mean and geometric mean of the available axial distances in each related design space. Therefore, each set contains three axial distances for each region. The arithmetic mean of a set of random variables, $\eta_1, \eta_2, \ldots, \eta_r$, is given by $\Lambda_a = r^{-1}\sum_{i=1}^{r}\eta_i$. The harmonic mean of the same set of random variables is $\Lambda_h = r\left[\sum_{i=1}^{r}\frac{1}{\eta_i}\right]^{-1}$ while their geometric mean is $\Lambda_G = \left[\prod_{i=1}^{r}\eta_i\right]^{\frac{1}{r}}$.

The axial distances developed from these functions were introduced in each central composite design for k = 3 to 8 factors. These designs were evaluated using the *D*-and *G*-efficiency design evaluation criteria as the single-value criteria. The design that has the highest *D*- and *G*-efficiency values is the most efficient with respect to the particular efficiency criteria. Two popular graphical methods, the variance dispersion graph and fraction of design space plots were used to display the prediction variance characteristics of the designs throughout the entire design region. The design that displays the smallest prediction variance throughout the design region is considered the most stable with minimum prediction variance.

3.2 *D*-and *G*-efficiencies

The *D*-efficiency makes use of the determinant, $|M|$, of the information matrix, $M = \mathbf{X}'\mathbf{X}$, or the determinant, $|M^{-1}|$, of the inverse of the information matrix, $M^{-1} = (\mathbf{X}'\mathbf{X})^{-1}$, where $\mathbf{X}$ is the design matrix extended to model form by including the linear, pure quadratic and mixed quadratic (interaction) terms. Under the standard normality assumptions, $|M|$ is inversely proportional to the square of the volume of the confidence ellipsoid (region) of the regression coefficients (Onukogu, 1997). The volume of the confidence ellipsoid is relevant because it reflects how well the set of coefficients are estimated. Therefore, the larger the value of $|M|$, the better the estimation of the model parameters. On the other hand, small $|M|$ and hence, large $|M^{-1}|$ implies poor estimation of the set of model parameters. The *D*-efficiency is very useful in quantifying the quality of the estimated model parameters and is defined as (Borkowski and Valeroso, 2001),

$$D - eff = \frac{|M|^{1/p} \times 100}{N}. \qquad (7)$$

The power, $1/p$, takes account of the *P*number of parameter estimates of the regression model being assessed when the determinant of the information matrix is being computed.

With the development of statistical softwares such as the JMP, Design Expert, and so on, which are based on numerous programs and algorithms, the computation of *D*-efficiency has been made easy. However, Borkowski and Valeroso (2001) developed exact *D*-efficiency for the central composite designs and used it to evaluate reduced models for the CCD in hypercube.

Since the primary target of so many response surface designed experiments is to allow for good prediction throughout the design space, the focus is on the variance of prediction, $\mathrm{var}\left[\hat{y}(X)\right]$. The *G*-efficiency is one of the design evaluation criteria that are based on the scaled prediction variance property of the design. The *G*-efficiency uses the maximum SPV, $\max\left[N\mathbf{x}'(\mathbf{X}'\mathbf{X})^{-1}\mathbf{x}\right]$, in design evaluation. The *G*-efficiency intuitively protects the experimenter against the worst-case scenario of the prediction variance being too undesirable since the user may wish to predict new responses anywhere in the design space. An interesting and important characteristic of the *G*-efficiency is that the lower bound for the maximum scaled prediction variance is equal to p, the number of model parameters. Therefore, when $\max\left[N\mathbf{x}'(\mathbf{X}'\mathbf{X})^{-1}\mathbf{x}\right] = p$, then the design is 100% *G*-efficient. Therefore, the *G*-efficiency is given by

$$G_{eff} = 100p/\max\left[N\mathbf{x}'(\mathbf{X}'\mathbf{X})^{-1}\mathbf{x}\right]. \tag{8}$$

For the *D*-and *G*-efficiencies, the closer the values are to 1 (that is, 100%), the better the design. Recent studies have shown that the lower bound of the *G*-efficiency may not be all the time. This was demonstrated by Anabri and Lucas (2008) and Lucas (2009) that some split-plot response surface designs have maximum SPV that are less than p such that *G*-efficiency could be greater than 100%. They termed these designs 'super-efficient' designs. Also, Borkowski and Valeroso (2001) developed exact *G*-optimality for evaluating the CCD for reduced models in the hypercube.

3.3 Graphical methods for comparison

Several graphical techniques have been developed to enhance comparisons of different designs in the design space. The most popular and most used are the variance dispersion graph (VDG) and fraction of design space graphs (FDSG).The

VDG was first introduced through the works of Giovannitti-Jensen and Myers (1989) as a graphical procedure that is dependent on the prediction variance properties of response surface designs for evaluating the designs. This graphical method displays the distribution of the unscaled and scaled prediction variances of response surface designs of a multi-dimensional design region on two-dimensional graphs. In constructing the VDG, the prediction variance is plotted against the radius, *r*, of the sphere from zero up to the outer region of the sphere covering the region of interest in order to evaluate the prediction capability of the design. If the region is cuboidal, the radius ranges from zero to one.

Giovannitti-Jensen and Myers (1989) developed the VDG first, for the first-order response surface designs. They showed that, for the first-order response surface models, the maximum SPV is $\max \frac{N \operatorname{var}[y(\mathbf{x})]}{\sigma^2} = 1 + N(\lambda_{\max})r^2$, the minimum SPV is $\min \frac{N \operatorname{var}[y(\mathbf{x})]}{\sigma^2} = 1 + N(\lambda_{\min})r^2$ and the average SPV is $V^r = 1 + \frac{Nr^2}{k}\sum_{i=1}^{k}\lambda_i$. The parameters, $\lambda_{\max}$, $\lambda_{\min}$ and λ_i, are respectively, the maximum, minimum and i^{th} eigenvalues of the inverse of the information matrix, $(X'X)^{-1}$. If the eigenvalues are equal, the design is said to be an orthogonal and rotatable first-order response surface design. Also, Giovannitti-Jensen and Myers (1989) employed a FORTRAN-based computer algorithm developed by Vinning (1988) for computing the prediction variances of the second-order response surface designs on a sphere of radius, *r*, and made the algorithm adaptable even for the first-order problems. However, this algorithm can only compute the prediction variances for up to $k = 7$ design variables and does not guarantee finding the global optimum. Apart from that, the computing time required in using the algorithm makes it less attractive for users. Following the

development of the VDG as an acceptable graphical procedure for design comparison, Vinning (1993) wrote a FORTRAN-based computer program to generate the VDG for response surface designs.

Following the drawbacks of the computer programs for plotting the variance dispersion graphs highlighted above and the uncertainties about obtaining the exact results for the designs, Borkowski (1995) developed analytical forms for evaluating the exact prediction variances for the CCD as more viable alternative to the optimization algorithm. He showed that the exact minimum and maximum scaled prediction variances for the second-order response surface design at radius, r, of the spherical region are as follows:

$$V_{rMIN} = N\left[A + Br^2 + \left(C + \frac{D}{k}\right)r^4\right] \text{ if } D > 0$$

$$= N\left[A + Br^2(C + D)r^4\right] \text{ if } D \leq 0.$$

$$V_{rMAX} = N\left[A + Br^2 + \left(C + \frac{D}{k}\right)r^4\right] \text{ if } D \leq 0$$

$$= N\left[A + Br^2(C + D)r^4\right] \text{ if } D > 0.$$

The values of the coefficients, as given by Borkowski (1995), are:

$$A = \alpha_{11} = \frac{kf + 2n_s\alpha^4}{Q}, \qquad B = 2\alpha_{12} + \frac{1}{f + 2n_s\alpha^2}, \qquad \alpha_{12} = -\frac{f + 2n_s\alpha^2}{T},$$

$$C = \frac{1}{2}\left(\frac{1}{f} - \frac{\alpha_{22}}{n_s\alpha^4}\right), \qquad \alpha_{22} = \frac{Nf - \left(f + 2n_s\alpha^2\right)^2}{Q}, \qquad D = \frac{1}{2}\left(\frac{1}{n_s\alpha^2} - \frac{1}{f}\right) \text{and}$$

$$Q = 2Nn_s\alpha^4 + kNf - k\left(f + 2n_s\alpha^2\right)^2,$$

where the meanings of N, r, k, f, and α are as have been given earlier in this work while n_s is the number of replications of the star portion.

As pointed out by Zahran et al (2003), the VDG portrays the prediction variance characteristic of a design at every point in the design space, helping the user to have knowledge of points of best and worst predictions, points where the prediction variance is maximized and where it is minimized in the design region. However, the VDG hides the fact that different volumes are associated with each radius or shrinkage factor, in the case of mixture experiments. The plots deal with the prediction variance on a sphere of radius, r, ignoring the associated volume.

The VDG has been extensively employed in comparing and solving several response surface related designs and problems: Trinca and Gilmour (1998), Borror et al (2002), anderson-Cook et al (2009), Chigbu et al (2009), Myers et al (2009) and Ukaegbu and Chigbu (2015a) for the application of the variance dispersion graphs procedure in the spherical region. Also, designs in the cuboidal regions were studied using the VDG in Rozum and Myers (1991), Borkowski (1995), Block and Mee (2001), Park et al (2005) and Ukaegbu and Chigbu (2015b). Goldfarb et al (2004) extended the VDG to three-dimensions to evaluate the prediction variance properties of mixture experiments. These plots are excellent tools to aid in selecting the designs, augmenting design points, or selecting appropriate fractions of experiments when full mixture-process design has large number of runs.

The fraction of design space graph (FDSG) was developed by Zahran et al. (2003) to complement the VDG for both spherical and cuboidal design spaces. The plots display the characteristics of the SPV of a multi-dimensional region on a two-dimensional graph with a single curve for each design. The graph displays the fraction of the design space at or below any given SPV value, ν, say. The concept of fraction of design space (FDS) puts into consideration, the volume of the fraction of the design

space not accounted for in VDG.According to Zahran et al (2003), the fraction of design space is defined as

$$FDS=\frac{1}{\Psi}\int \ldots \int I(X)dx_1..dx_k,$$

$$\text{where } I(X)=\begin{cases} 0.5^{\frac{(g-g)}{g}}; & g\neq 0 \\ 0 \quad ; & g=0 \end{cases}$$

$g=v(x)-v$, v is any given scaled prediction variance value, $v(x)$ is the prediction variance such that $v(x)<v$ and $g<0$ while $\Psi=2^k$ is the volume of the design space. If the design is rotatable, Zahran et al. (2003) defined the fraction of design space as

$$FDS=k\int_0^1 I(X)r^{k-1}dr.$$

The prediction variance is computed for each fraction of the design space, then the prediction variance is plotted against the cumulative fractions of the design space. They went ahead to develop a FORTRAN code that uses International Mathematics and Statistics Library (IMSL) multivariate numerical subroutine for calculating the FDS and plotting the graphs.

The prediction variance values of the FDS were originally calculated numerically using the software, Mathematica. Though this is feasible for lower dimensions up to five factors, this approach becomes computationally too cumbersome and slow for higher dimensions. For this reason, considerations have been vigorously assessed for other alternatives for obtaining the FDS and their corresponding prediction variances (PV). Consequently, Goldfarb et al .(2004) proposed uniform sampling throughout the entire design space. Using this approach, the FDS is constructed by sampling a large number of values, n, throughout the entire

design region and obtaining the corresponding PV values which are then ordered and plotted against the quantiles, $\left(\frac{1}{n},\frac{2}{n},...,\frac{n}{n}\right)$. This approach could be employed for any type of design space, regular or irregular. The original approach proposed by Zahran et al. (2003) considered only regular design regions.

Goldfarb et al. (2004) also adopted the FDS plots for evaluating mixture experiments. At constant shrinkage factor, they plotted the global FDS and the sliced FDS for the scaled prediction variance values. This enables the user to see which of the spaces contributes more to changes in the SPV. Liang et al. (2006) extended the FDS plots approach to the case of CCD for split-plot designs incorporating cost. The graphical tool enables the experimenter to evaluate and develop strategies for improving the prediction performance of split-plot designs. Li et al. (2009) utilized the FDS plots to evaluate the prediction variance properties of the CCD, SCD and MinResV designs in both cuboidal and spherical regions for various axial distances and for six to ten design factors. Examples of further works involving the fraction of design space graphs in design evaluation and comparisons include Ozol-Godfrey et al. (2005), Ozol-Godfrey et al. (2008),Anderson-Cook et al. (2009)and Jang and Anderson-Cook (2011).

CHAPTER FOUR

RESULTSAND DISCUSSION

4.1 Alternative axial distances

In this section, a set of axial distances were developed for the cuboidal and spherical design regions for the evaluation of the central composite designs (CCD).

4.1.1 Axial distances for Spherical Region

The three existing axial distances for the spherical region are, namely: spherical alpha, $\alpha = \sqrt{k}$; practical alpha, $\alpha = \sqrt[4]{k}$ and rotatable alpha, $\alpha = \sqrt[4]{f}$, where $f = 2^{k-q}$, k is the number of factors and q is a nonnegative integer less than k. The arithmetic, harmonic and geometric means of these three alpha values gave the three new axial distances for the placement of the star points in the spherical region. The first is the arithmetic axial distance.

Let $\Lambda_A = s^{-1}\sum_{i}^{s}\eta_i$ (9)

be the arithmetic mean of s random variables with subscript, A representing 'arithmetic', then the arithmetic mean of the spherical, practical and rotatable axial distances is given by

$$\alpha_{AS} = s^{-1}\left[k^{1/2} + k^{1/4} + 2^{(k-q)/4}\right], \quad s = 3 \text{ and } q \geq 0. \tag{10}$$

For the harmonic axial distance, let $\Lambda_H = s\left[\sum_{i=1}^{s}\frac{1}{\eta_i}\right]^{-1}$ be the harmonic mean of the s independent random variables, then the harmonic mean of the three existing axial distances is given by

$$\alpha_{HS} = s\left[\frac{1}{\sqrt{k}} + \frac{1}{\sqrt[4]{k}} + \frac{1}{\sqrt[4]{2^{k-q}}}\right]^{-1}$$

$$= s\left[k^{-1/2} + k^{-1/4} + 2^{-(k-q)/4}\right]^{-1}, s = 3 \text{ and} q \geq 0. \quad (11)$$

The geometric mean of a set of s independent random variables is $\Lambda_G = \left[\prod_{i=1}^{s} \eta_i\right]^{\frac{1}{s}}$.

Hence, the geometric axial distance in the spherical region is

$$\alpha_{GS} = \left[\sqrt{k} \times \sqrt[4]{k} \times \sqrt[4]{2^{k-q}}\right]^{\frac{1}{s}}$$

$$= \left[k^{\left(\frac{1}{2}+\frac{1}{4}\right)} \times 2^{\frac{k-q}{4}}\right]^{\frac{1}{s}} = \left[\left(2^{\frac{k-q}{4}}\right)\left(k^{\frac{3}{4}}\right)\right]^{\frac{1}{s}}$$

Therefore,

$$\alpha_{GS} = \left[k^3 \left(2^{k-q}\right)\right]^{\frac{1}{4s}}, s = 3 \text{ and} q \geq 0. \quad (12)$$

Equations (10), (111) and (12) are the alternative axial distances for the CCD in spherical region based on the three Pythagorean means.

4.1.2 Axial distances for Cuboidal Region

The two existing axial distances applicable to the cuboidal region is the cuboidal alpha, $\alpha = 1$, which defines the face-centered CCD and the practical alpha, $\alpha = \sqrt[4]{k}$ (k is as earlier defined). Then the three Pythagorean means are obtained.

For the arithmetic alpha,

$$\alpha_{AC} = s^{-1}\left[1 + k^{\frac{1}{4}}\right], s = 2. \quad (13)$$

The harmonic alpha for the cuboidal region is

$$\alpha_{HC} = s\left[1 + \frac{1}{\sqrt[4]{k}}\right]^{-1}, s = 2. \quad (14)$$

The geometric alpha is

$$\alpha_{GC} = \left[1 \times \sqrt[4]{k}\right]^{1/s} = (k)^{1/4r}, s = 2. \quad (15)$$

Equations (13), (14) and (15) are the three alternative axial distances of the CCD in the cuboidal region. Catalogues of the values of these alternative axial distances with those of the existing axial distances, the cuboidal, α_C, spherical, α_S, practical, α_P, and rotatable, α_R, axial distances, from which they were derived are presented in Tables 1 and2, respectively, for the spherical and cuboidal regions.

4.2 Design Efficiencies for Comparison

The D- and G-efficiency values are computed for the six variations of the CCD in spherical region and five variations of the CCD in cuboidal region. The variations of the CCD are based on the various axial distances defining the central composite designs under comparison. The D- and G-efficiencies are used to measure any improvement on the performances of the designs by the alternative axial distances. The closer the efficiency value is to 100 percent, the more preferable the design. The designs having the same number of experimental runs makes it easier for comparison as no design will have undue advantage over the others with respect to the number of runs. The number of factors under consideration here is k = 2 to 8 factors. Each set of factors was evaluated with three centre points in line with the recommendations of Montgomery (2013) which stated that for CCD, 3-5 centre points area acceptable. The values of the D- and G-efficiencies for the axial distances for the spherical regions are presented in Tables 3 and 4, respectively.

Table 1 presents the catalogue of Alpha value for the Spherical Region. The values of the six axial distances in the Spherical Region as evaluated using 2 to 10 factors are presented in the table.

The catalogue of Alpha value for the Cuboidal Region is presented in table 2. The table is made up of the results of evaluation of the five axial distances in the region using varying number of factors, 2 to 10 in experiment. Table 3 and 4 show the D- and G- efficiency values, respectively, with the three centre points in the Spherical Region.

The best results for the D-efficiency in spherical region is given by the CCD with rotatable axial distance, α_R. This is followed by the CCD with spherical axial distances, α_S. The central composite designs with the three alternative axial distances, α_{AS}, α_{HS} and α_{GS}, consistently give D-efficiency values that are better than the CCD with practical axial distance, α_P. Among the arithmetic, harmonic and geometric axial distances, the CCD with arithmetic axial distance is the best in terms of D-efficiency, followed by the CCD with geometric axial distance. The CCD with harmonic axial distance consistently gave the worst D-efficiency performance among the three alternative axial distances. Therefore, the central composite designs with arithmetic, harmonic and geometric axial distances should be used in place of the CCD with practical axial distance when the D-efficiency is the criterion chosen by the experimenter for response surface exploration.

The CCDs with arithmetic, harmonic and geometric axial distances, α_{AS}, α_{HS} and α_{GS}, gave the highest G-efficiency values for k = 5, 7 and 8 factors. Only the G-efficiency values of the CCD with spherical axial distance, α_S, are higher than those of the arithmetic, harmonic and geometric axial distances for k = 3, 4 and 6 factors. In the spherical region, the CCD with practical axial distance offered the lowest G-efficiency values, followed by the CCD with rotatable axial distance. It is only at k = 8 that the CCD with rotatable and spherical axial distances have the same G-

TABLE 1

Catalogue of alpha value for the spherical region

K	F	α_S	α_P	α_R	α_{AS}	α_{HS}	α_{GS}
2	2^2	1.4142	1.1892	1.4142	1.3392	1.3303	1.3348
3 4	2^3	1.7321	1.3161	1.6818	1.5766	1.5530	1.5651
5	2^4	2.0000	1.4142	2.0000	1.8047	1.7574	1.7818
6	2^5	2.2361	1.4954	2.3784	2.0366	1.9526	1.9961
7	2^6	2.4495	1.5651	2.8284	2.2810	2.1417	2.2134
	2^{6-1}	2.4495	1.5651	2.3784	2.1310	2.0441	2.0891
8	2^7	2.6458	1.6266	3.3636	2.5453	2.3255	2.4371
	2^{7-1}	2.6458	1.6266	2.8284	2.3669	2.2283	2.3003
9	2^{7-2}	2.6458	1.6266	2.3784	2.2169	2.1229	2.1712
	2^8	2.8284	1.6818	4.0000	2.8367	2.5038	2.6697
10	2^{8-1}	2.8284	1.6818	3.3636	2.5246	2.4088	2.5198
	2^{8-2}	2.8284	1.6818	2.8284	2.4462	2.3047	2.3784
	2^9	3.0000	1.7321	4.7568	3.1630	2.6764	2.9130
	2^{9-1}	3.0000	1.7321	4.0000	2.9107	2.5847	2.7495
	2^{9-2}	3.0000	1.7321	3.3636	2.6986	2.3415	2.5952
	2^{10}	3.1623	1.7783	5.6569	3.5325	2.8427	3.1686
	2^{10-1}	3.1623	1.7783	4.7568	3.2325	2.7554	2.9907
	2^{10-2}	3.1623	1.7783	4.0000	2.9802	2.6583	2.8229
	2^{10-3}	3.1623	1.7783	3.3636	2.7681	2.4197	2.6644

TABLE 2

Catalogue of alpha value for the cuboidal region

K	F	α_c	α_P	α_{AS}	α_{HS}	α_{GS}
2	2^2	1.0000	1.1892	1.0946	1.0864	1.0905
3	2^3	1.0000	1.3161	1.1580	1.1365	1.1472
4	2^4	1.0000	1.4142	1.2071	1.1716	1.1892
5	2^5	1.0000	1.4954	1.2477	1.1985	1.2229
6	2^6	1.0000	1.5651	1.2826	1.2203	1.2511
	2^{6-1}	1.0000	1.5651	1.2826	1.2203	1.2511
7	2^7	1.0000	1.6266	1.3133	1.2386	1.2754
	2^{7-1}	1.0000	1.6266	1.3133	1.2386	1.2754
	2^{7-2}	1.0000	1.6266	1.3133	1.2386	1.2754
8	2^8	1.0000	1.6818	1.3409	1.2542	1.2968
	2^{8-1}	1.0000	1.6818	1.3409	1.2542	1.2968
	2^{8-2}	1.0000	1.6818	1.3409	1.2542	1.2968
9	2^9	1.0000	1.7321	1.3661	1.2680	1.3161
	2^{9-1}	1.0000	1.7321	1.3661	1.2680	1.3161
	2^{9-2}	1.0000	1.7321	1.3661	1.2680	1.3161
10	2^{9-3}	1.0000	1.7321	1.3661	1.2680	1.3161
	2^{10}	1.0000	1.7783	1.3892	1.2801	1.3335
	2^{10-1}	1.0000	1.7783	1.3892	1.2801	1.3335
	2^{10-2}	1.0000	1.7783	1.3892	1.2801	1.3335
	2^{10-3}	1.0000	1.7783	1.3892	1.2801	1.3335

TABLE 3

D-efficiency values with three centre points in spherical region

k	F	N	α_S	α_P	α_{AS}	α_{HS}	α_{GS}	α_R
2	2^2	11	61.76	44.77	57.59	57.12	57.36	61.76
3 4	2^3	17	70.05	52.51	62.53	53.04	53.20	100
5	2^4	27	76.40	55.80	68.98	67.30	68.16	100
6 7	2^5	45	80.70	58.70	74.42	71.93	73.51	85.60
8	2^{6-1}	47	83.50	59.60	74.62	72.33	73.51	100
	2^{7-1}	81	85.94	62.16	79.41	76.29	77.91	90.61
	2^{8-2}	83	87.87	63.38	79.84	76.94	78.46	87.87

TABLE 4

G-efficiency values with three centre points in spherical region

k	F	N	α_S	α_P	α_{AS}	α_{HS}	α_{GS}	α_R
2	2^2	11	87.27	57.65	83.52	83.52	83.30	61.76
3	2^3	17	89.03	79.25	85.20	79.54	79.63	77.30
4	2^4	27	95.21	58.50	92.50	91.84	92.63	76.30
5	2^5	45	86.00	80.90	88.60	89.19	88.92	83.00
6	2^{6-1}	47	94.90	90.00	92.88	92.36	92.63	86.10
7	2^{7-1}	81	83.68	81.64	85.37	85.52	85.46	81.06
8	2^{8-2}	83	94.58	95.48	97.35	96.93	97.14	94.58

efficiency values which are however, lower than those of the three new alternative axial distances. Hence, if the G-efficiency is the experimenter's preferred criterion for response surface exploration in spherical region, the CCD with arithmetic axial distance should be used or any of harmonic and geometric axial distances. It is only for k = 3, 4 and 6 factors that the CCD with spherical axial distance should be preferred.

The results of the *D*- and *G*-efficiencies for the cuboidal region are presented in Tables 5and 6, respectively, for k = 3 to 8 factors of the central composite design. D- and G- efficiency values with three centre points in the Cuboidal Region are presented in Table 5 and 6 respectively.

As depicted by the results in Table 5, the CCDs with arithmetic, harmonic and geometric axial distances are consistently the best with the highest D-efficiency values for all the factors considered in the cuboidal design region. Among the three alternative axial distances, the CCD with the arithmetic axial distance gives the highest D-efficiency values which are followed by the CCD with geometric axial distance and then, the CCD with harmonic axial distance giving the lowest percentage D-efficiency values. Also, the CCDs with arithmetic, harmonic and geometric axial distances provide the highest G-efficiency values as compared to the values of those of the cuboidal and practical axial distances. The only exceptions are for k = 5 and 7 where the CCD with cuboidal axial distance, α_C, have the highest G-efficiency values. The CCD with arithmetic axial distance again provided the highest G-efficiency values for k = 3, 4, 6 and 8 factors among the three alternative axial distance. This is followed by the CCD with geometric axial distancesand then, the CCD with harmonic axial distance. Obviously, the central composite designs with

TABLE 5

D-efficiency values with three centre points in cuboidal region

K	*F*	*N*	α_C	α_P	α_{AC}	α_{HC}	α_{GC}
2	2^2	11	42.84	44.77	46.43	46.03	46.36
3	2^3	17	41.30	42.95	46.83	46.08	46.45
4	2^4	27	42.10	44.07	49.05	47.88	48.46
5	2^5	45	43.30	48.16	51.24	49.71	50.47
6	2^{6-1}	47	43.20	49.77	51.66	49.84	50.74
7	2^{7-1}	81	45.11	51.28	54.00	51.95	52.97
8	2^{8-2}	83	45.88	51.40	55.07	52.82	53.93

TABLE 6

G-efficiency values with three centre points in cuboidal region

K	*F*	*N*	α_C	α_P	α_{AC}	α_{HC}	α_{GC}
2	2^2	11	68.71	57.65	72.18	71.79	72.03
3	2^3	17	74.00	69.42	76.37	76.02	76.20
4	2^4	27	84.30	73.91	85.86	85.57	85.71
5	2^5	45	95.01	82.20	92.22	92.52	92.37
6	2^{6-1}	47	88.14	84.14	88.95	88.74	88.85
7	2^{7-1}	81	89.20	86.30	87.82	88.12	87.97
8	2^{8-2}	83	94.37	91.96	94.88	94.75	94.81

arithmetic axial distance would be the experimenter's choice should the D-efficiency be the criterion for response surface exploration. The same is also true of the CCD with arithmetic axial distance if the G-efficiency is the experimenter's choice for response surface exploration in cuboidal region. Following the results of the D- and G-efficiencies, the central composite designs with geometric and harmonic axial distance provide formidable alternatives to the CCD with arithmetic axial distances since in most cases, the results of the three CCDs only slightly differ.

4.3 Graphical comparison

The variance dispersion graphs (VDG) and fraction of design space graphs (FDSG) were used in comparing the alternative axial distances for the central composite designs with the existing axial distances in the cuboidal and spherical regions. As earlier pointed out, single point criteria like the D- and G-efficiencies cannot completely reflect the performances of a design throughout the entire design region. The graphical methods possess this unique quality and could reveal points of strengths and weaknesses of the competing designs within the design region by displaying the designs performances throughout the design space (Li et al, 2009 and Chigbu et al, 2009).The variance dispersion graphs (VDG) assess the prediction variance properties of the designs under study by displaying their scaled prediction variance performances at every point radius in the design space. A design with low and stable scaled prediction variances at every point radius is preferred. The fraction of design space graphs (FDSG) assess the prediction variance characteristics of competing designs by displaying the scaled prediction variances of the designs per volume of the design space (Ozol-Godfrey et al, 2005). Therefore, a design with small and stable scaled prediction variance at every fraction of the design space is preferred. The term 'stability' refers to a design maintaining small prediction variance over substantial portion of the design space or the entire design region. The variance dispersion graphs were plotted in MATLAB software package (Version 2014a) with

the aid of computer programs developed in this work. The fraction of design space graphs were plotted in MATLAB software package (Version 2014a) after the fractions of design space and corresponding scaled prediction variance have been computed in Design Expert software package, Version 11. Three centre points were considered for each design for all the k factors under consideration.

4.3.1 Comparison using VDG

The designs are compared in the spherical and cuboidal design regions using the variance dispersion graphs (VDG). The graphs displayed the prediction variances of the competing designs throughout the entire design space on a two dimensional scale. The graphs are presented in Figures 4-10 for the spherical region and Figures 11-17 for the cuboidal region.

The graphs for the spherical region show that the CCD with arithmetic axial distance displayed the smallest and stable scaled prediction variances throughout the design regions for the k = 2to 8 factors considered. This was followed by the CCD with practical axial distance. The designs with spherical and rotatable axial distances displayed the worst performances with the highest scaled prediction variances throughout the design space. The CCD with harmonic and geometric axial distances are only better than the CCD with spherical and rotatable axial distances in the distribution of small scaled prediction variances at every point radius in the spherical region. For the cuboidal design space, the CCD with cuboidal axial distance, α_C, displayed the smallest prediction variances which remained stable for r = 0.5.Beyond this radius, the scaled prediction variance of the cuboidal CCD deteriorates and becomes very unstable. The three alternative axial distances, harmonic, arithmetic and geometric axial distances, displayed relatively similar but stable scaled prediction variance characteristics. The CCD with harmonic axial distances is the best of the three in cuboidal region with the lowest prediction variance. The CCD with practical

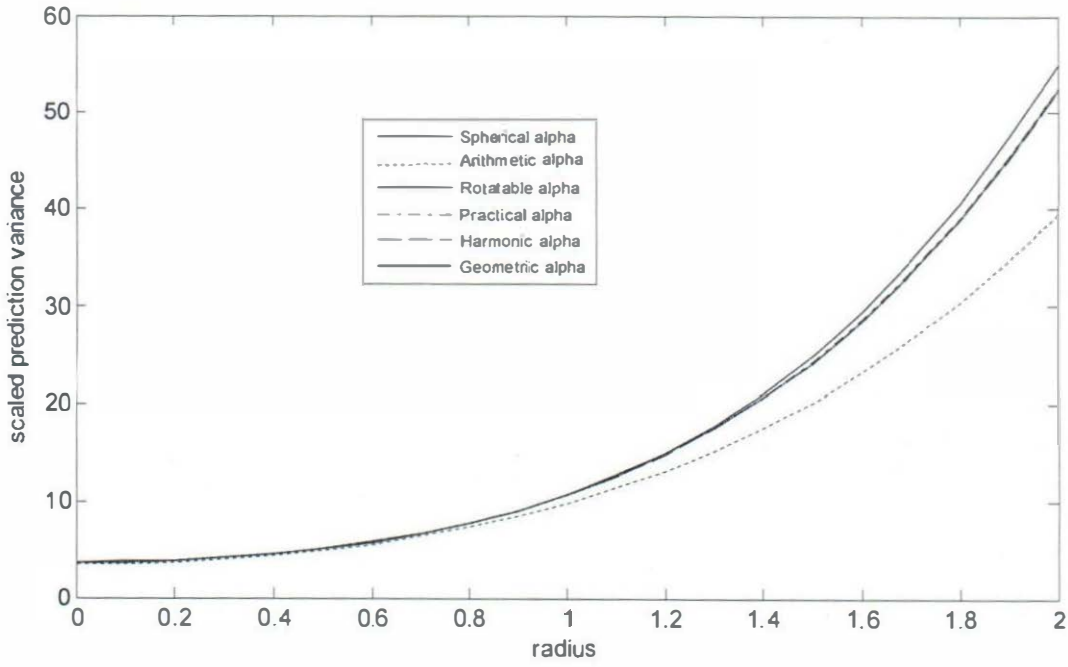

FIG.4: VDG for the Two-factor CCDs in spherical region

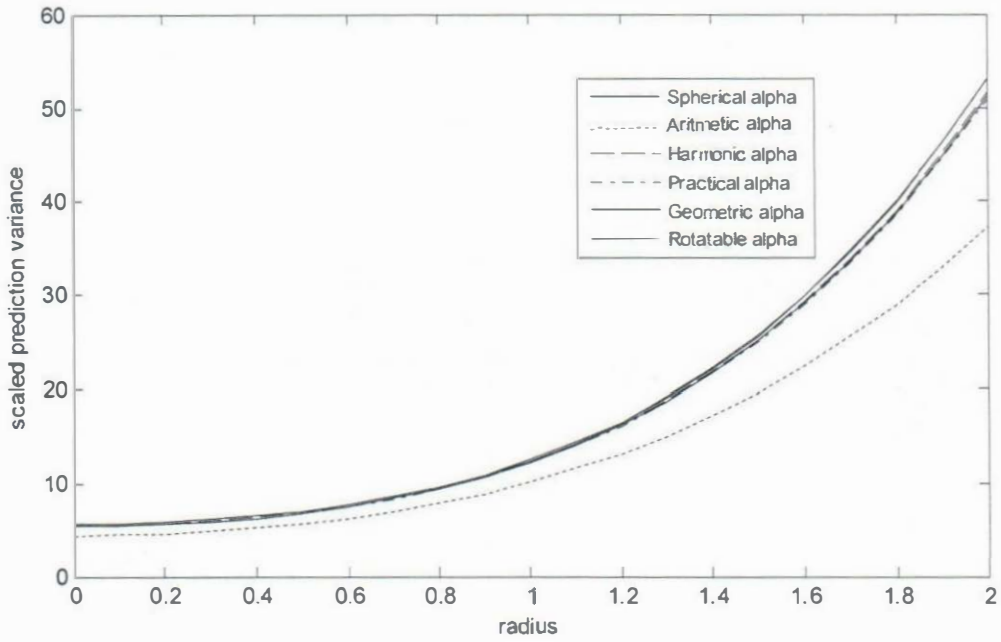

FIG.5: VDG for the three-factor CCDs in spherical region

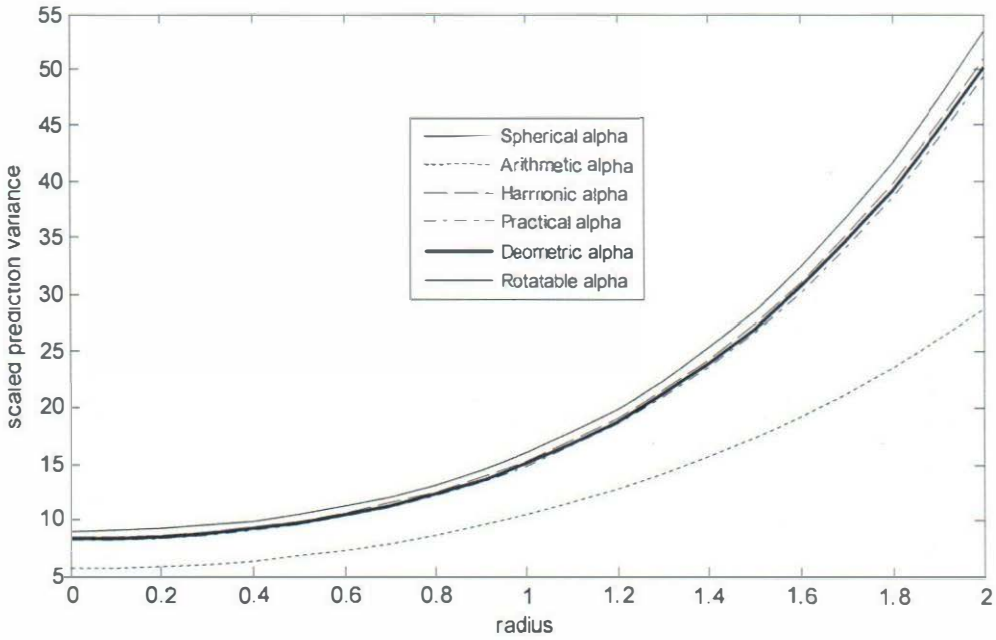

FIG. 6: VDG for the four-factor CCDs in spherical region

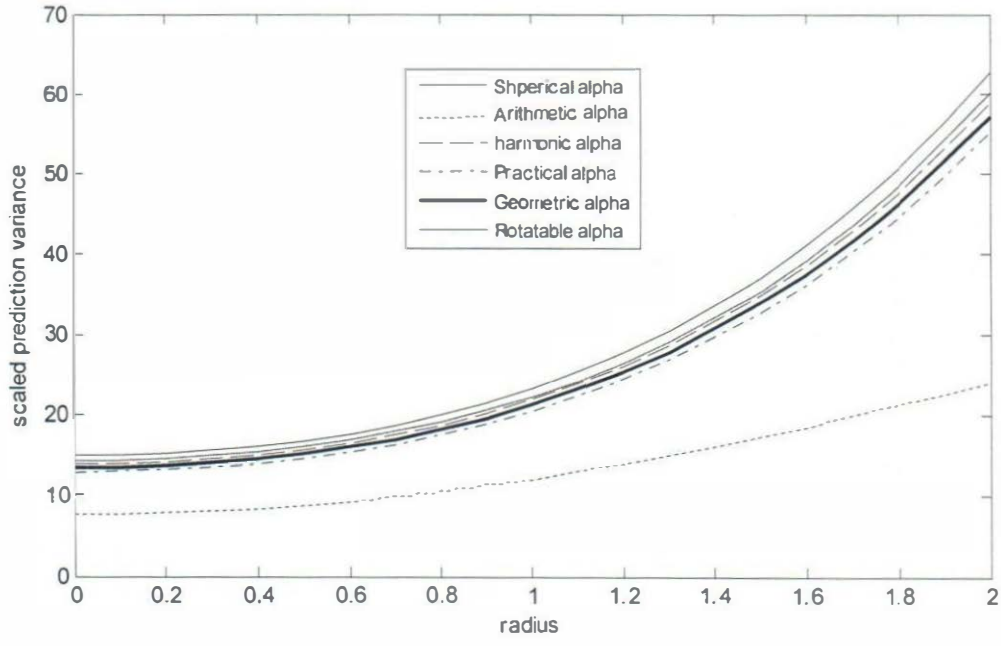

FIG.7: VDG for the five-factor CCDs in spherical region

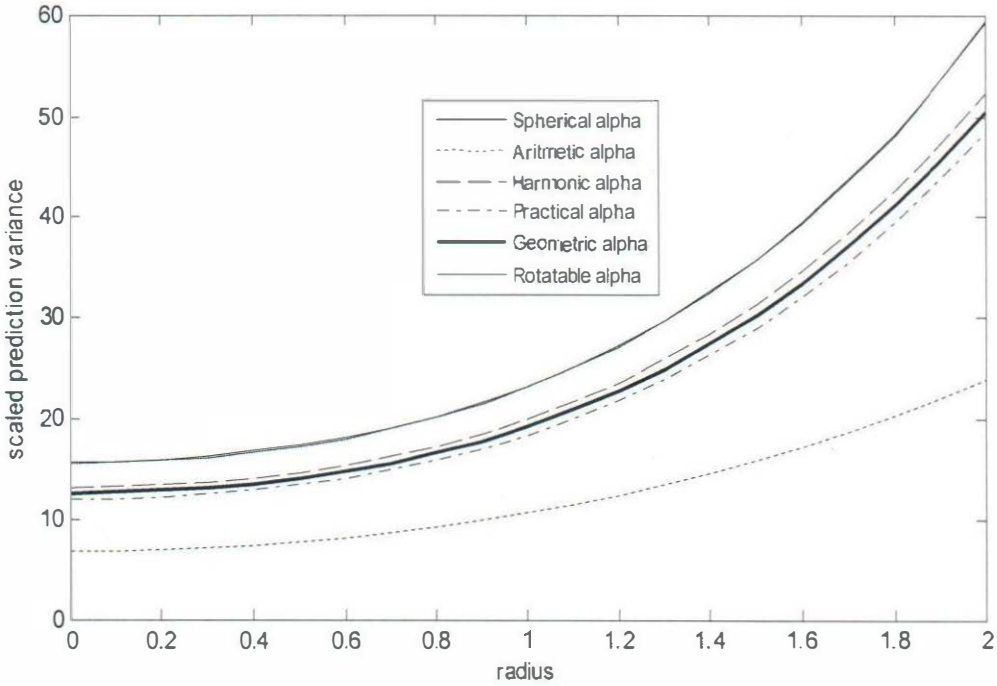

FIG.8: VDG for the six-factor CCDs in spherical region

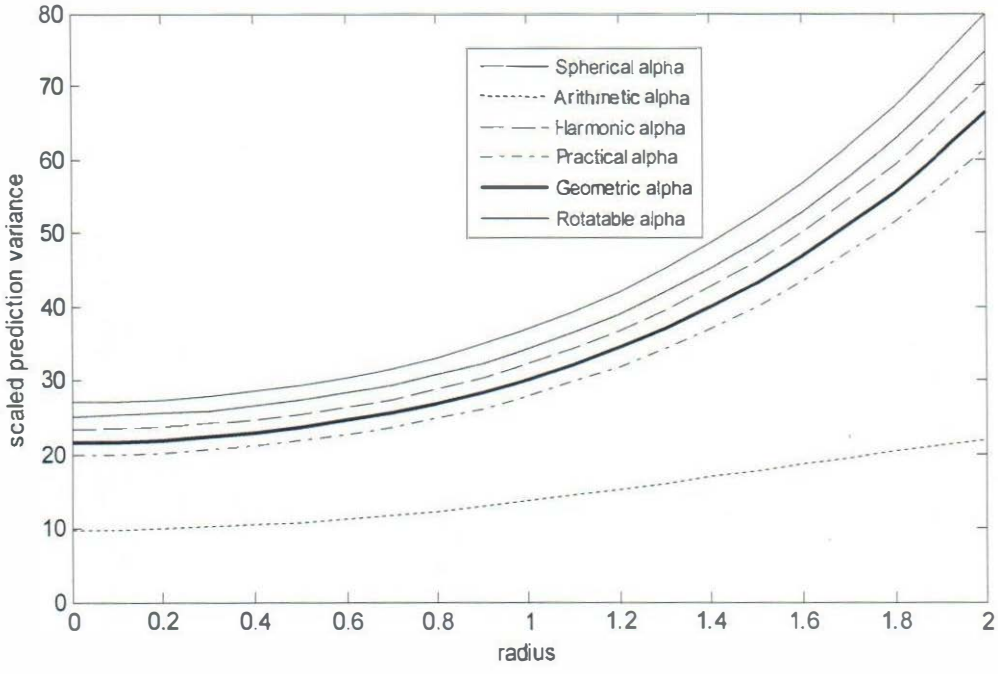

FIG.9: VDG for the seven-factor CCDs in spherical region

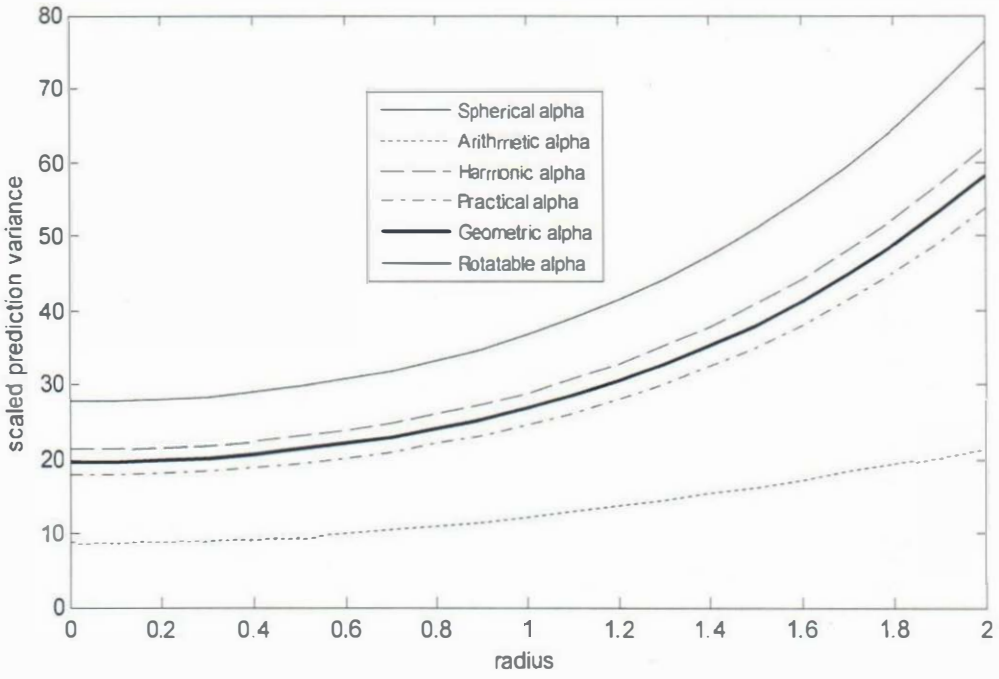

FIG. 10: VDG for the eight-factor CCDs in spherical region

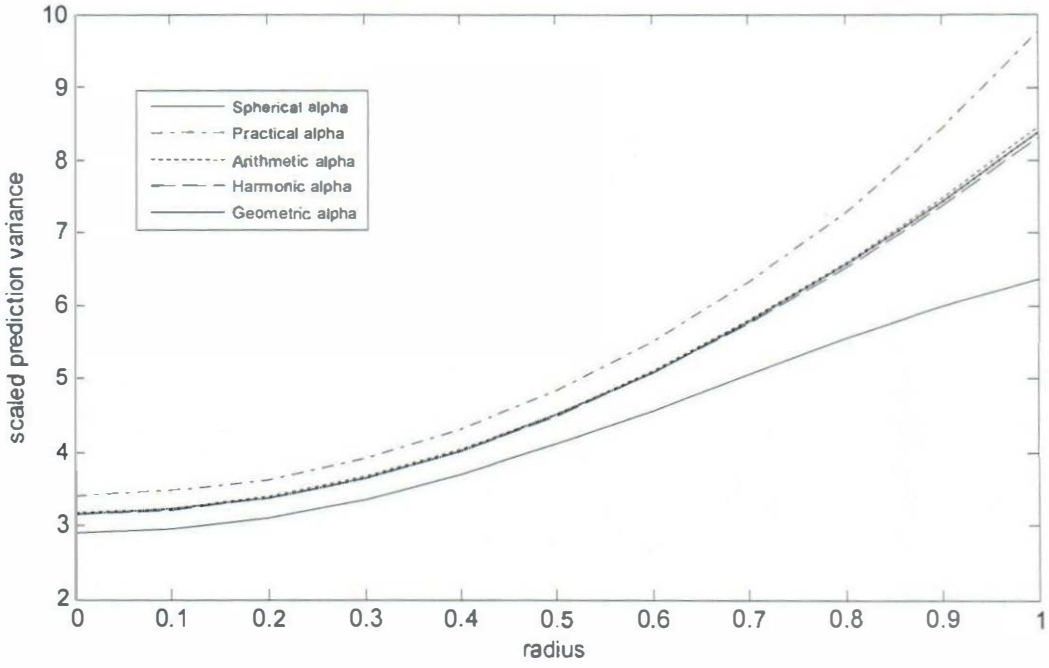

FIG. 11: VDG for the two-factor CCDs in cuboidal region

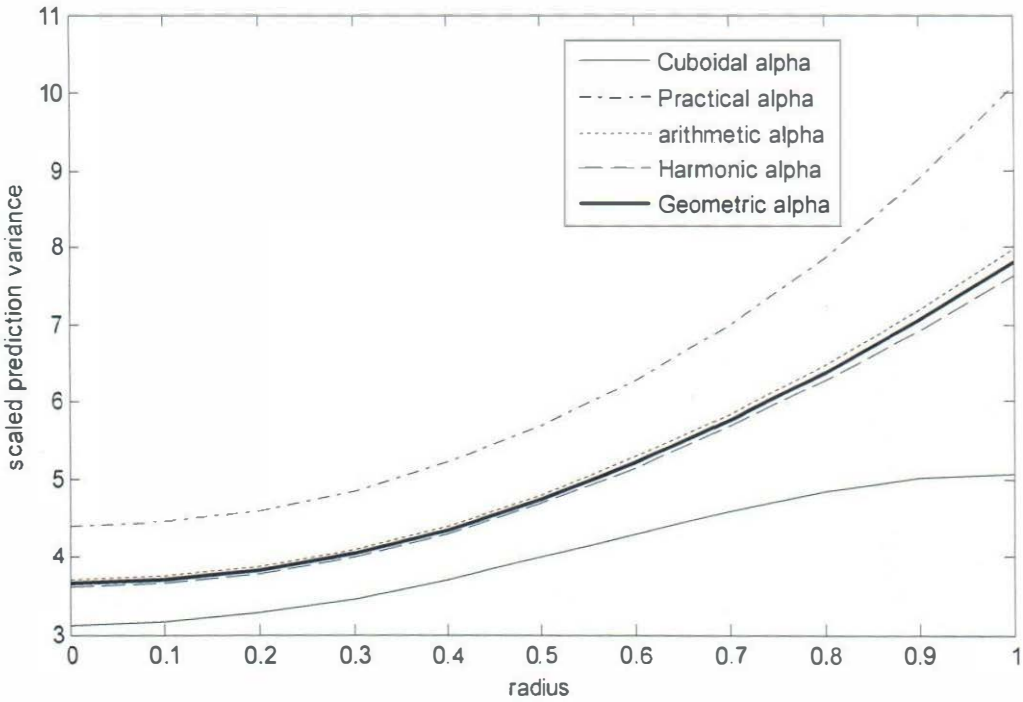

FIG. 12: VDG for the three-factor CCDs in cuboidal region

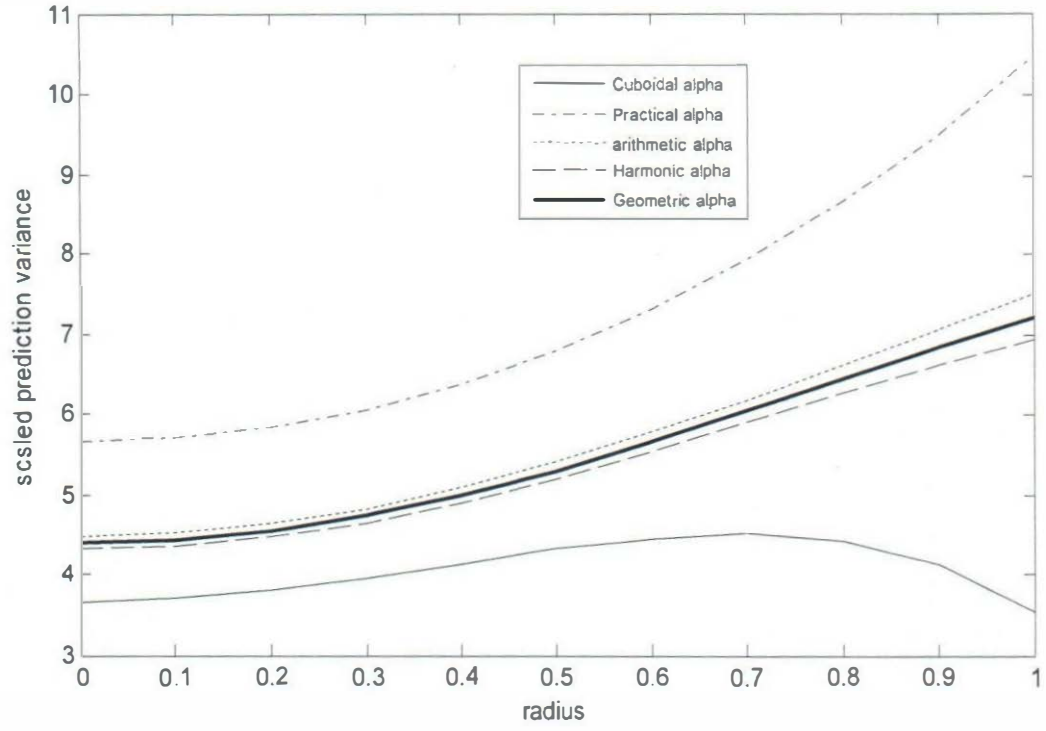

FIG. 13: VDG for the four-factor CCDs in cuboidal region

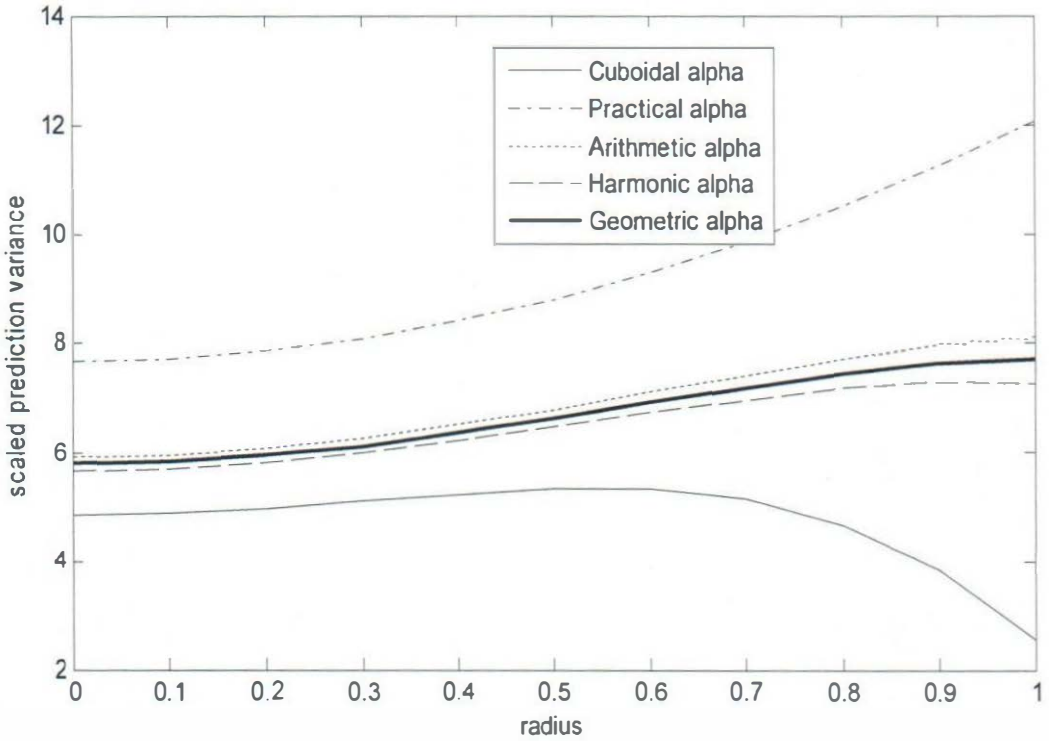

FIG. 14: VDG for the five-factor CCDs in cuboidal region

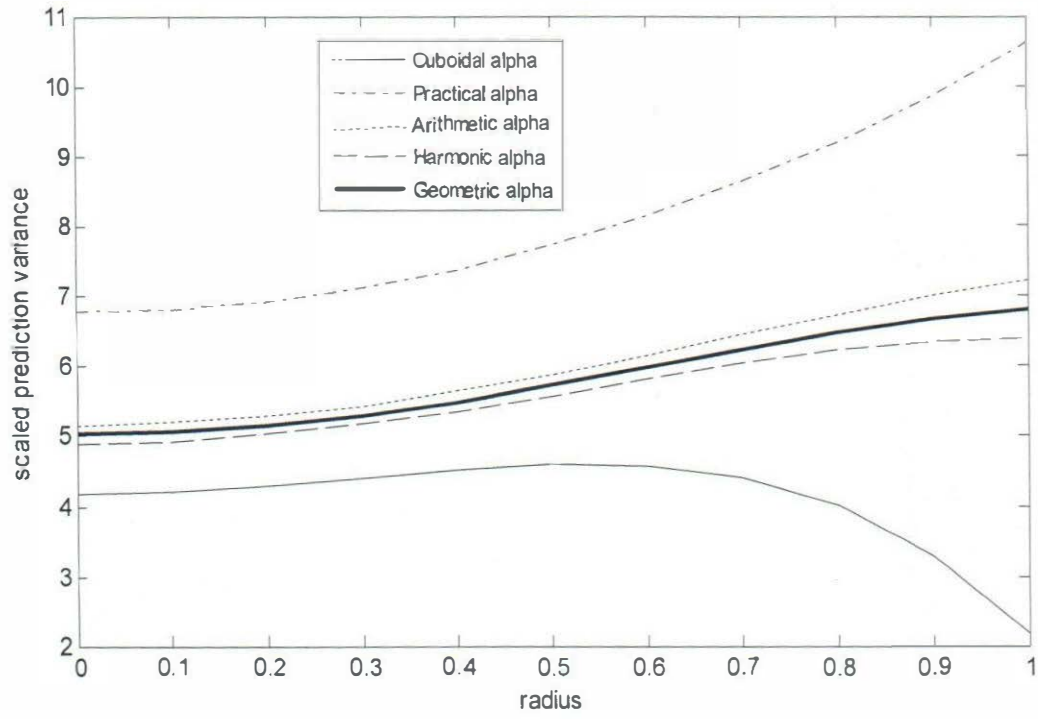

FIG.15: VDG for the six-factor CCDs in cuboidal region

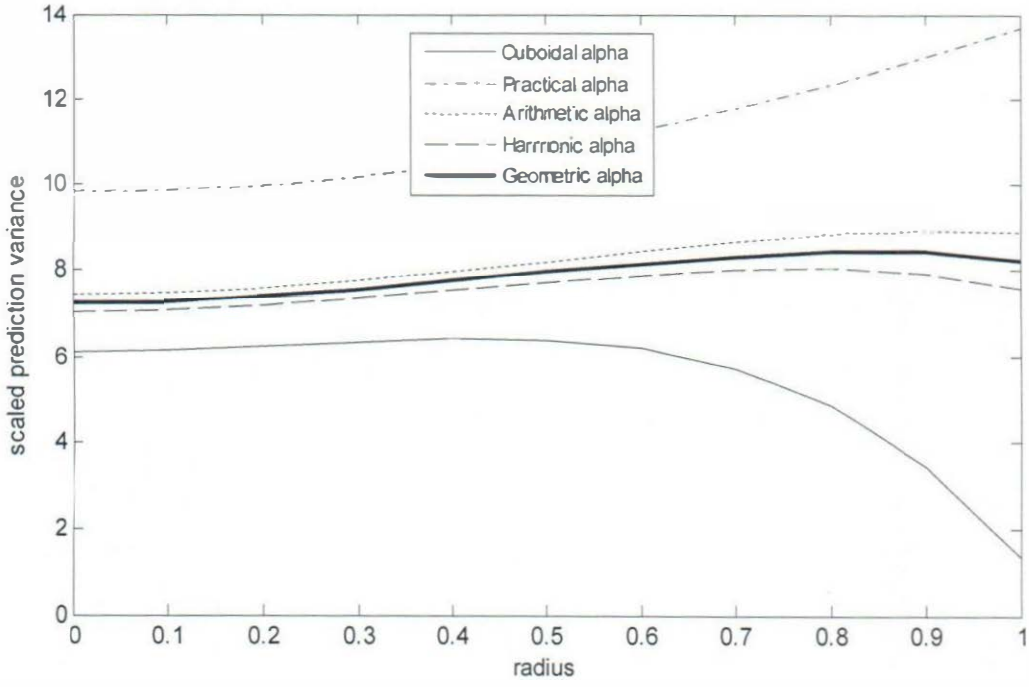

FIG. 16: VDG for the seven-factor CCDs in cuboidal region

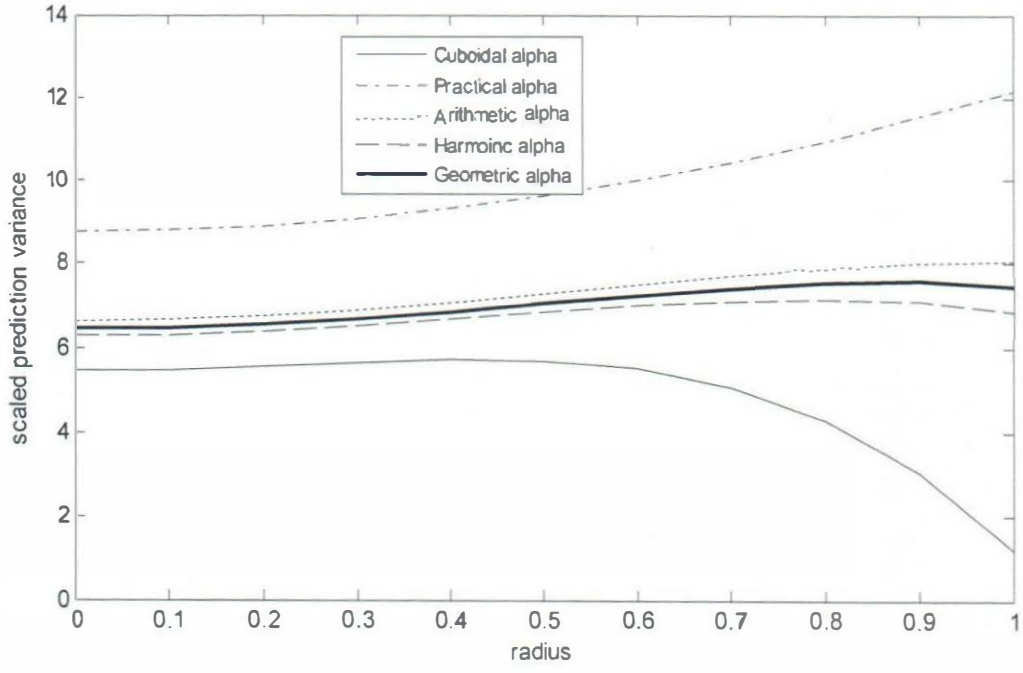

FIG. 17: VDG for the eight-factor CCDs in cuboidal region

axial distance displayed the worst prediction characteristics with the highest and unstable scaled prediction variance spread throughout the entire cuboidal design region, followed by the CCD with arithmetic axial distance. Obviously, the alternative three axial distances have shown amazing prediction potentials for predicting responses in the spherical and cuboidal regions. The three axial distances are better than the spherical axial distance in the spherical region and practical axial distance in the cuboidal region. However, none of the three axial distances is overall better than the other two alternative axial distances in both the spherical and cuboidal design regions. The arithmetic axial distance is better than the other axial distances in the spherical region, followed by the geometric and then harmonic axial distances. In the cuboidal region, the harmonic axial distance gave better prediction potential, followed by the geometric and then arithmetic axial distances. Prediction variance is very vital in the choice of design for predicting responses. Therefore, for the spherical region, the CCD with arithmetic axial distance is the ultimate choice. Considering the apparent instability displayed by the CCD with cuboidal axial distance, the CCD with harmonic axial distance could be preferred instead for predicting responses in the cuboidal region.

4.3.2 Comparison using FDSG

The prediction variance characteristics of the competing designs were also evaluated using the fraction of design space graphs. The graph displays the scaled prediction variances of multi-factor experimental design region on a two-dimensional scale. The lower to the horizontal scale and more stable the prediction variance is, the better the design for predicting responses in the design region. The graphs are displayed in Figures 18 to 24 for the designs in spherical region and Figures 25 to 31 for the designs in cuboidal region.

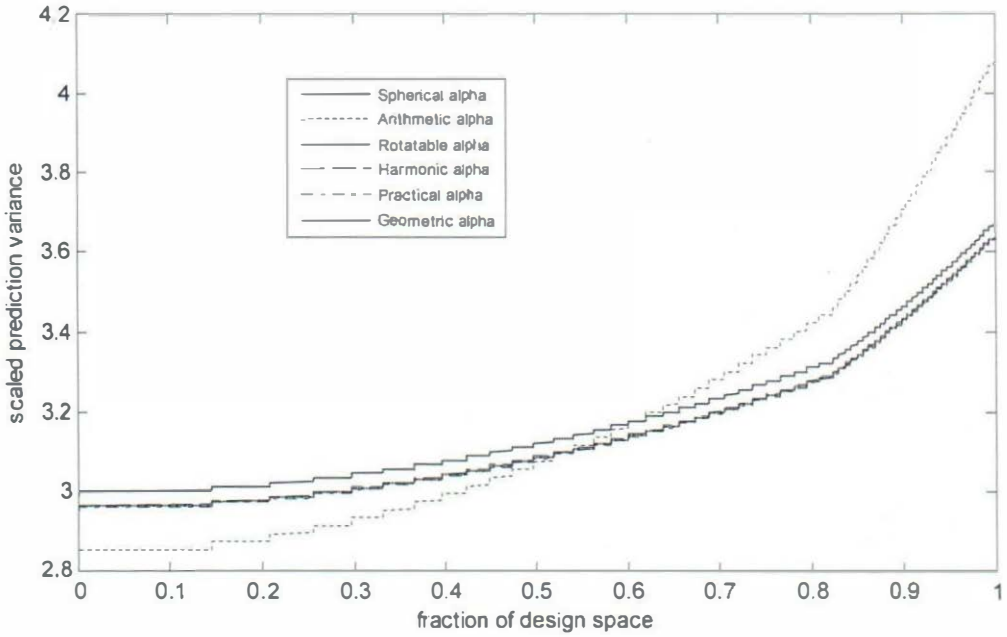

FIG. 18: FDSG for two-factor CCDs in spherical region

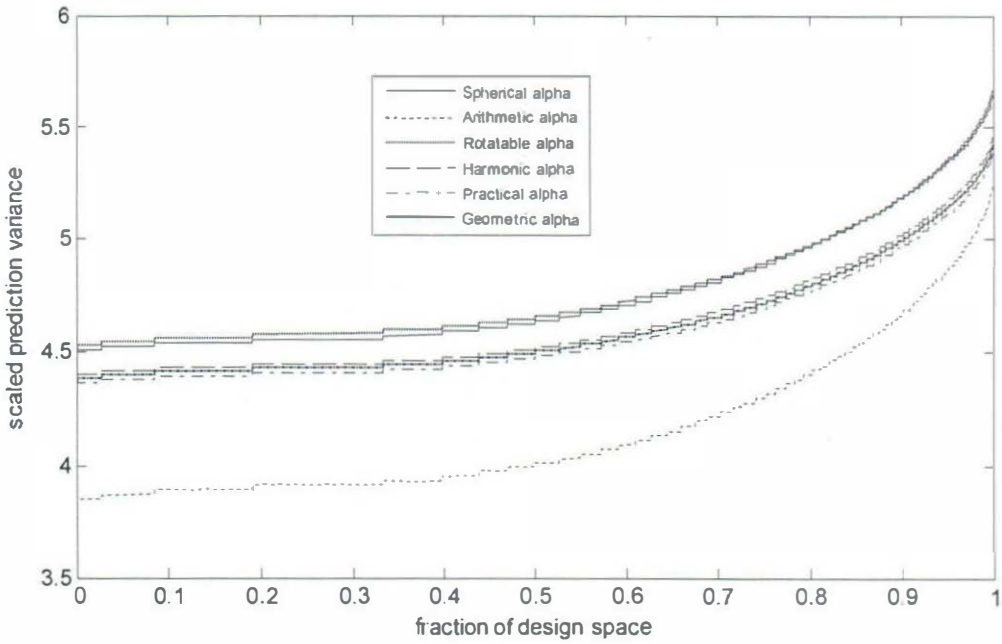

FIG. 19: FDSG for three-factor CCDs in spherical region

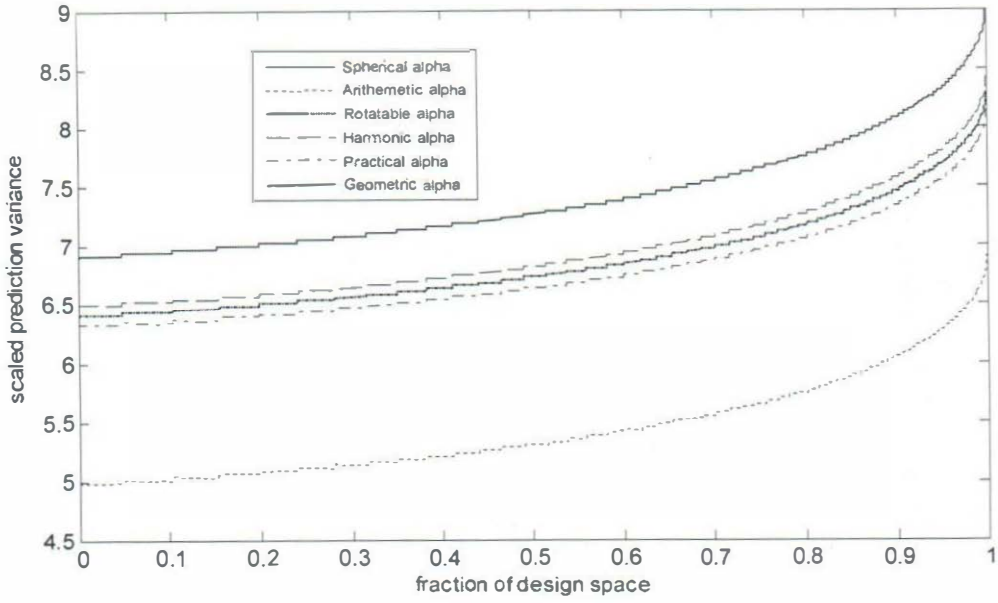

FIG. 20: FDSG for four-factor CCDs in spherical region

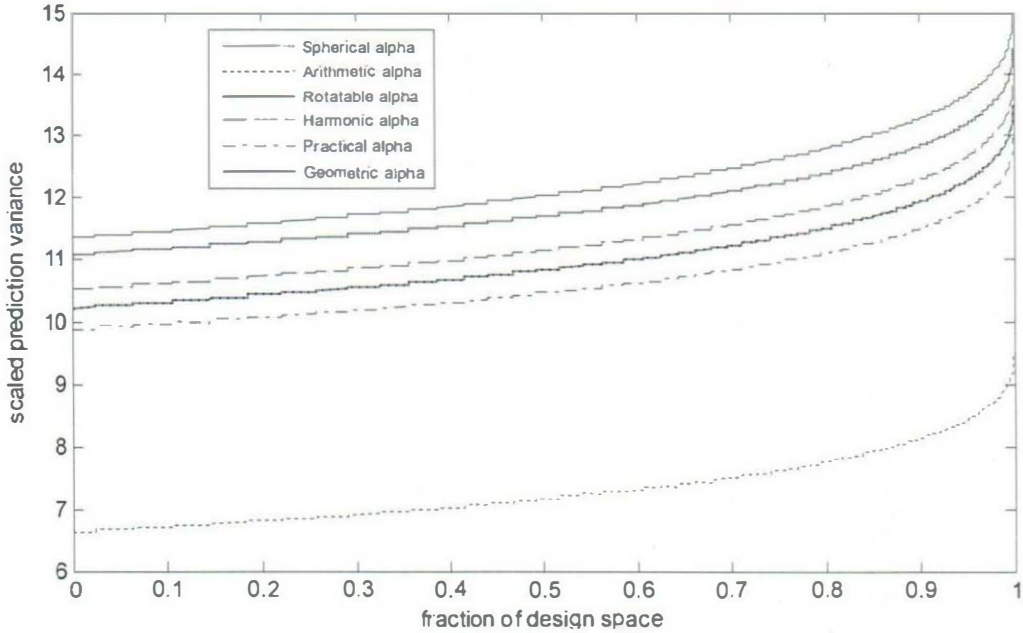

FIG. 21: FDSG for five-factor CCDs in spherical region

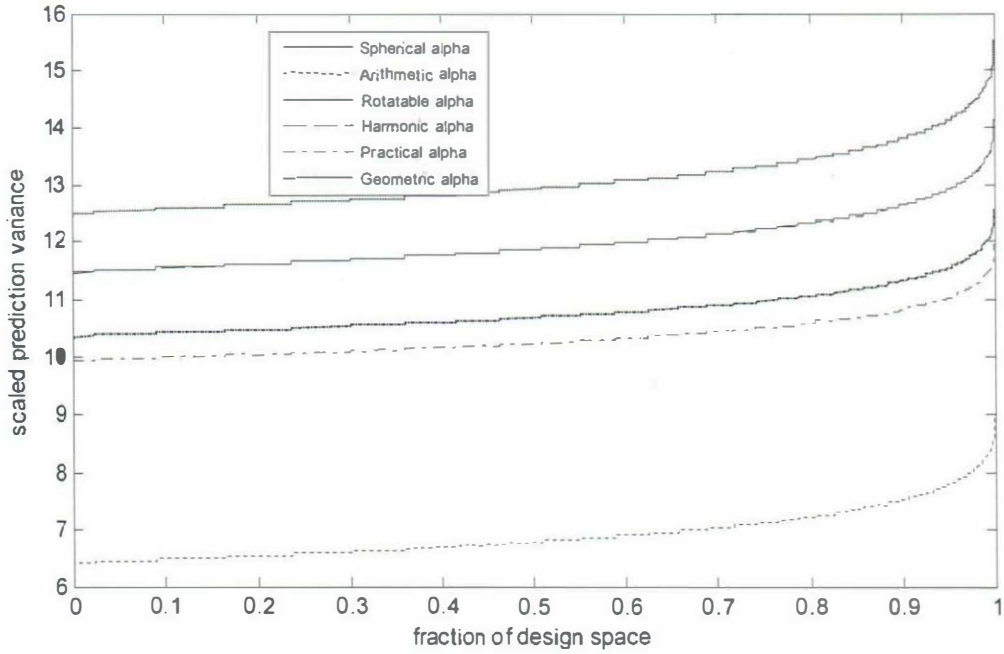

FIG. 22: FDSG for six-factor CCDs in spherical region

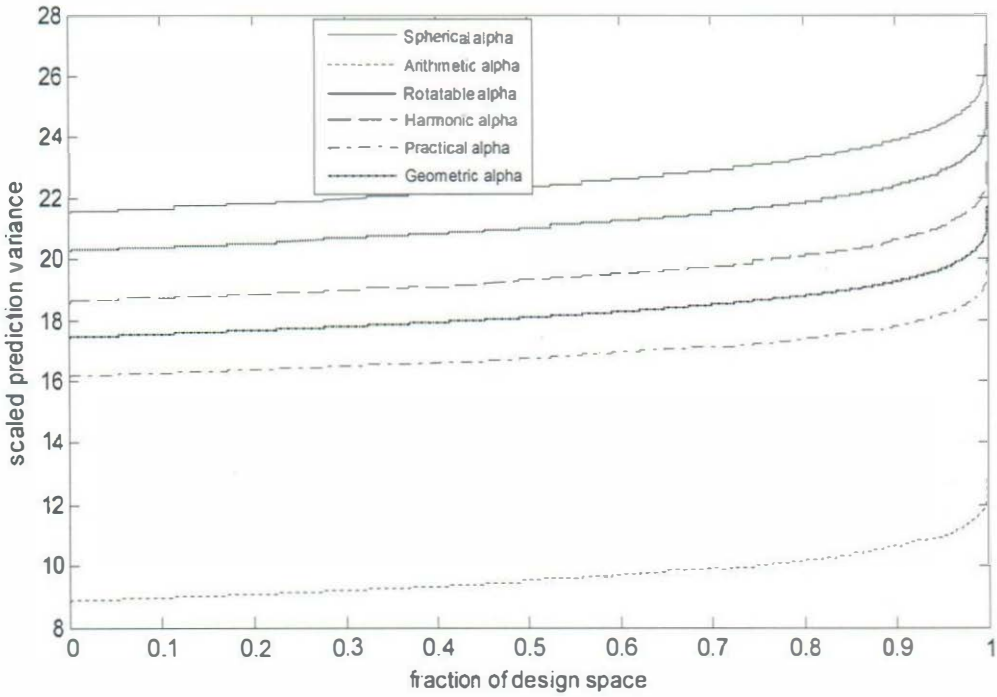

FIG. 23: FDSG for seven-factor CCDs in spherical region

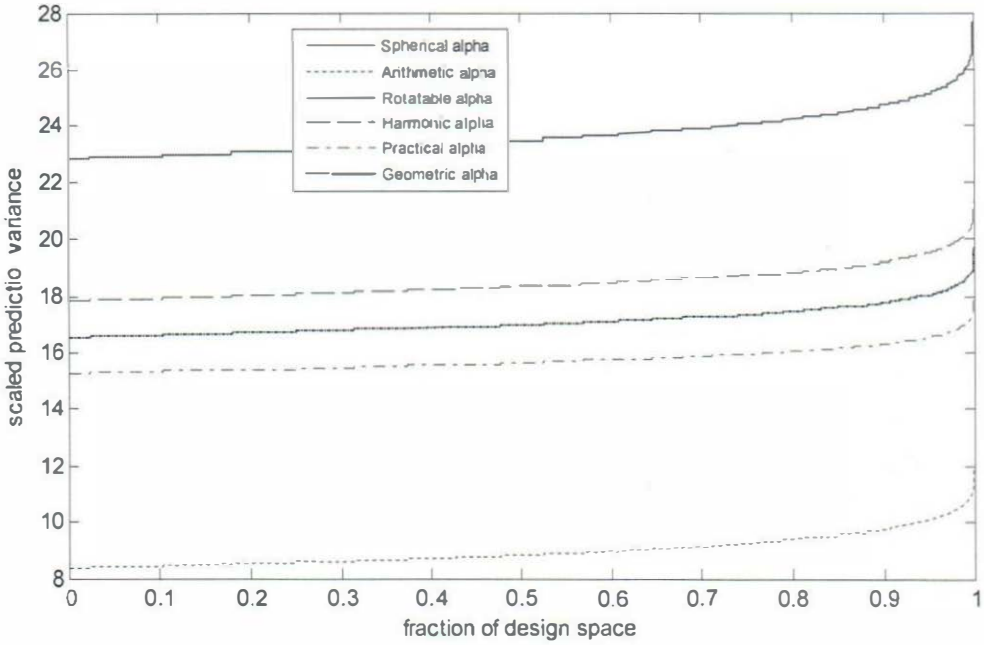

FIG. 24: FDSG for eight-factor CCDs in spherical region

The fraction of design space graphs (FDSG) in Figures 18 to 24 reveal that the CCD with arithmetic axial distance, α_{AS}, in the spherical region has the smallest and most stable scaled prediction variance throughout the entire design space for all the factors under consideration. Though for $k = 2$, the CCD with arithmetic axial distance maintained the smallest scaled prediction variance for only 50 percent of the fractions of the design space. This design deteriorates with rapid increase in scaled prediction variance which accounts for the high level of instability displayed by the design. The central composite designs with spherical axial distance, α_S, and rotatable axial distance, α_R, displayed the worst scaled prediction variance characteristics in the spherical region for all the $k = 2, 3, \ldots, 8$ factors. The central composite designs with geometric axial distance is better than the CCD with harmonic axial distance with smaller scaled prediction variance. Though both designs maintained high stability throughout the entire design space, they are only better than the spherical and rotatable CCDs. Obviously, the CCD with arithmetic axial distance would be the appropriate choice for predicting responses in the spherical region.

The cuboidal CCD with axial distance, α_C, produced the lowest scaled prediction variances for $k = 2$ and 3 factors in the cuboidal region. With higher factors, $k = 4, \ldots, 8$, the prediction variance characteristics of the cuboidal CCD deteriorates with the highest and most unstable scaled prediction variances. The CCD with practical axial distance, α_P, performed only better than the cuboidal CCD but worse than the arithmetic, harmonic and geometric CCDs. The arithmetic, harmonic and geometric CCDs produced the same small and stable scaled prediction variances for all the factors under consideration.

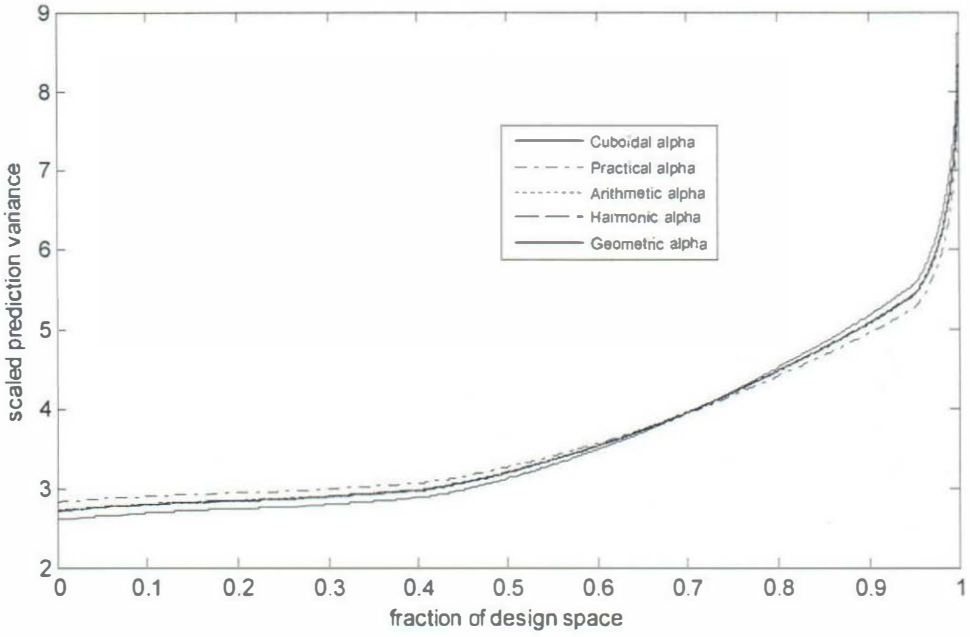

FIG. 25: FDSG for two-factor CCDs in cuboidal region

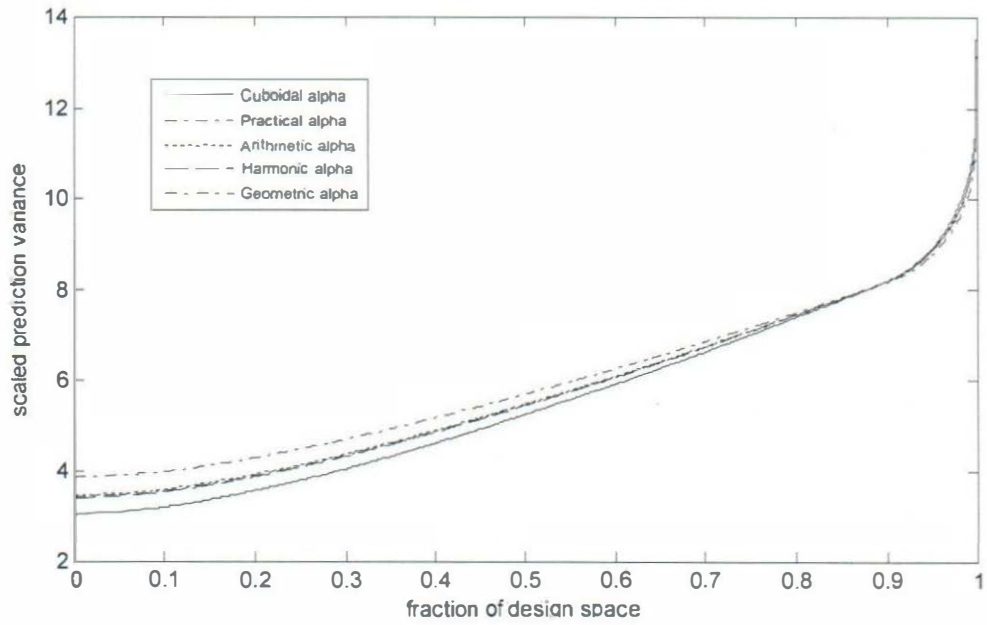

FIG. 26: FDSG for three-factor CCDs in cuboidal region

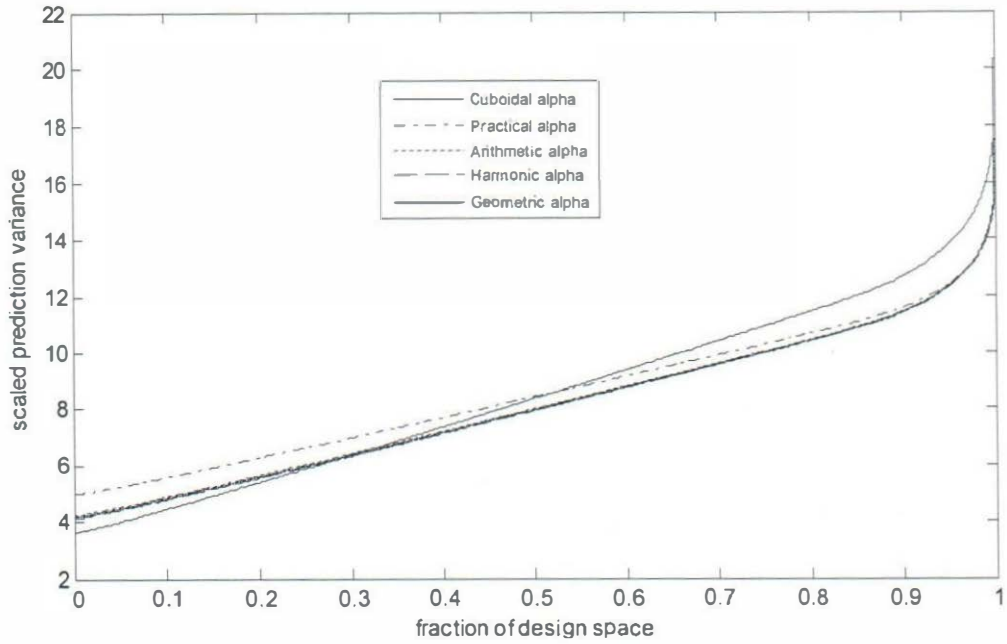

FIG. 27: FDSG for four-factor CCDs in cuboidal region

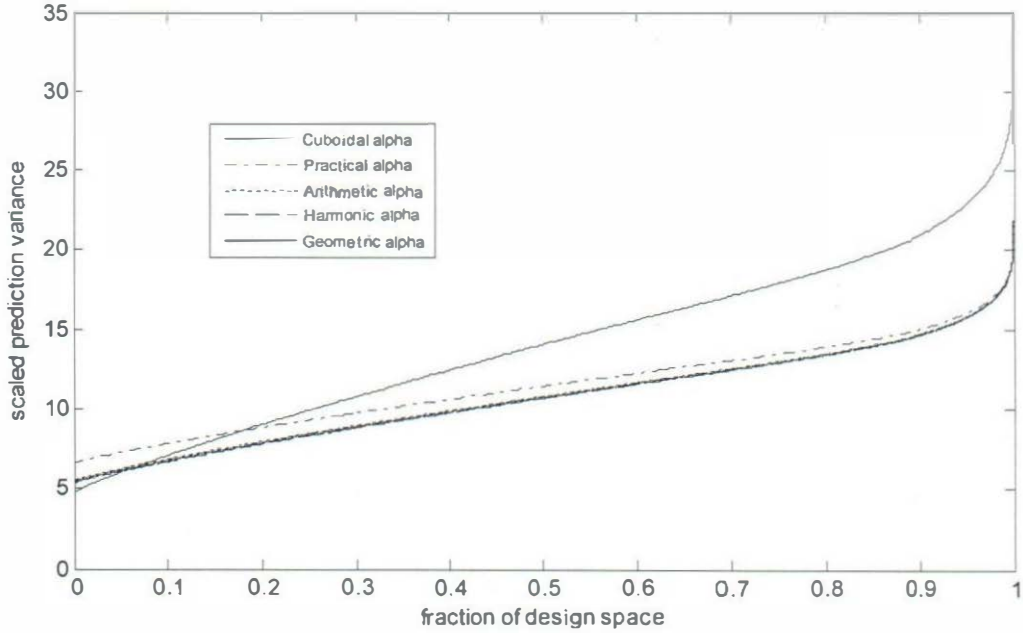

FIG. 28: FDSG for five-factor CCDs in cuboidal region

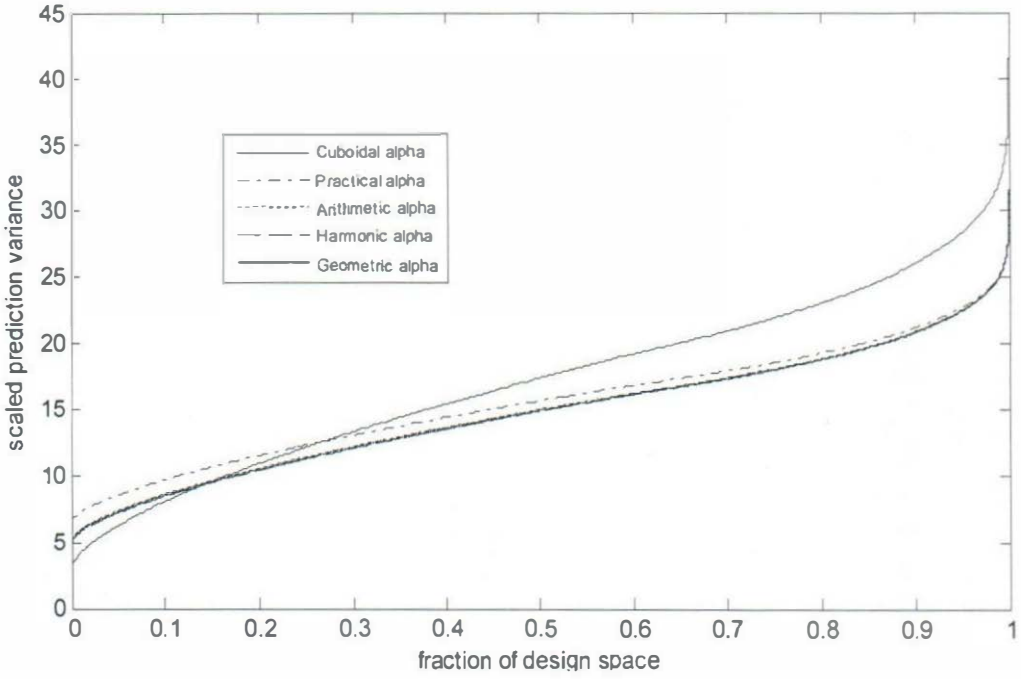

FIG. 29: FDSG for six-factor CCDs in cuboidal region

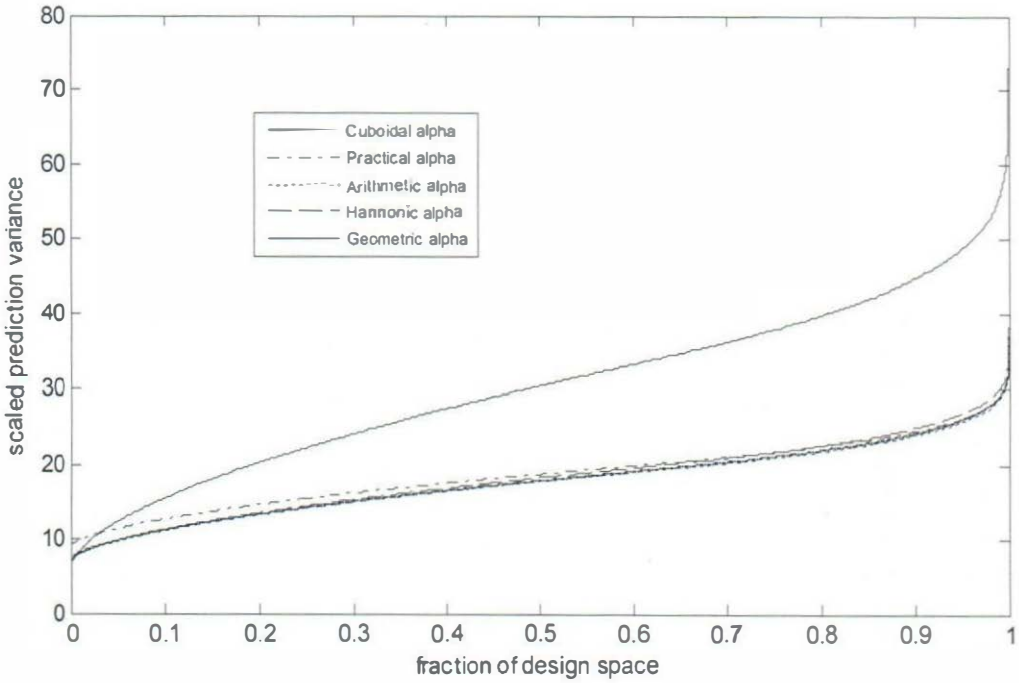

FIG. 30: FDSG for seven-factor CCDs in cuboidal region

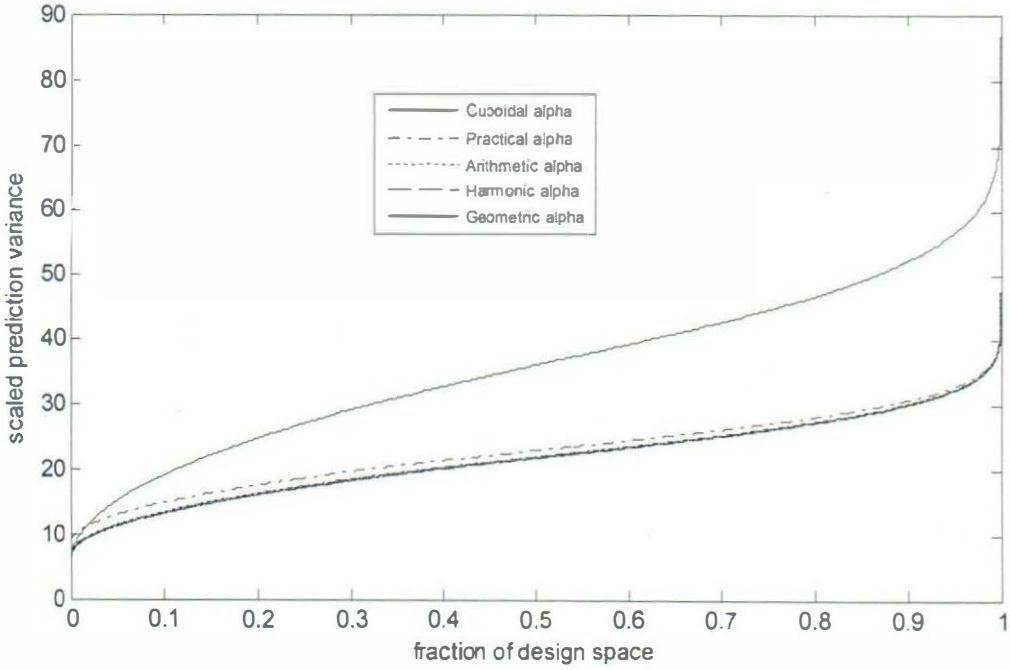

FIG. 31: FDSG for eight-factor CCDs in cuboidal region

4.4 Partial Replications of the CCDs

The concept of replication of factorial components of the designs other than the centre point of the design was first introduced by Dykstra (1959). He argued that the measure of error obtained in factorial experiments in which each factor combination is run once does not provide true estimate of the experimental error in estimating the factor effects since the measure of the experimental error is obtained from the scatter among resulting measurements from design samples. This measure of experimental error, he considered to be the same as having repeated measures on one sample. Therefore, Dykstra (1959) proposed changing the experimental conditions after each run in order to obtain real duplicates that will provide true estimate of the experimental error even though this may incur higher number of experimental runs and cost of experimentation.

The idea of replicating factorial designs was extended to the replication of the cube and star portions of the central composite designs by Dykstra (1960).He argued that replicating only at the centre could be misleading since there is no assurance that the experimental error will be constant throughout the entire design region. He pointed out that variability might increase away from the centre of the design such that the estimate of the experimental error may be too small for proper evaluation of the coefficients of the second-order models. The cube and star portions of the CCD were examined for partial replication and suggestions made on possible advantages of replicating these portions of the CCD.

Draper (1982) examined the appropriate number of centre points that offers minimum prediction variance for central composite and Box-Behnken designs. To achieve this, he considered three variations of the CCD, namely: (i) one cube plus two stars, (ii) one cube plus one star and (iii) two cubes plus one star, for k = 5, 6, 7 and 8

factors. The designs are evaluated by varying the number of centre points to know the design option that minimizes the integrated variance function proposed by Draper in the study.

Focus on improving prediction variance characteristics of the central composite design through the replication of cube and star portions of the design was recommended by Giovannitti-Jensen and Myers (1989).The variance dispersion graph developed by Giovannitti-Jensen and Myers (1989) for evaluating the prediction variances of response surface designs was extended to the central composite design with star replications by Borkowski (1995). The procedure adopted by Borkowski (1995) for the variance dispersion graph involved the development of analytical procedure as opposed to the Fortran-based programme used by Giovannitti-Jensen and Myers (1989) which becomes almost impossible to use for higher number of factors.

Borkowski (1995) approach has been adopted since its introduction as easier and more reliable approach for plotting variance dispersion graphs of the central composite designs. Chigbu et al. (2009) and Ukaegbu and Chigbu (2015a, 2015b) are some of the authors that have utilized the approach in plotting variance dispersion graphs for the evaluation of the central composite designs in both the spherical and cuboidal design regions. The same approach has been extended to the evaluation of prediction variance properties of split-plot central composite designs by Wesley et al. (2009).

Works by Chigbu and Ohaegbulem (2011) and Ukaegbu (2017) involved the evaluation and comparisons of the partially replicated variations of the central composite designs using single value criteria like the D- and G- criteria. In general, their works have shown that replicating the cube and star portions of the central

composite designs does not improve the values of the D- and G-efficiencies of the design. Therefore, in this work, attention was paid mainly on the evaluation of the prediction variance characteristics of the central composite designs using the variance dispersion graphs and fraction of design space graphs when only the star portion is replicated.

As earlier pointed out in the literature, the value of the rotatable axial distance with cube and star replications, n_1 and n_2, respectively, is $\alpha_R = \sqrt[4]{n_1 f / n_2}$. With the replication of the star only, the rotatable axial distance becomes $\alpha_R = \sqrt[4]{f / n_2}$. This axial distance, $\alpha_R = \sqrt[4]{f / n_2}$, was used to develop another set of arithmetic, harmonic and geometric axial distances that accommodate the replication of the star portions of the central composite designs (CCD). The new set of axial distances for the spherical region are presented below.

For the arithmetic axial distance,

$$\alpha_{AS} = \frac{1}{s}\left\{k^{1/2} + k^{1/4} + \left[\frac{2^{k-q}}{n_2}\right]^{1/4}\right\}, s = 3, q > 0. \qquad (16)$$

For the harmonic axial distance,

$$\alpha_{HS} = s\left\{k^{-1/2} + k^{-1/4} + \left[\frac{2^{-(k-q)/4}}{n_2^{1/4}}\right]\right\}^{-1}, \quad s = 3, q > 0. \qquad (17)$$

For the geometric axial distance,

$$\alpha_{GS} = \left\{k^{\frac{3}{4}} \times \frac{1}{n_2}\left(2^{\frac{k-q}{4}}\right)\right\}^{\frac{1}{s}}$$

$$= \left\{\frac{k^3 2^{k-q}}{n_2}\right\}^{\frac{1}{4s}}. \qquad (18)$$

The catalogue of values for the arithmetic, harmonic and geometric axial distances in the spherical region when the star point is replicated for k = 2 to 10 factors are presented in Tables 7and 8, respectively for n_2 = 2 and 3.

Catalogue of Alpha values for replicating the star portion of all CCDs twice in the Spherical Region is presented in Table 7.

Catalogue of Alpha values for replicating the star portion of all the CCDs three times in the Spherical Region is shown in table 8.

It could be observed from comparing the values in Tables 1, 7 and 8 that replicating the star portion of the central composite design reduces the rotatable, arithmetic, harmonic and geometric axial distances for the spherical region. The consequences of the reduction of the axial distances will now be measured on the prediction variance characteristics of the star-replicated central composite designs. The variance dispersion graphs and fraction of design space graphs of the star-replicated CCD are presented henceforth.

TABLE 7

Catalogue of Alpha Values for the Spherical Region with $n_2 = 2$

K	F	$2n_2k$	α_S	α_P	α_R	α_{AS}	α_{HS}	α_{GS}
2	2^2	8	1.4142	1.1892	1.1892	1.2642	1.2558	1.2599
3	2^3	12	1.7321	1.3161	1.4142	1.4874	1.4675	1.4772
4	2^4	16	2.0000	1.4142	1.6818	1.6987	1.6651	1.6818
5	2^5	20	2.2361	1.4954	2.0000	1.9105	1.8565	1.8840
6	2^6	24	2.4495	1.5651	2.3784	2.1300	2.0441	2.0891
	2^{6-1}	24	2.4495	1.5651	2.0000	2.0049	1.9390	1.9719
7	2^7	28	2.6458	1.6266	2.8284	2.3699	2.2283	2.3003
	2^{7-1}	28	2.6458	1.6266	2.3784	2.2169	2.1228	2.1712
	2^{7-2}	28	2.6458	1.6266	2.0000	2.0908	2.0097	2.0494
8	2^8	32	2.8284	1.6818	3.3636	2.6246	2.4088	2.5198
	2^{8-1}	32	2.8284	1.6818	2.8284	2.4462	2.3047	2.3784
	2^{8-2}	32	2.8284	1.6818	2.3784	2.2962	2.1920	2.2449
9	2^9	36	3.0000	1.7321	4.0000	2.9107	2.5847	2.7496
	2^{9-1}	36	3.0000	1.7321	3.3636	2.6986	2.4835	2.5951
	2^{9-2}	36	3.0000	1.7321	2.8284	2.5202	2.3730	2.4495
10	2^{10}	40	3.1623	1.7783	4.7568	3.2325	2.7553	2.9907
	2^{10-1}	40	3.1623	1.7783	4.0000	2.9802	2.6582	2.8228
	2^{10-2}	40	3.1623	1.7783	3.3636	2.7681	2.5513	2.6644
	2^{10-3}	40	3.1623	1.7783	2.8284	2.5897	2.4348	2.5149

TABLE 8

Catalogue of Alpha Values for the Spherical Region with $n_2 = 3$

K	F	$2n_2k$	α_S	α_P	α_R	α_{AS}	α_{HS}	α_{GS}
2	2^2	12	1.4142	1.1892	1.0746	1.2260	1.2104	1.2181
3	2^3	18	1.7321	1.3161	1.2779	1.4420	1.4153	1.4282
4	2^4	24	2.0000	1.4142	1.5197	1.6446	1.6085	1.6259
5	2^5	30	2.2361	1.4954	1.8072	1.8462	1.7972	1.8214
6	2^6	36	2.4495	1.5651	2.1491	2.0546	1.9835	2.0197
	2^{6-1}	36	2.4495	1.5651	1.8072	1.9406	1.8744	1.9064
7	2^7	42	2.6458	1.6266	2.5558	2.2760	2.1676	2.2239
	2^{7-1}	42	2.6458	1.6266	2.1491	2.1405	2.0575	2.0991
	2^{7-2}	42	2.6458	1.6266	1.8072	2.0265	1.9404	1.9813
8	2^8	48	2.8284	1.6818	3.0393	2.5165	2.3489	2.4361
	2^{8-1}	48	2.8284	1.6818	2.5558	2.3553	2.2398	2.2994
	2^{8-2}	48	2.8284	1.6818	2.1491	2.2198	2.1224	2.1703
9	2^9	54	3.0000	1.7321	3.6144	2.7822	2.5266	2.6581
	2^{9-1}	54	3.0000	1.7321	3.0393	2.5905	2.4199	2.5089
	2^{9-2}	54	3.0000	1.7321	2.5558	2.4293	2.3042	2.3681
10	2^{10}	60	3.1623	1.7783	4.2983	3.0796	2.6997	2.8913
	2^{10-1}	60	3.1623	1.7783	3.6144	2.8517	2.5969	2.7291
	2^{10-2}	60	3.1623	1.7783	3.0393	2.6600	2.4843	2.5759
	2^{10-3}	60	3.1623	1.7783	2.5558	2.4988	2.3625	2.4313

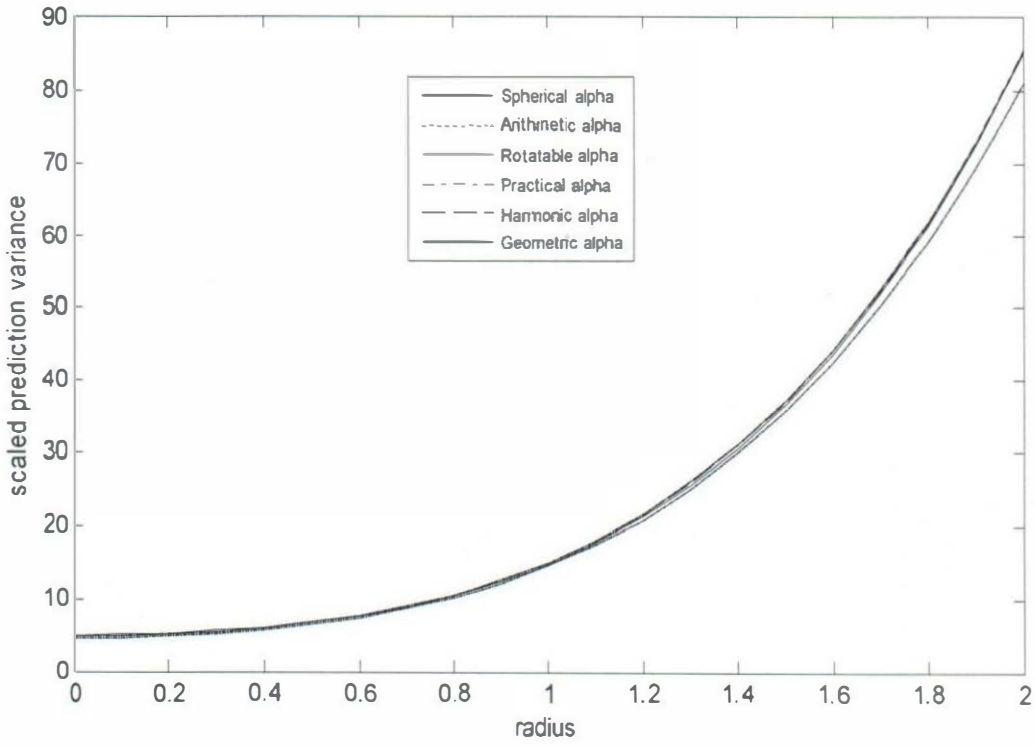

FIG. 32: VDG for two-factor star-replicated CCD with $n_2 = 2$ in spherical region

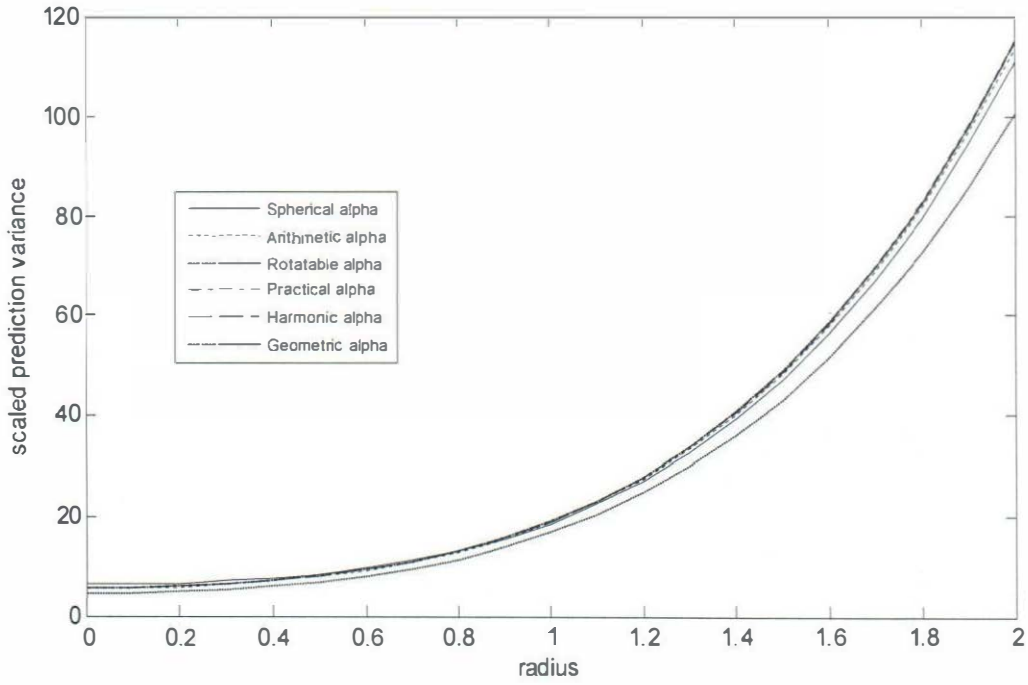

FIG. 33: VDG for two-factor star-replicated CCD with $n_2 = 3$ in spherical region

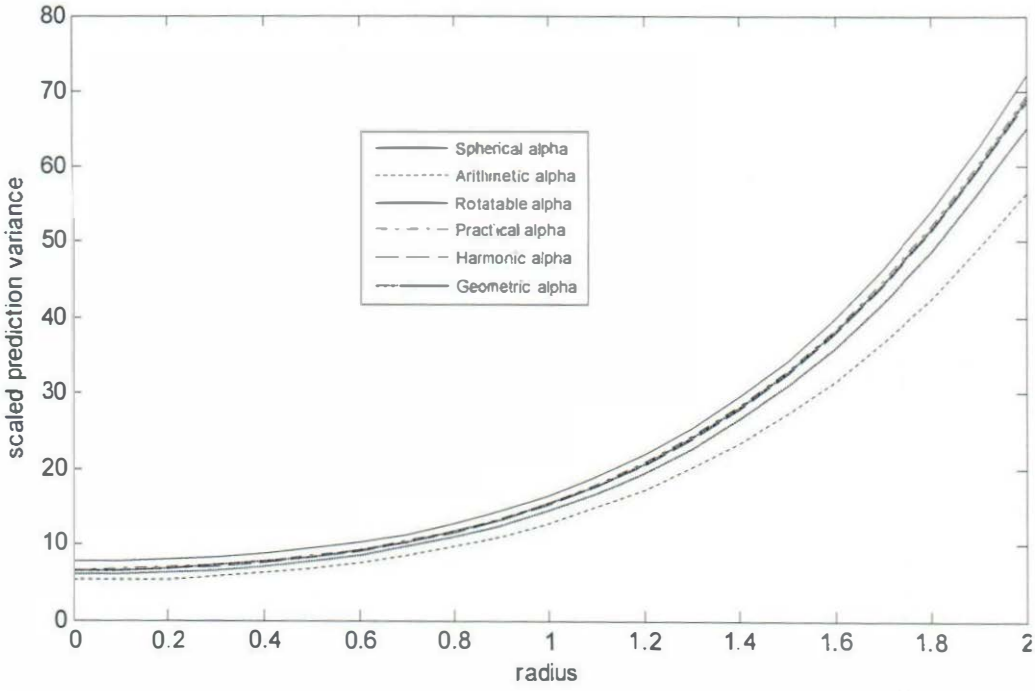

FIG. 34: VDG for three-factor star-replicated CCD with $n_2 = 2$ in spherical region

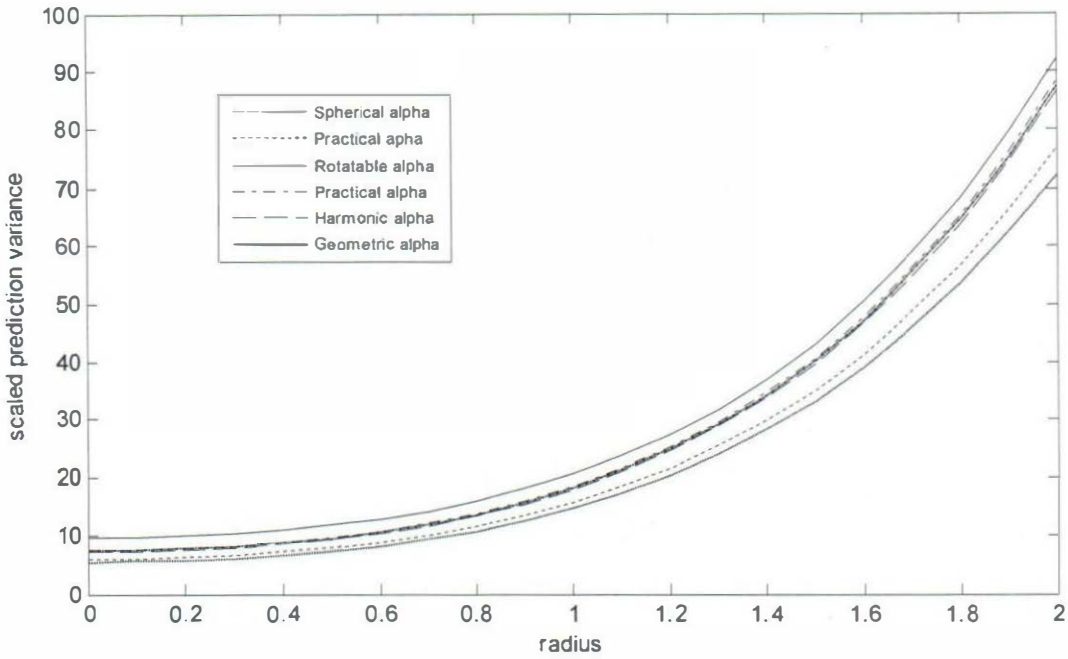

FIG. 35: VDG for three-factor star-replicated CCD with $n_2 = 3$ in spherical region

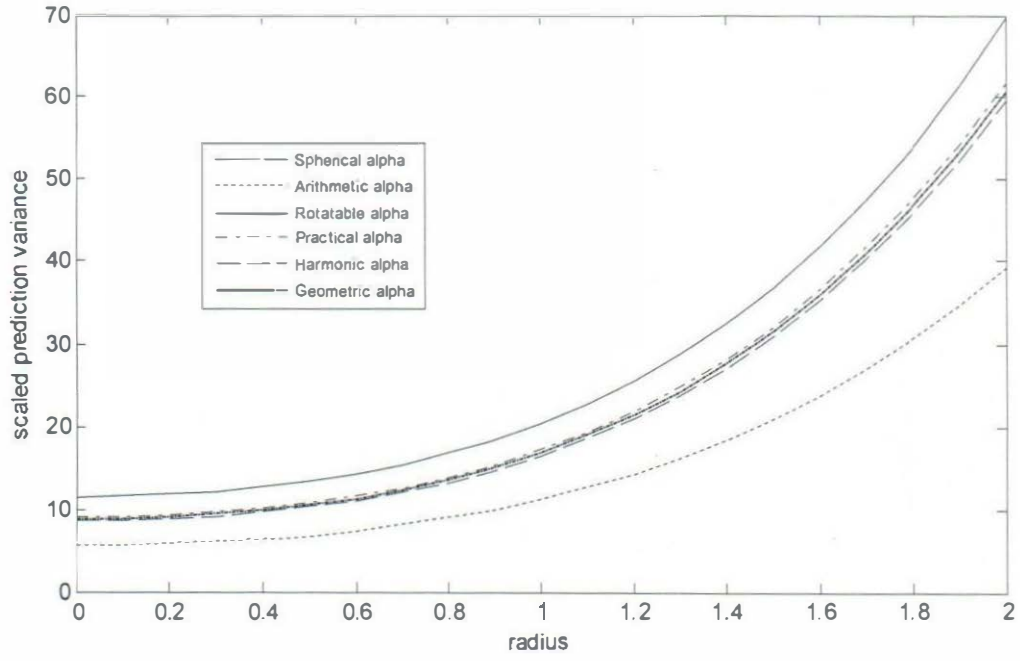

FIG. 36: VDG for four-factor star-replicated CCD with $n_2 = 2$ in spherical region

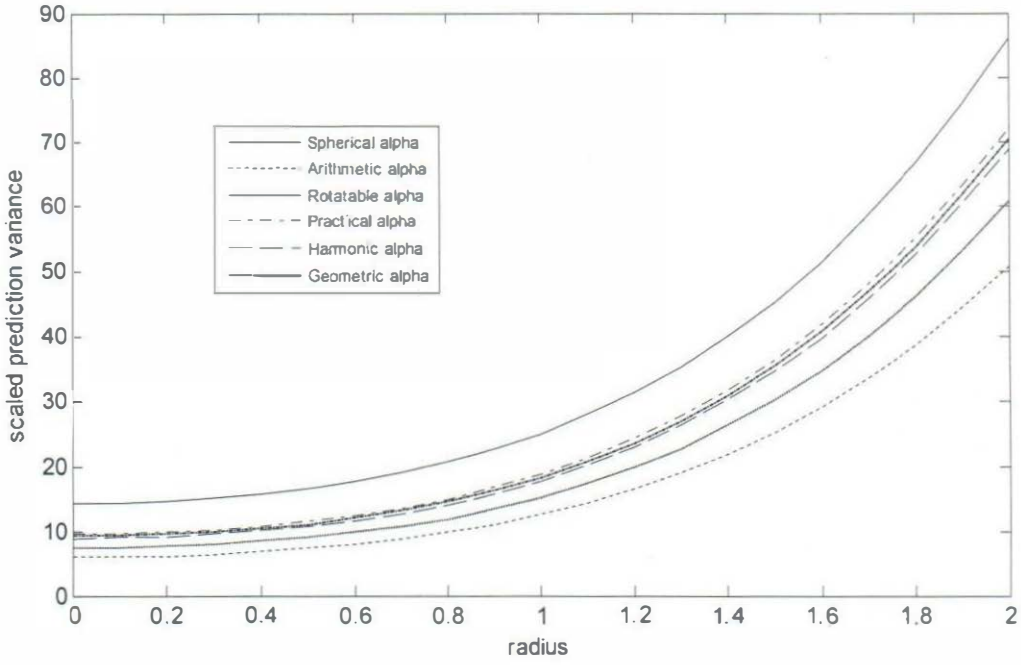

FIG. 37: VDG for four-factor star-replicated CCD with $n_2 = 3$ in spherical region

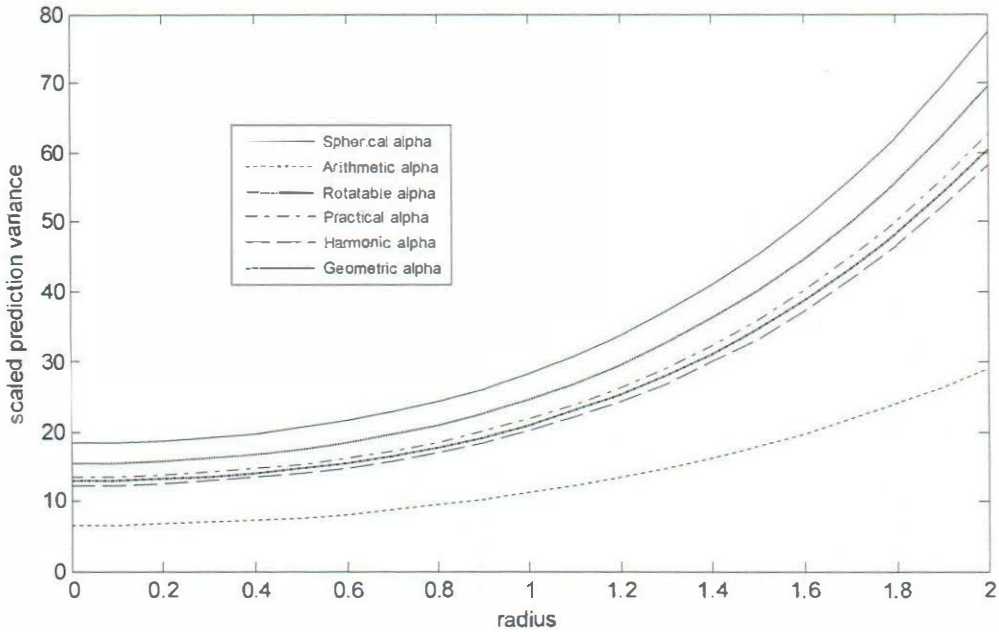

FIG. 38: VDG for five-factor star-replicated CCD with $n_2 = 2$ in spherical region

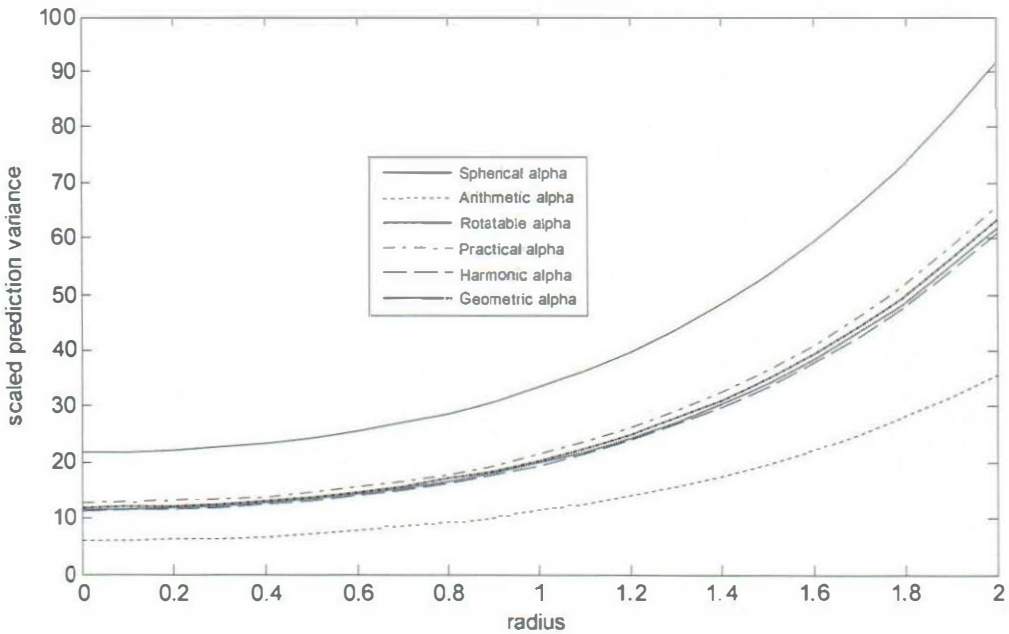

FIG. 39: VDG for five-factor star-replicated CCD with $n_2 = 3$ in spherical region

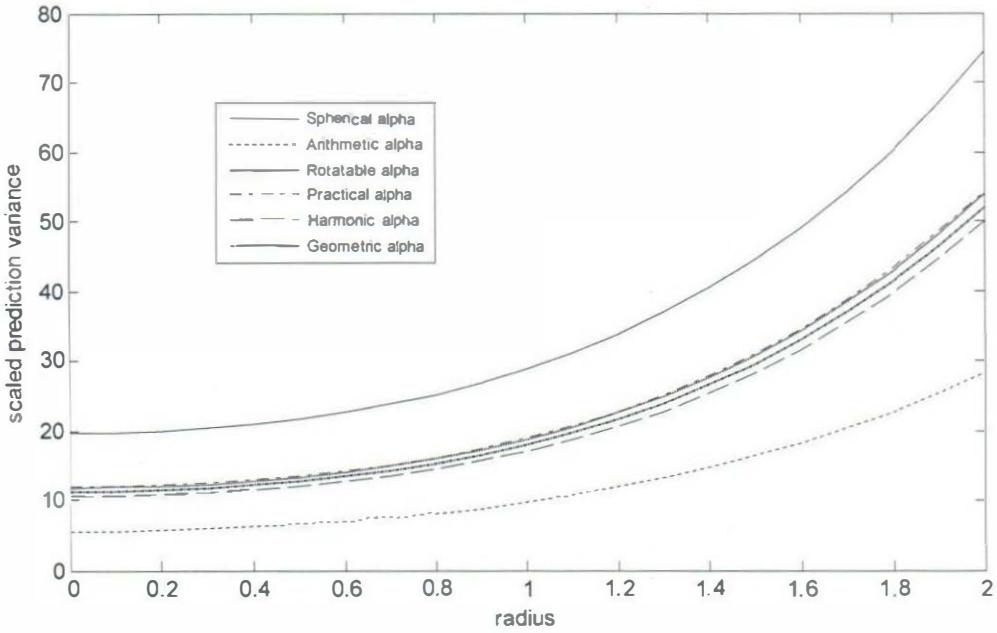

FIG. 40: VDG for six-factor star-replicated CCD with $n_2 = 2$ in spherical region

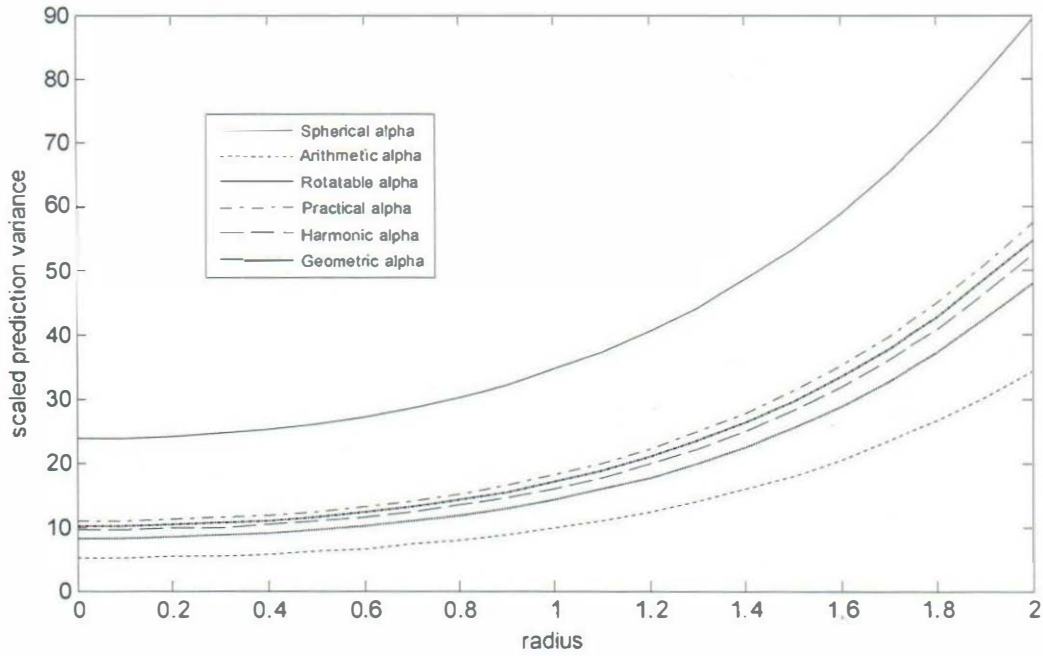

FIG. 41: VDG for six-factor star-replicated CCD with $n_2 = 3$ in spherical region

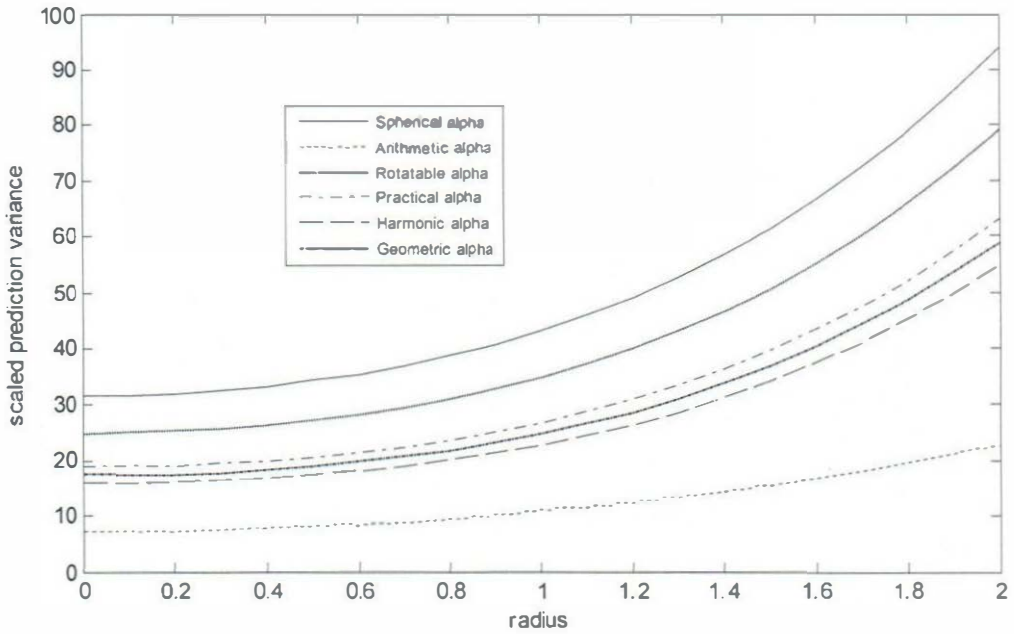

FIG. 42: VDG for seven-factor star-replicated CCD with $n_2 = 2$ in spherical region

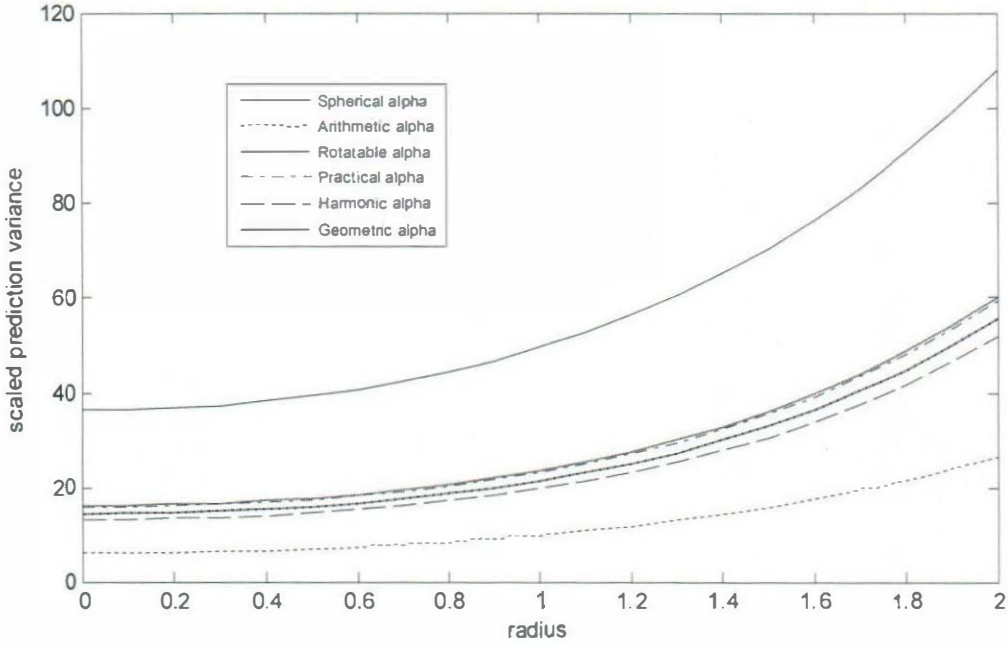

FIG. 43: VDG for seven-factor star-replicated CCD with $n_2 = 3$ in spherical region

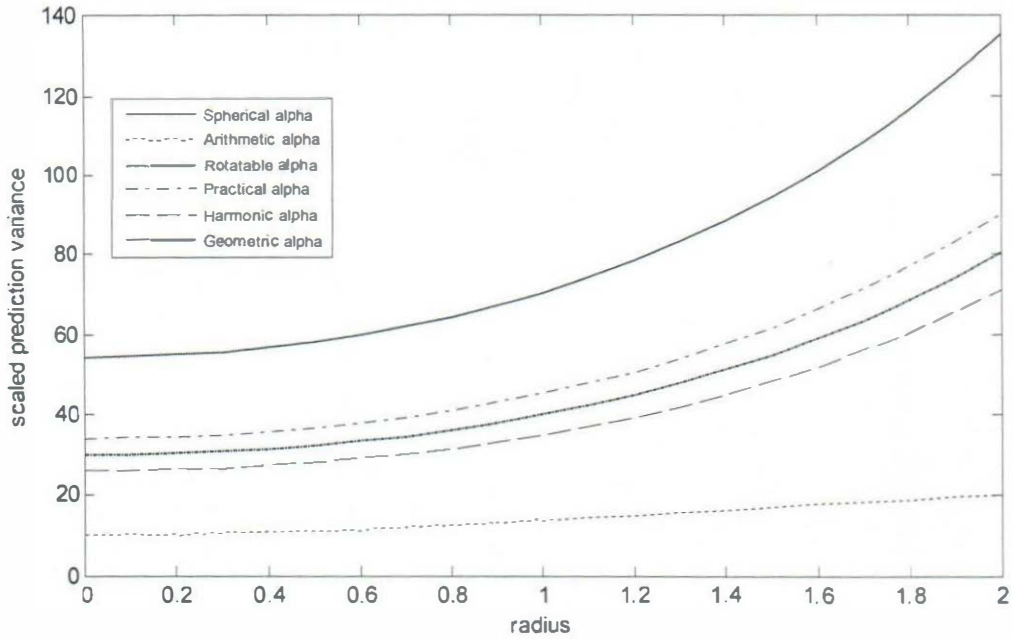

FIG. 44: VDG for eight-factor star-replicated CCD with $n_2 = 2$ in spherical region

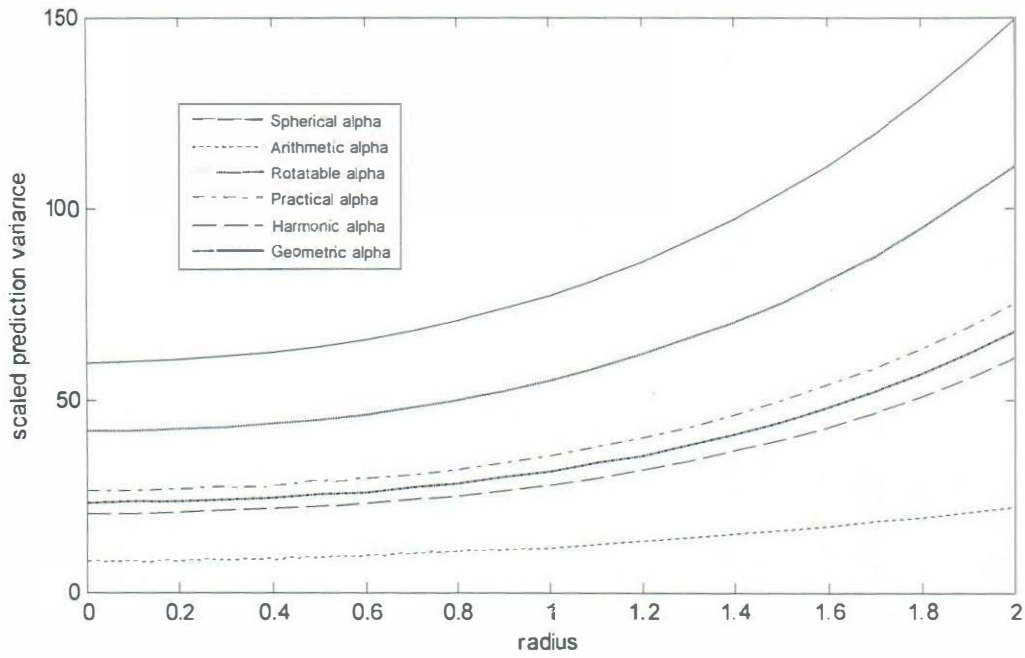

FIG. 45: VDG for eight-factor star-replicated CCD with $n_2 = 3$ in spherical region

The variance dispersion graphs (VDG) for the star-replicated central composite designs are shown in Figures 32 to 45for n_2 = 2 and 3. For k = 2 factors, all the six competing designs display very similar scaled prediction variance characteristics with almost equal scaled prediction variances and could be described to have equal prediction capabilities, especially for n_2 = 2. For n_2 = 3, the CCD with rotatable axial distance gives the lowest scaled prediction variance which is slightly different from the others. The CCD with arithmetic axial distance displayed the lowest and most stable scaled prediction variances for k = 3 to 8 factors and mostly for the n_2 = 2 and 3 replications of the star portion. This is followed by the CCD with harmonic axial distance for some factors and the CCD with rotatable axial distance for other factors. The CCD with spherical axial distance displayed the worst scaled prediction variance distribution with the highest scaled prediction variance values for all the factors and for n_2 = 2 and 3 replications of the star portion. This is followed by the CCD with practical axial distance.

Should the experimenter decide to harness the advantages of replicating the star portion of the CCD in predicting responses in the spherical region, the CCD with arithmetic axial distance should be the ideal choice. The fact that these competing designs have equal number of experimental runs and centre points shows that the best design in terms of small and stable scaled prediction variance has no undue advantage over the other designs. The fraction of design space graphs of Figures 46 to 59show that the CCD with arithmetic axial distance gives the smallest scaled prediction variances throughout the spherical region for $n_2 = 2$ and 3 replications of the star portion and for the k = 2, 3, . . ., 8 experimental factors under consideration.

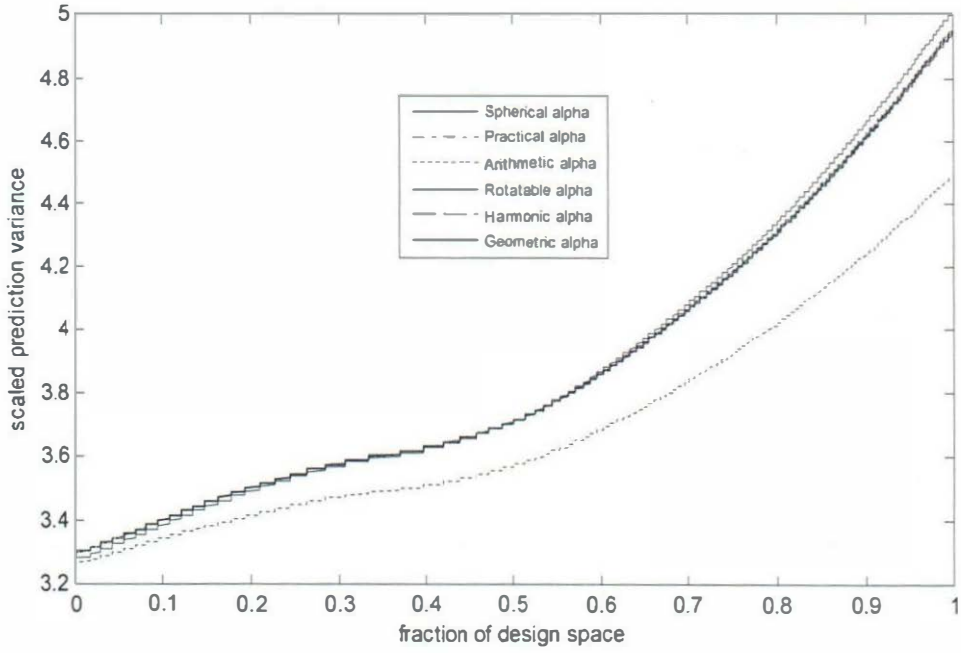

FIG. 46: FDSG for two-factor star-replicated CCD with $n_2 = 2$ in spherical region

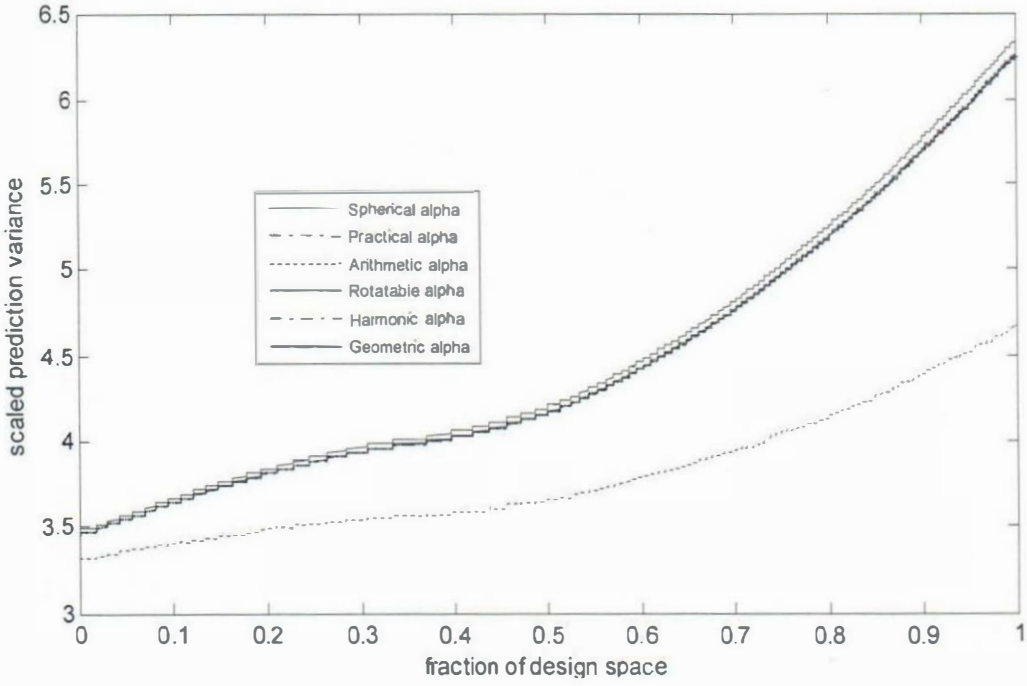

FIG. 47: FDSG for two-factor star-replicated CCD with $n_2 = 3$ in spherical region

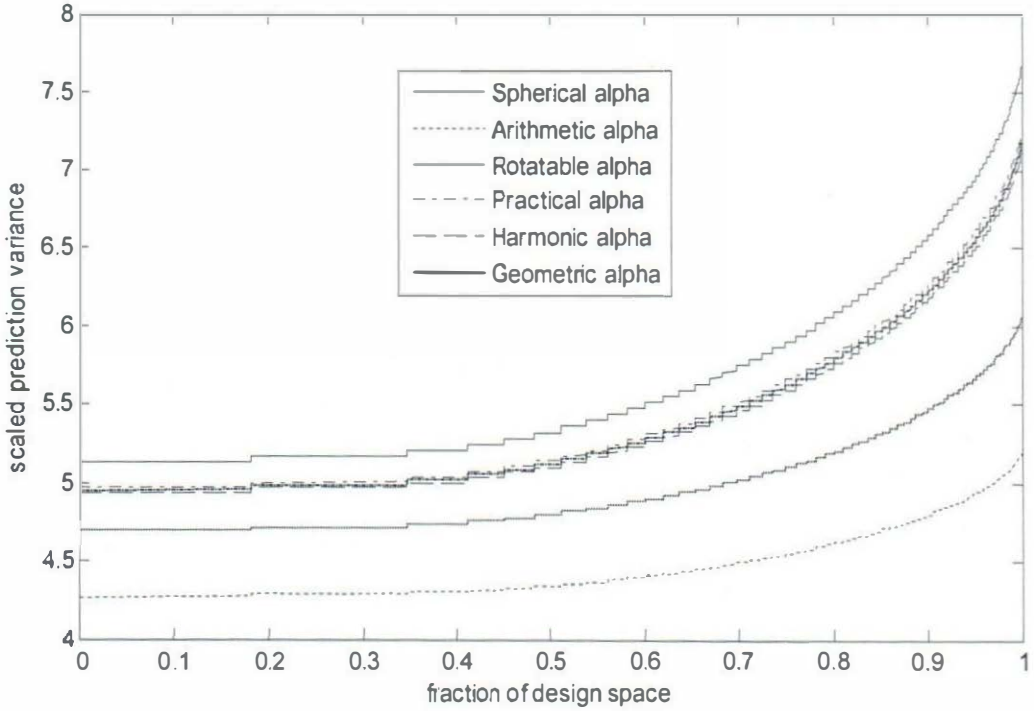

FIG. 48: FDSG for three-factor star-replicated CCD with $n_2 = 2$ in spherical region

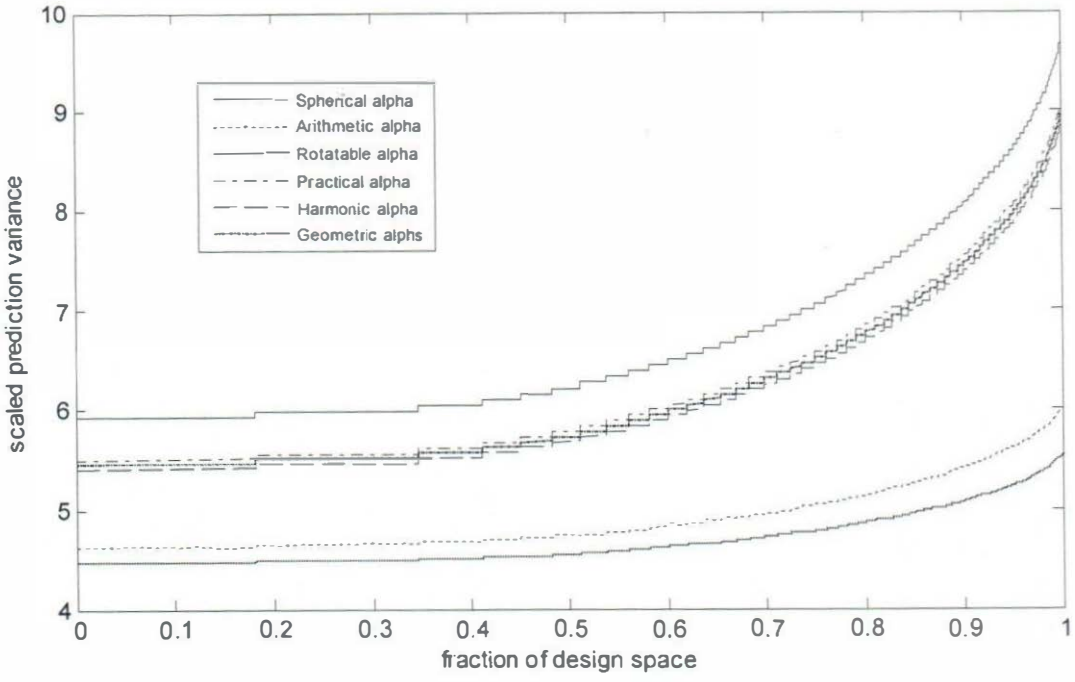

FIG. 49: FDSG for three-factor star-replicated CCD with $n_2 = 3$ in spherical region

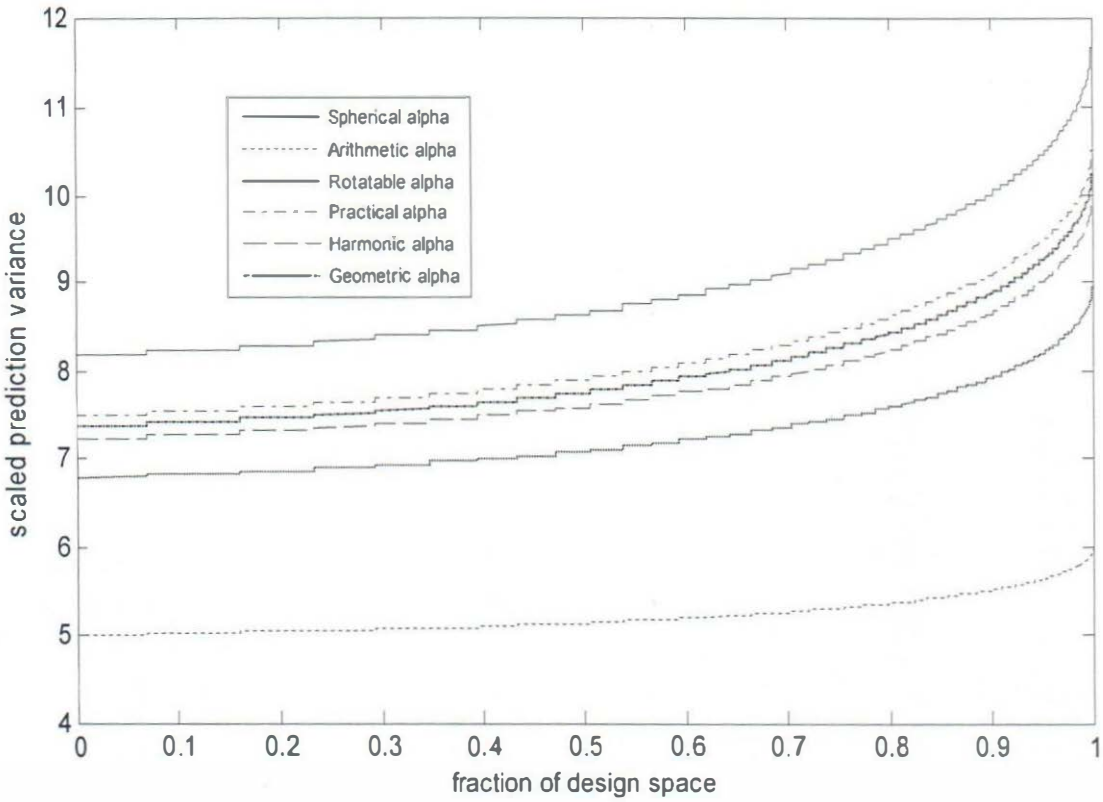

FIG. 50: FDSG for four-factor star-replicated CCD with $n_2 = 2$ in spherical region

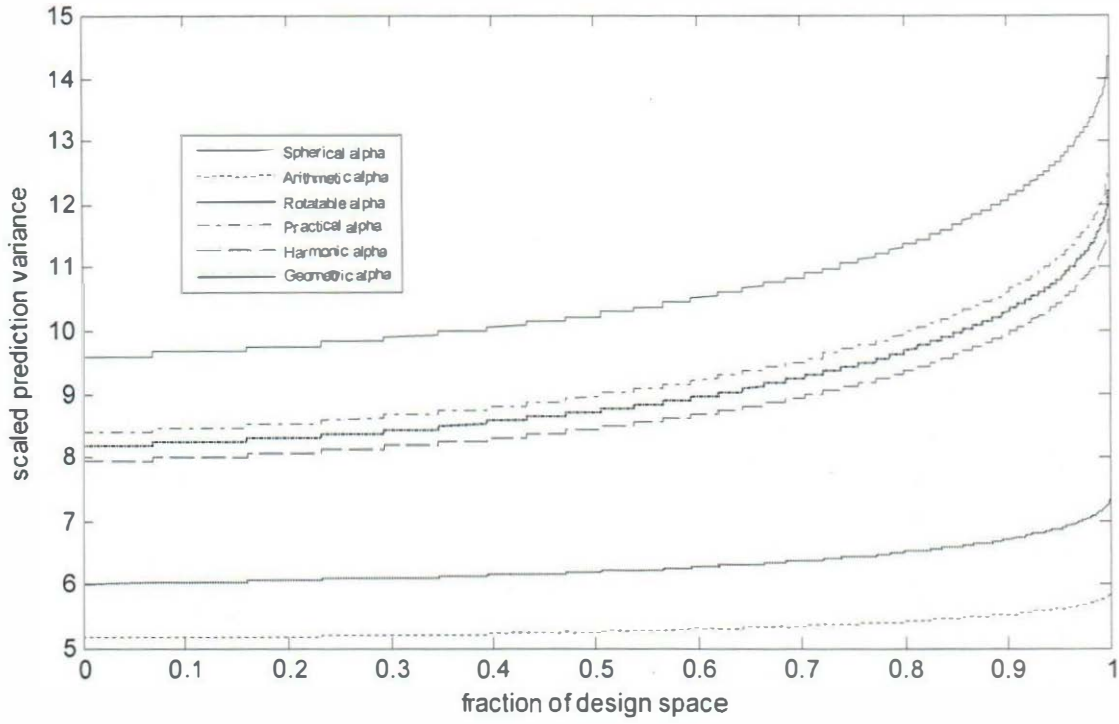

FIG. 51: FDSG for Four-factor star-replicated CCD with $n_2 = 3$ in spherical region

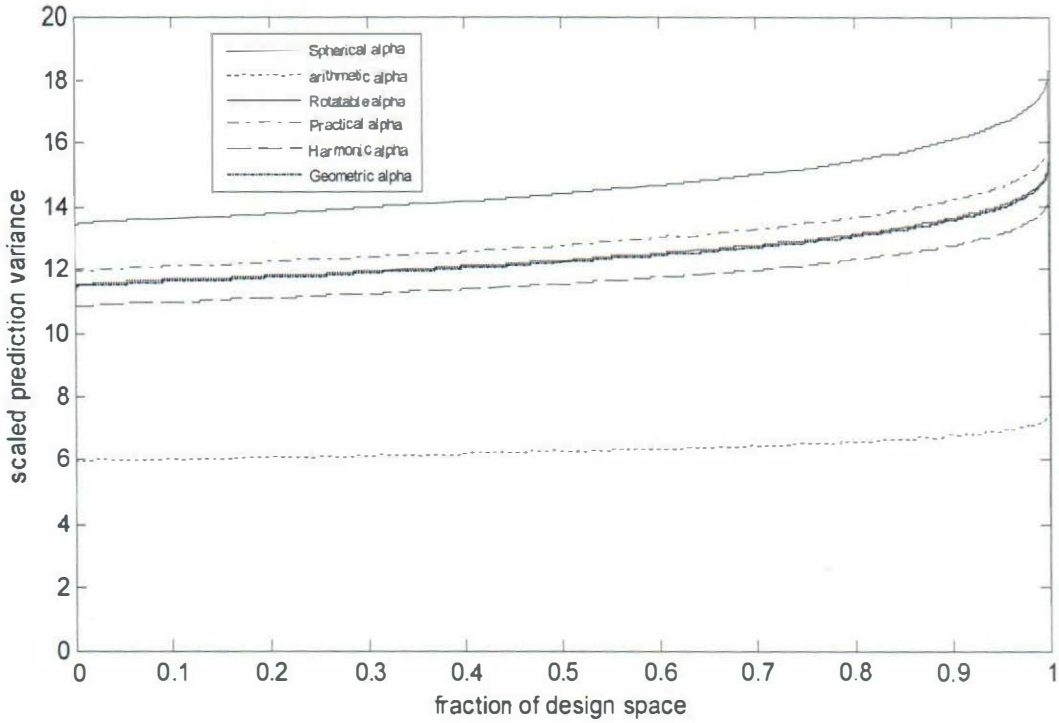

FIG. 52: FDSG for five-factor star-replicated CCD with $n_2 = 2$ in spherical region

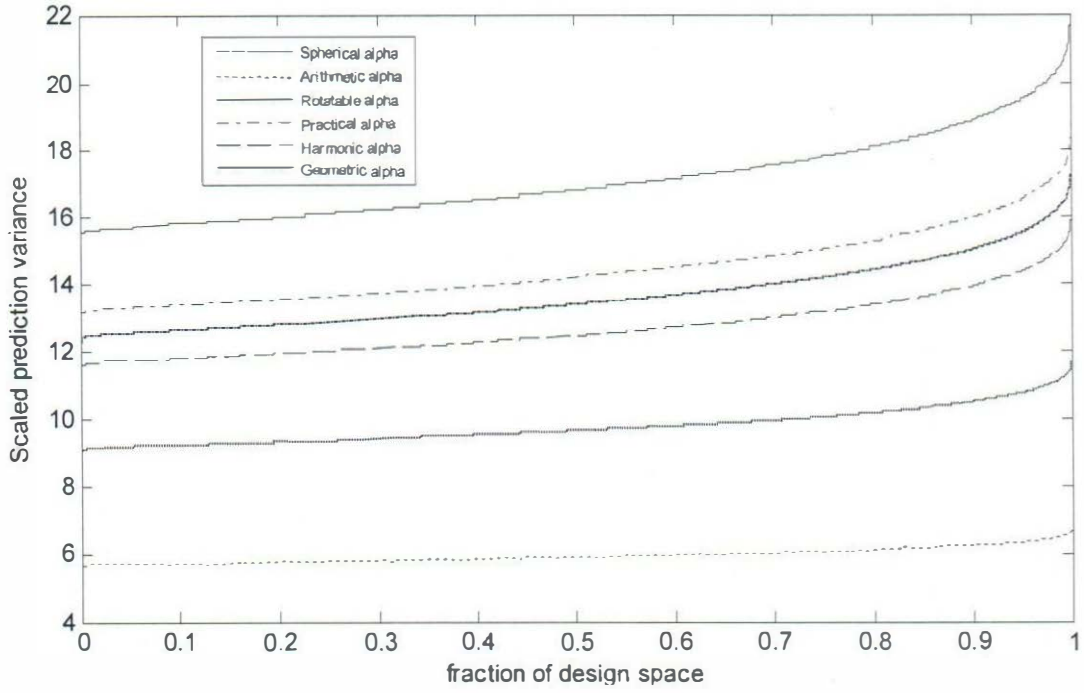

FIG. 53: FDSG for five-factor star-replicated CCD with $n_2 = 3$ in spherical region

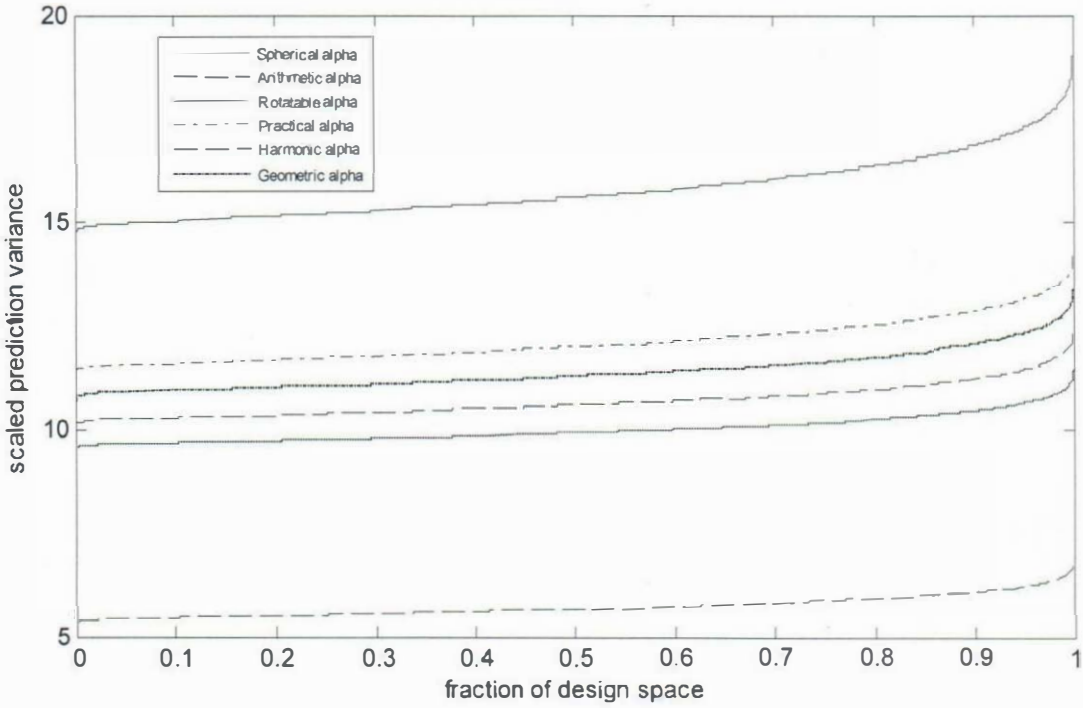

FIG. 54: FDSG for six-factor star-replicated CCD with $n_2 = 2$ in spherical region

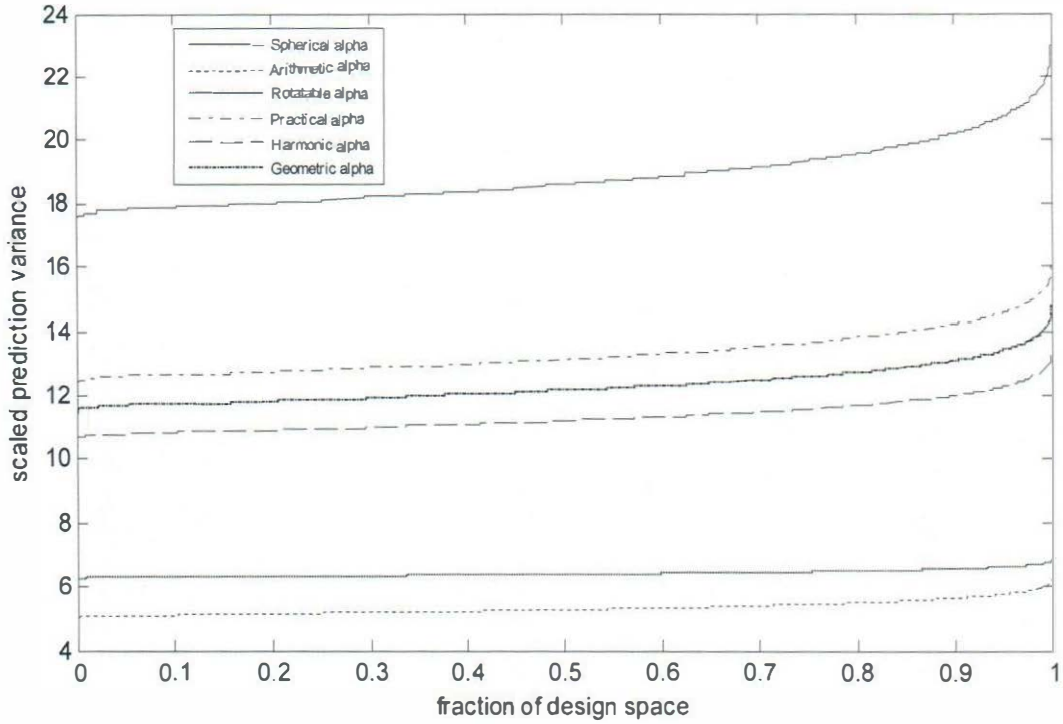

FIG. 55: FDSG for six-factor star-replicated CCD with $n_2 = 3$ in spherical region

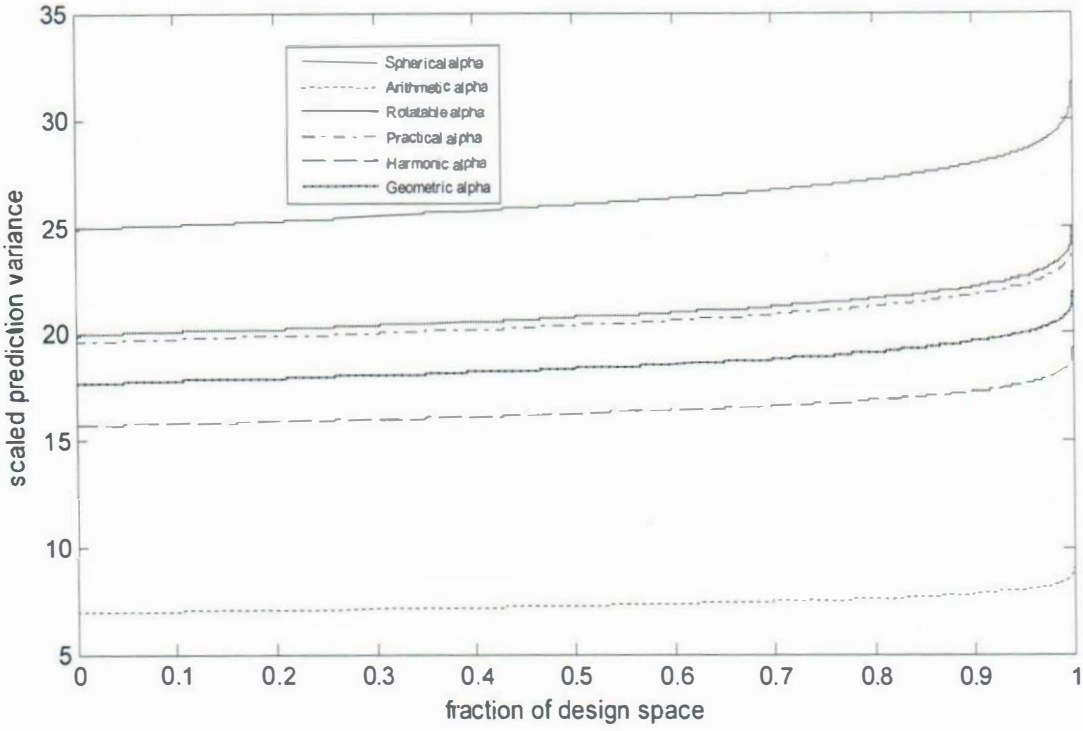

FIG. 56: FDSG for seven-factor star-replicated CCD with $n_2 = 2$ in spherical region

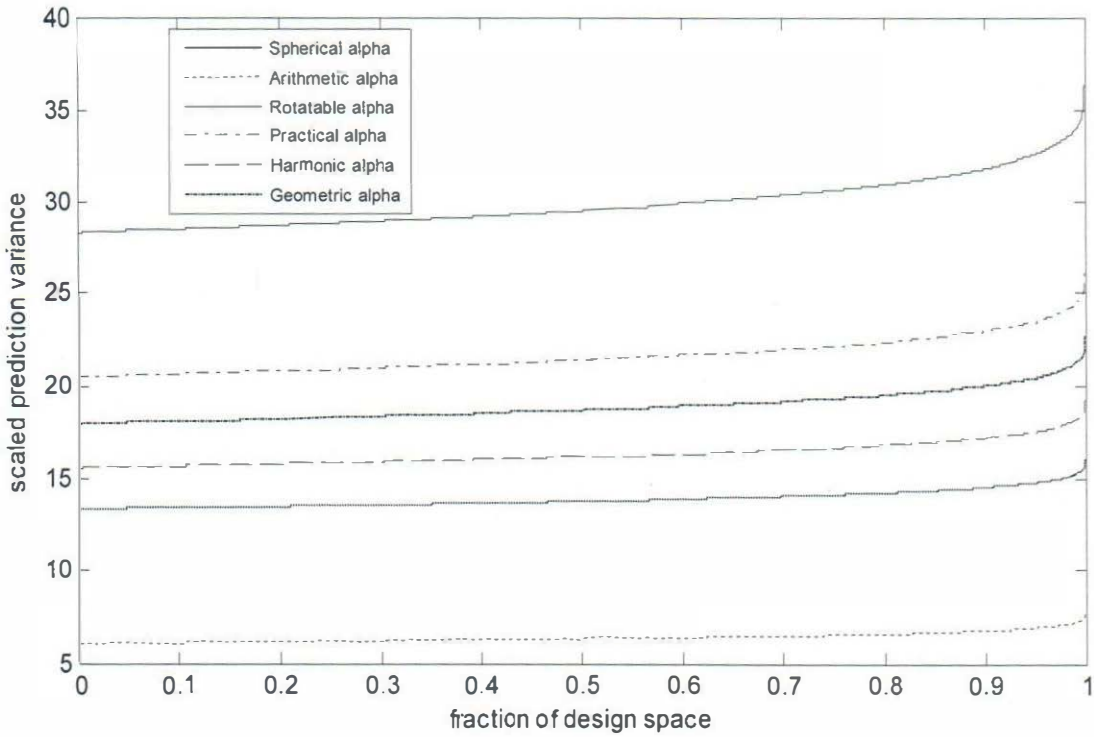

FIG. 57: FDSG for seven-factor star-replicated CCD with $n_2 = 3$ in spherical region

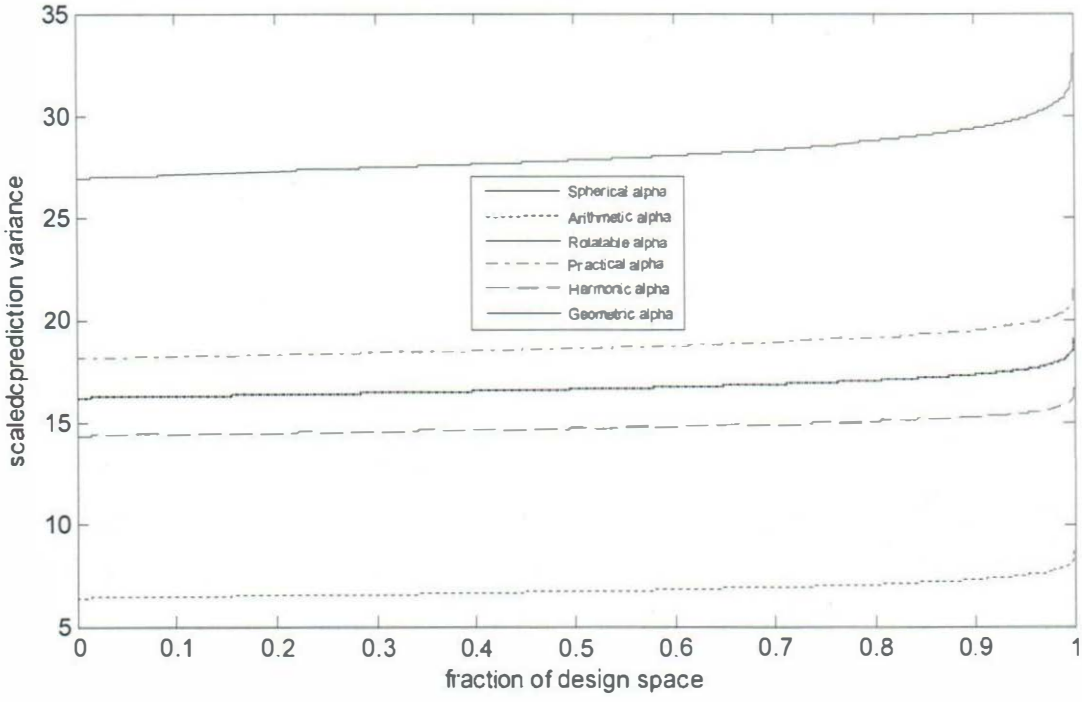

FIG. 58: FDSG for eight-factor star-replicated CCD with $n_2 = 2$ in spherical region

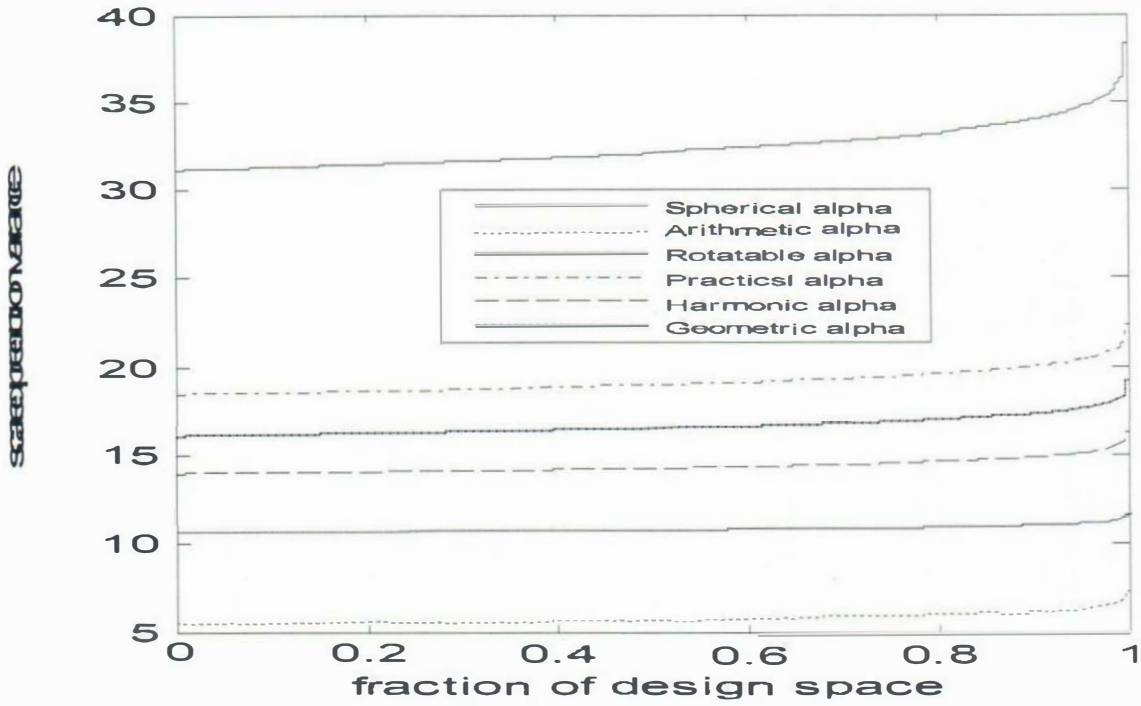

FIG. 59: FDSG for eight-factor Star-replicated CCD with $n_2 = 3$ in spherical region

The CCD with harmonic alpha is the second best for all the factors only when there is $n_2 = 2$ replication of the star portion. The scaled prediction variances of the CCD with rotatable axial distance get smaller and better as the replication of the star portion increases from $n_2 = 2$ to $n_2 = 3$ and performed better than the CCD with arithmetic alpha for $k = 3$ with $n_2 = 3$. The CCD with spherical axial distance gives the worst prediction variance performances with the highest and most unstable scaled prediction variances for $n_2 = 2$ and 3 and for all the factors under consideration. This is followed by the CCD with practical axial distance which displayed the second worst scaled prediction variance characteristics throughout the entire design space. The graphs did not reflect any improvement in the prediction capabilities of the CCDs with spherical and practical axial distances with the replication of the star portion.

The fraction of design space graphs for the star-replicated CCDs are shown in Figures 60 to 73 for the cuboidal design space. As earlier stated, the values of the five axial distances, cuboidal, practical, arithmetic, harmonic and geometric, for the cuboidal design region are not affected by the replication of the star portion of the CCD. The fraction of design space graphs (FDSG) of the star-replicated CCDs in cuboidal region are displayed in Figures 60 to 73 for all the factors under consideration. The graphs show that for the CCD with cuboidal axial distance yielded the smallest scaled prediction variances for about eighty percent (80 %) of design space for k = 2 to 4 factors irrespective of the number of replications of the star portion. For k = 5 to 8 factors, the prediction variance performances of the CCD with cuboidal alpha become almost the same with those of the arithmetic, harmonic and geometric axial distances. The CCD with cuboidal alpha becomes very unstable with

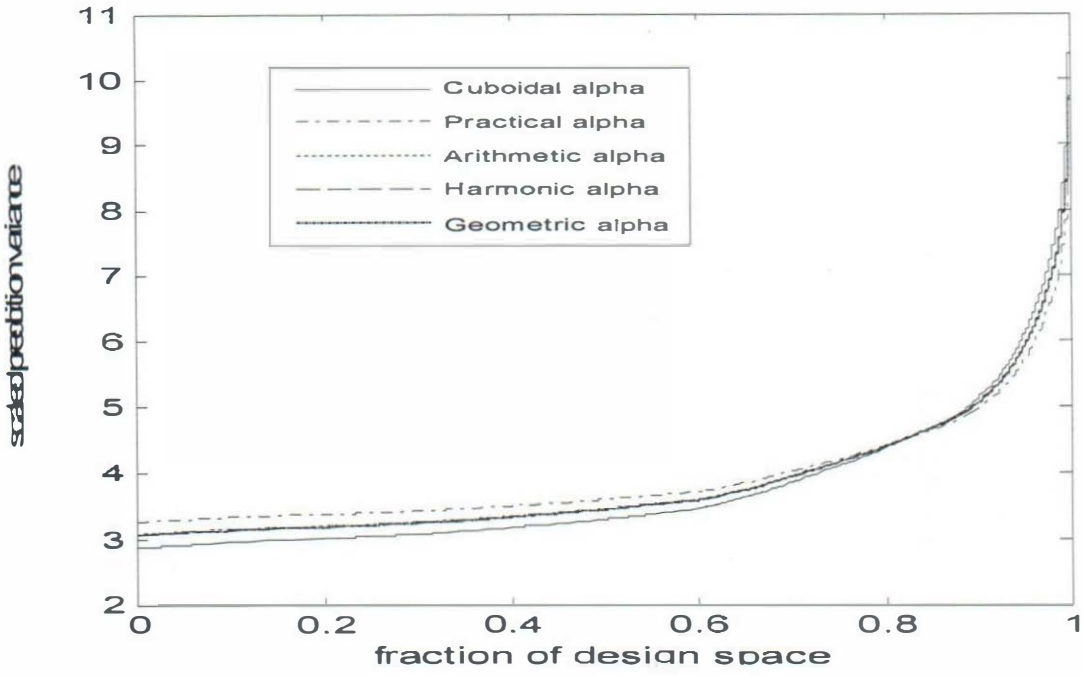

FIG. 60: FDSG for two-factor star-replicated CCD with $n_2 = 2$ in cuboidal region

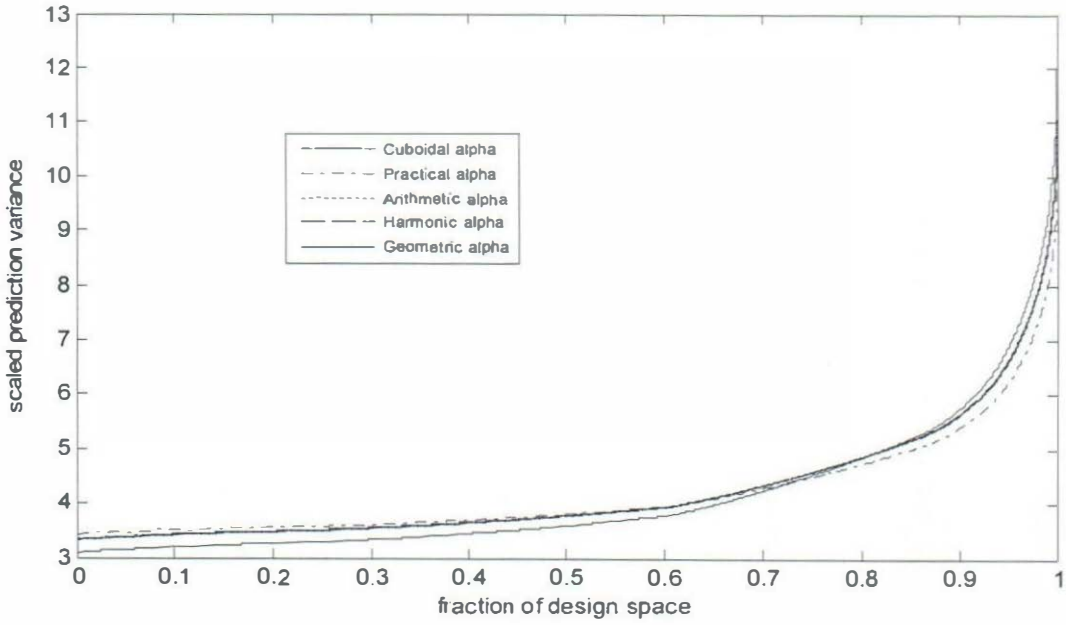

FIG. 61: FDSG for two-factor star-replicated CCD with $n_2 = 3$ in cuboidal region

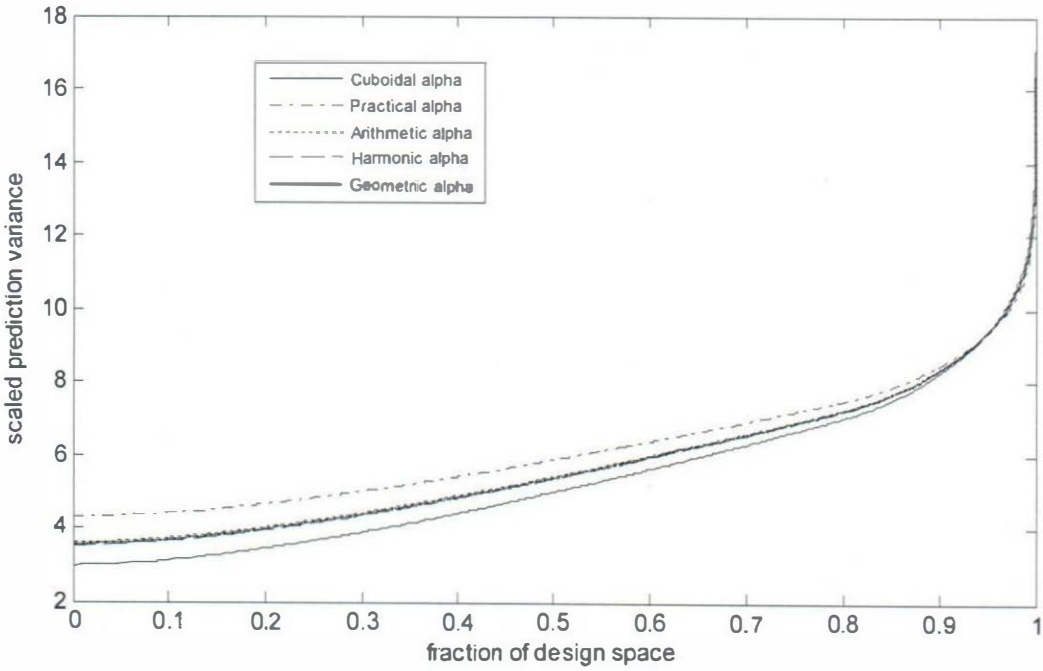

FIG. 62: FDSG for three-factor star-replicated CCD with $n_2 = 2$ in cuboidal region

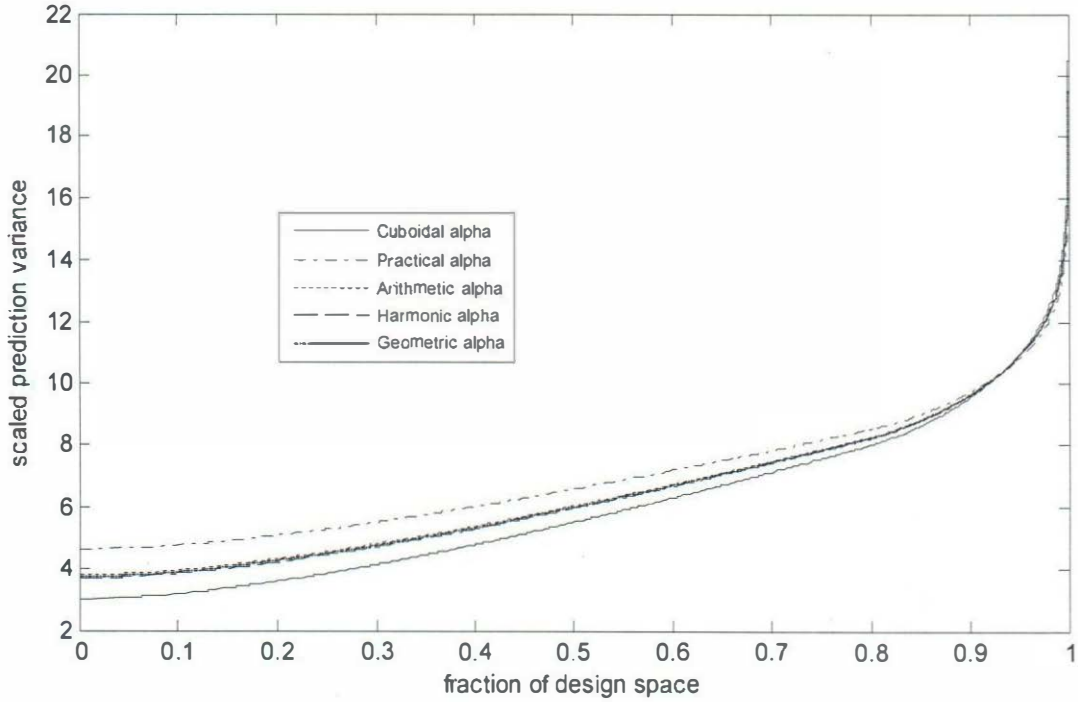

FIG. 63: FDSG for three-factor star-replicated CCD with $n_2 = 3$ in cuboidal region

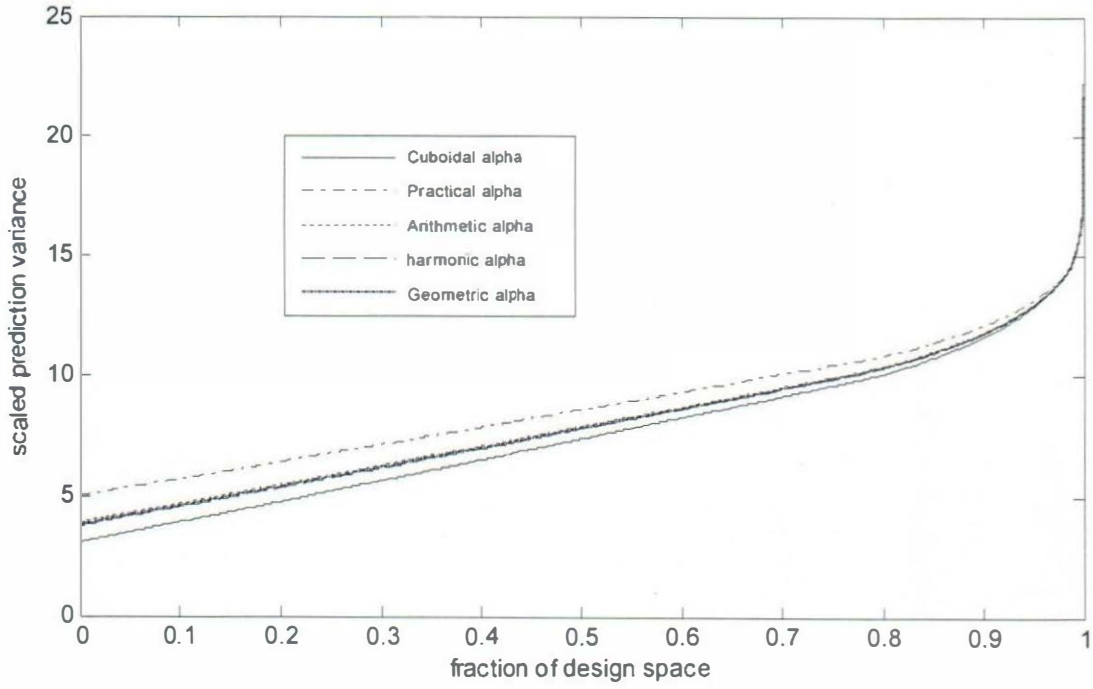

FIG. 64: FDSG for four-factor star-replicated CCD with $n_2 = 2$ in cuboidal region

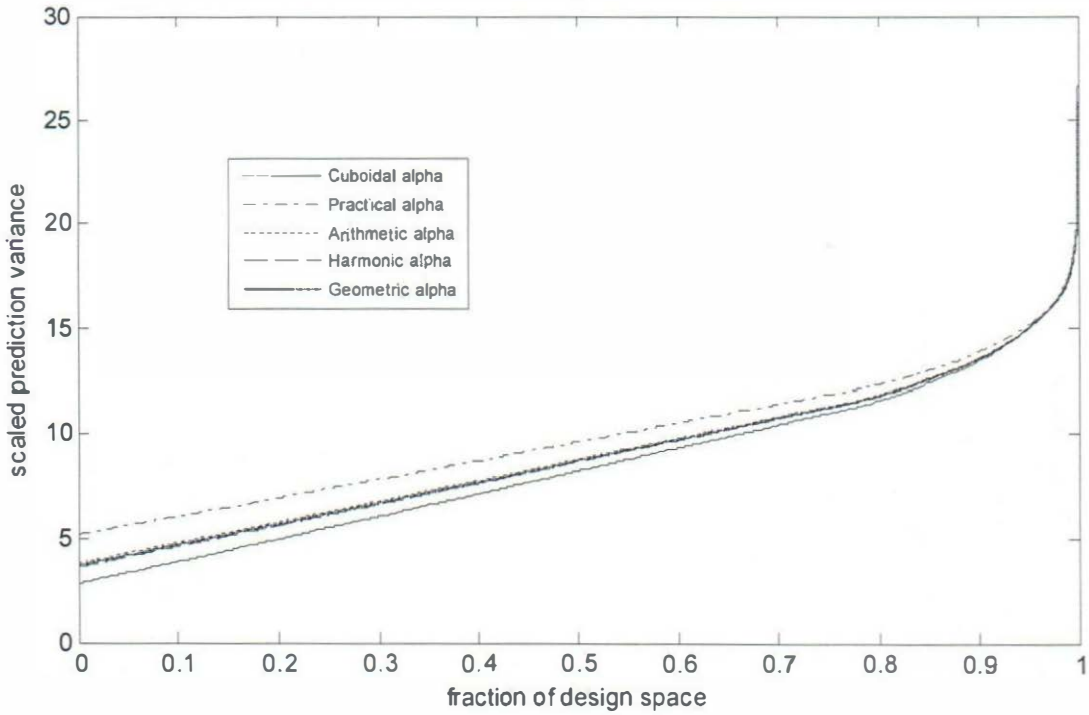

FIG. 65: FDSG for four-factor star-replicated CCD with $n_2 = 3$ in cuboidal region

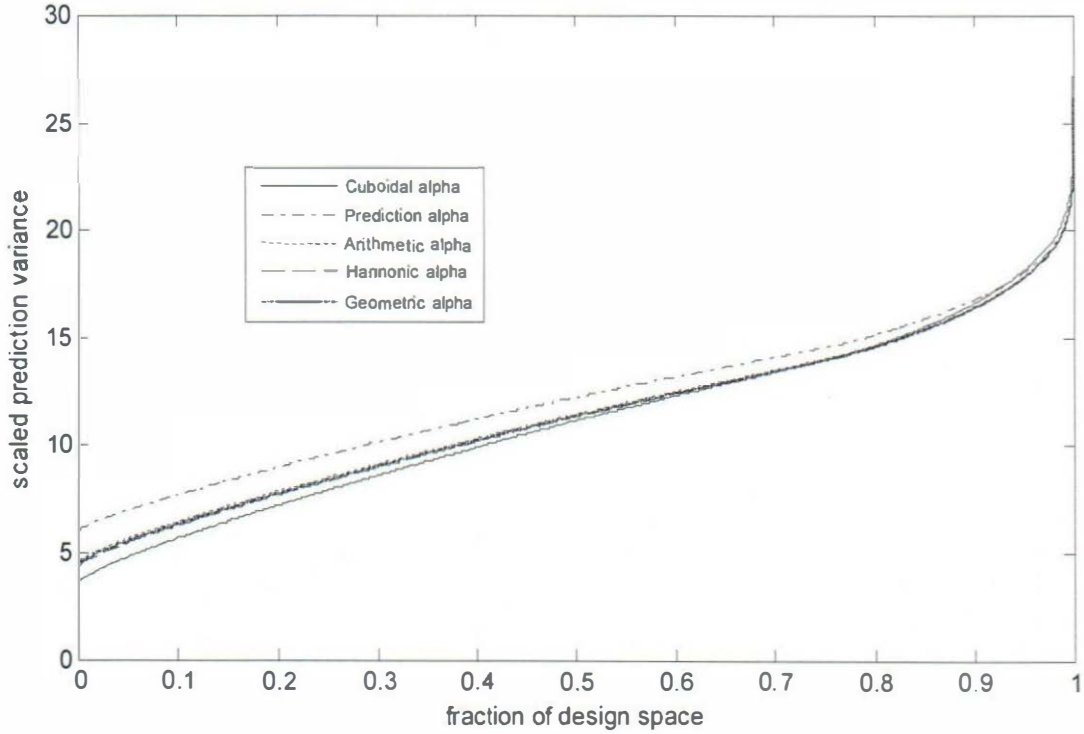

FIG. 66: FDSG for five-factor star-replicated CCD with $n_2 = 2$ in cuboidal region

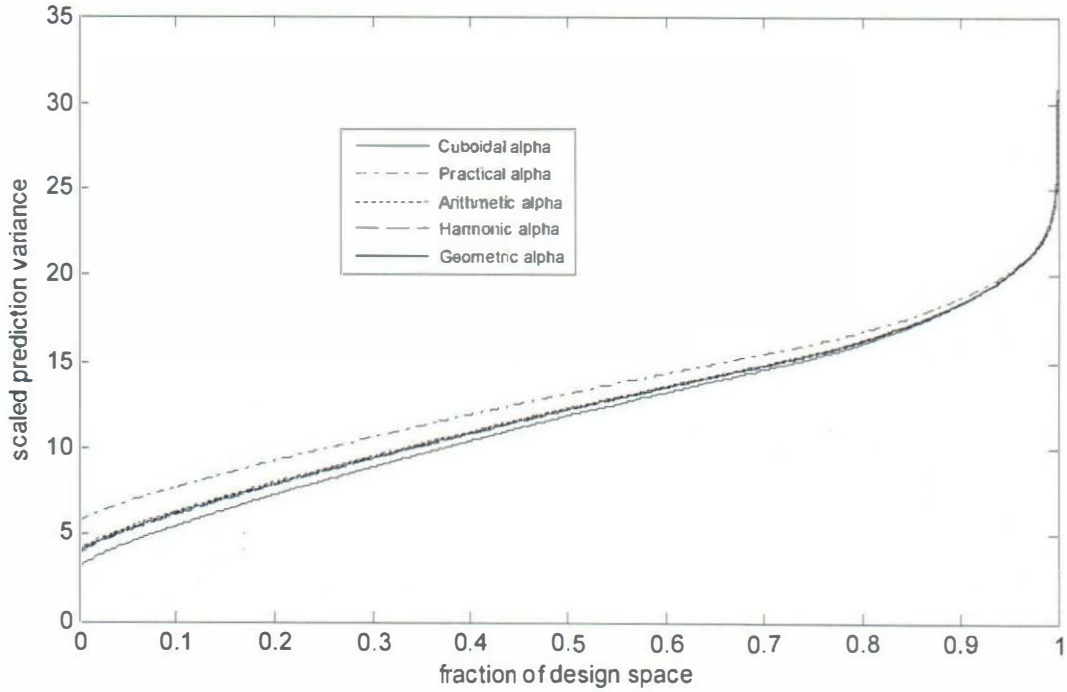

FIG. 67: FDSG for five-factor star-replicated CCD with $n_2 = 3$ in cuboidal region

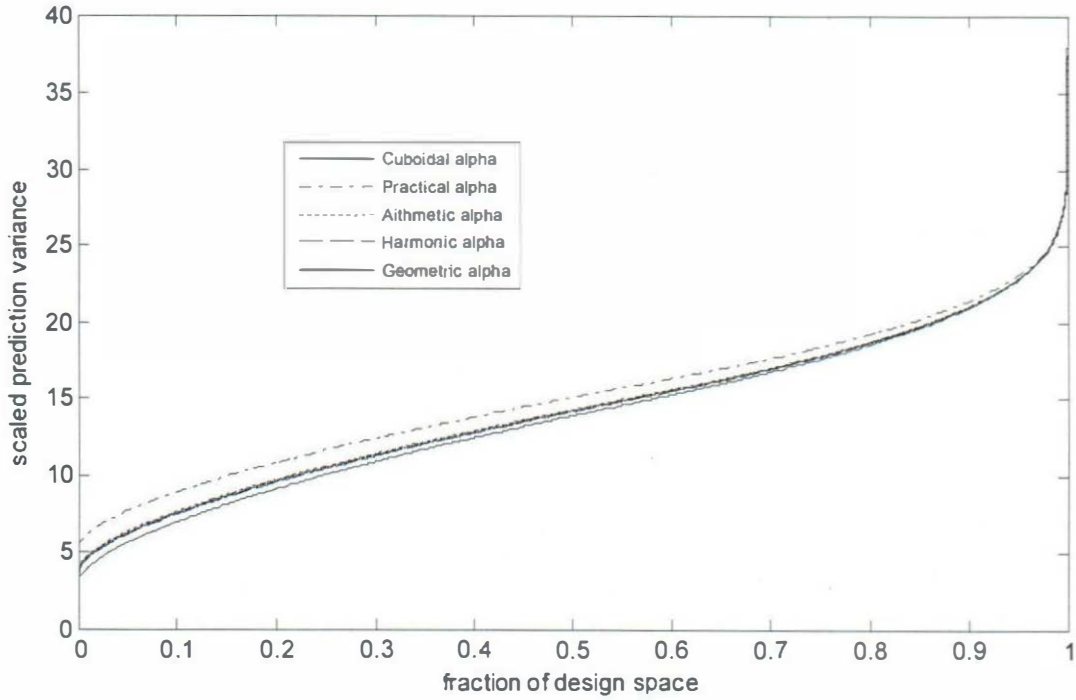

FIG. 68: FDSG for six-factor star-replicated CCD with $n_2 = 2$ in cuboidal region

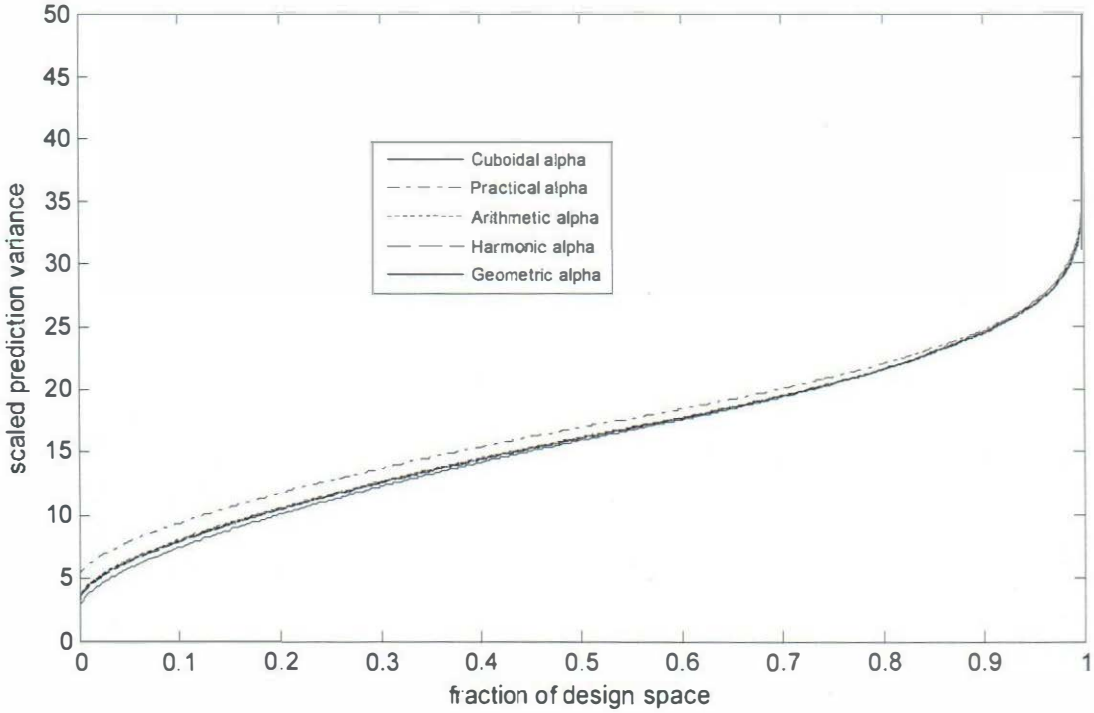

FIG. 69: FDSG for six-factor star-replicated CCD with $n_2 = 3$ in cuboidal region

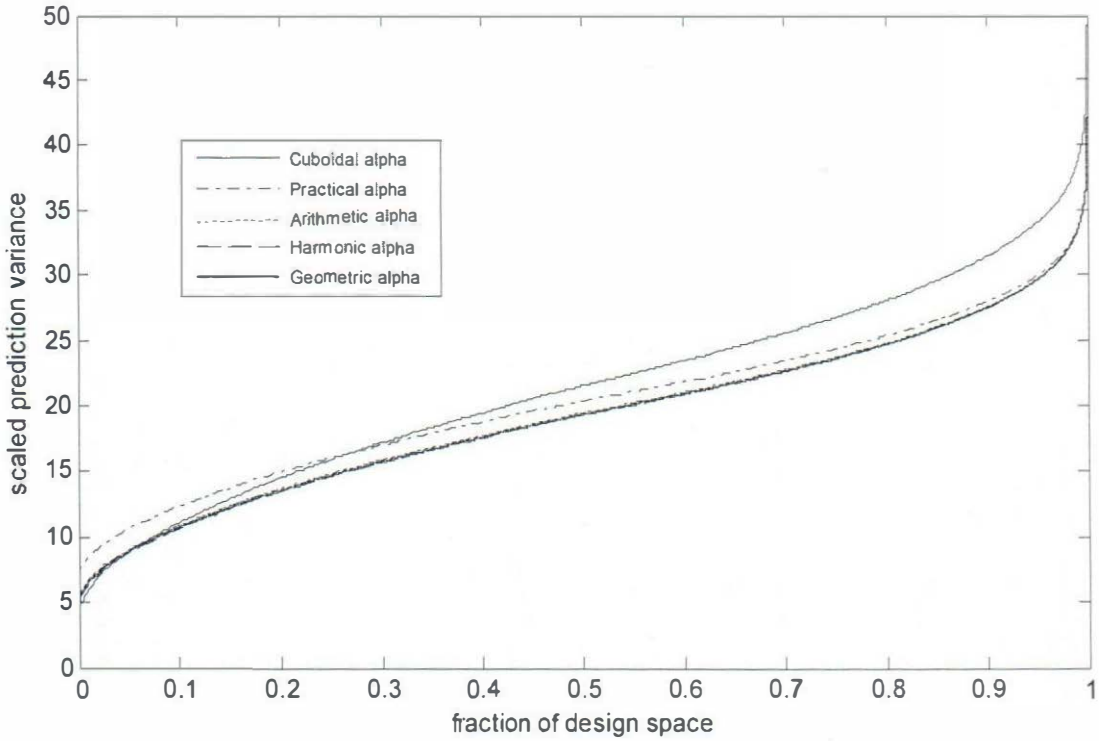

FIG. 70: FDSG for Seven-factor star-replicated CCD with $n_2 = 2$ in cuboidal region

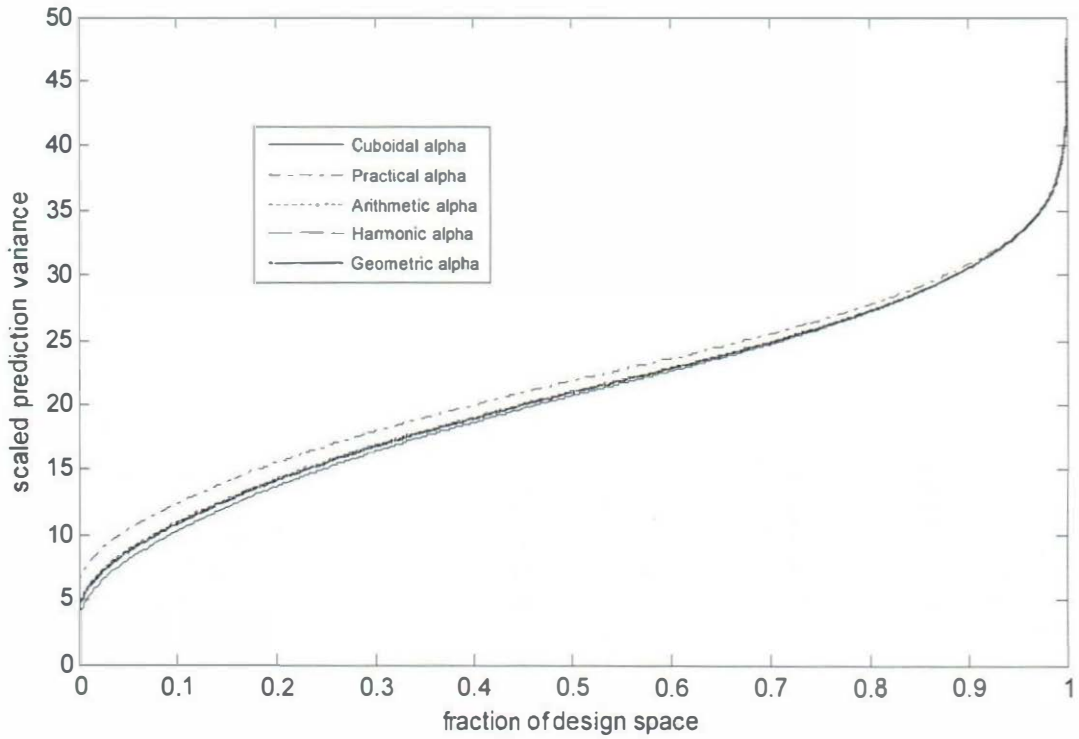

FIG. 71: FDSG for seven-factor star-replicated CCD with $n_2 = 3$ in cuboidal region

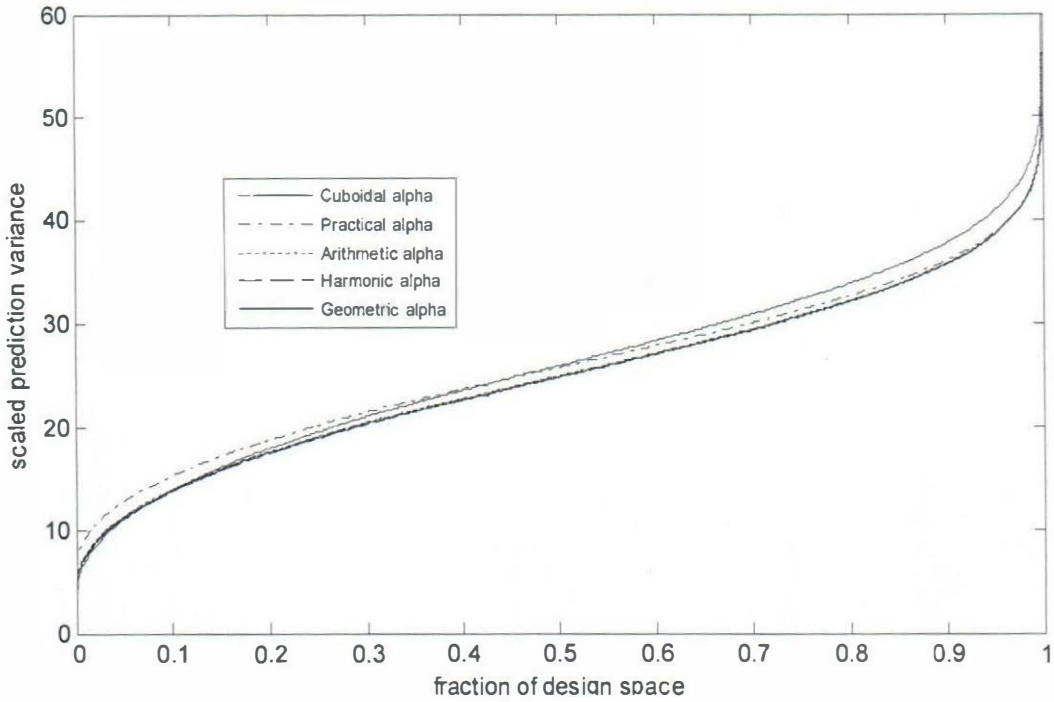

\FIG. 72: FDSG for eight-factor star-replicated CCD with $n_2 = 2$ in cuboidal region

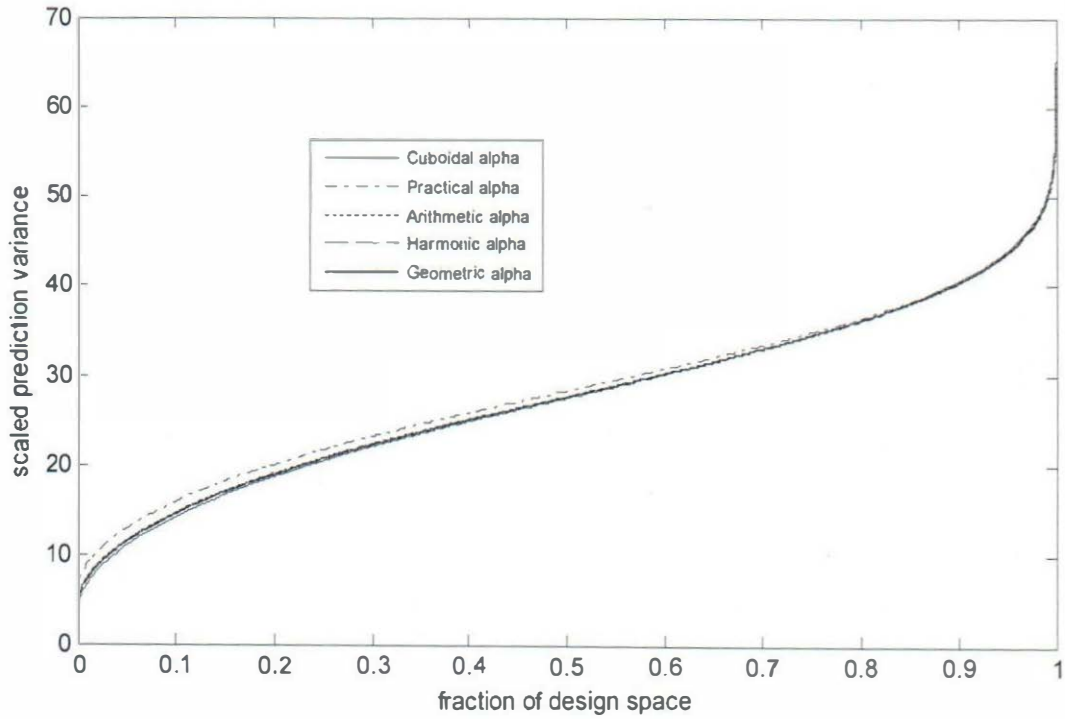

FIG. 73: FDSG for eight-factor star-replicated CCD with $n_2 = 3$ in cuboidal region

small scaled prediction variances which increases so rapidly that it becomes the worst prediction variance at more than ninety five percent (95 %) of the design spaces for k = 6, 7 and 8 factors. This improves as the number of star replication increases from 2 to 3.

The CCD with arithmetic, harmonic and geometric axial distances displayed the same and most stable scaled prediction variance characteristics in the cuboidal region. The CCD with practical axial distance displayed the worst scaled prediction variance characteristics in the cuboidal region with the highest scaled prediction variances irrespective of the number of replication of the star portion. In response surface exploration in the cuboidal region involving the replication of the star portion of the CCD, the CCD with cuboidal axial distance will be recommended mainly for k = 2 to 4 experimental factors. However, due to the instability of the CCD with cuboidal alpha, any of the CCDs with arithmetic, harmonic and geometric axial distances would be preferred for k = 5 to 8 factors. On the other hand, the CCD with practical axial distance cannot be recommended for response surface exploration in cuboidal region involving the replication of the star portion of the CCD.

4.5 Inscribed CCD

The inscribed CCD is a rotatable CCD whose cube component is located inside the sphere unlike the circumscribed CCD where the edges of the cube are circumscribed by the sphere. The factorial portion of the inscribed CCD is obtained by dividing the unit length of the cube, ± 1, by α, the axial distance. This causes the cube to shrink within the circumference of the sphere.

In this section, the variations of the central composite design whose axial distances associated with the rotatable axial distance were used to construct the

inscribed CCD and the *D*-and *G*-efficiencies obtained for comparison. The results are presented in Tables 9 and10, respectively, for the *D*-and *G*-efficiencies.

Table 9 and 10 shows the D- and G- efficiency values, respectively, for inscribed CCD. The values of the *D*-efficiency for the inscribed central composite designs displayed in Table 9 show that the designs have low *D*-efficiency values. The designs having the same number of experimental runs for each particular set of factors makes comparison easier. The inscribed CCD with harmonic axial distance consistently gives the highest *D*-efficiency values except for $k = 7$ where the inscribed CCD with geometric axial distance gives the highest value of the *D*-efficiency. The second inscribed CCD with geometric alpha has the second best *D*-efficiency values that are only lower than those of the harmonic axial distance, followed by the inscribed CCD with arithmetic axial distance. The inscribed CCD with rotatable axial distance consistently yielded the poorest *D*-efficiency values. Therefore, if the D-efficiency is the experimenter's choice criterion for exploring the design region for the inscribed central composite design, the harmonic axial distance should be used in constructing the factorial portion of the inscribed CCD. But for $k = 7$, the geometric axial distance should be used to construct the inscribed CCD.

The variations of the inscribed CCD displayed commendably high *G*-efficiency values as shown in Table 10.For $k = 2, 3, 4$ and 6 factors, the inscribed CCD with rotatable axial distance gives the highest *G*-efficiency values. For $k = 5$ factors, the inscribed CCD with geometric alpha gives the highest *G*-efficiency value, the harmonic axial distance gives the best for $k = 7$ factors while the highest *G*-efficiency for $k = 8$ is given by the arithmetic axial distance. If the experimenter chooses the G-efficiency for the experimental region, the rotatable axial distance is most suitable for constructing the inscribed CCD for $k = 2, 3, 4$ and 6 factors. The

TABLE 9

D-efficiency Values for Inscribed CCD

K	*F*	*N*	α_R	α_{AS}	α_{HS}	α_{GS}
2	2^2	11	24.51	26.43	26.69	26.56
3	2^3	17	14.21	16.03	16.50	16.26
4	2^4	27	08.32	10.43	11.08	10.73
5	2^5	45	04.77	06.95	07.31	07.17
6	2^{6-1}	47	02.71	04.66	05.50	05.04
7	2^{7-1}	81	00.14	00.22	00.23	00.26
8	2^{8-2}	83	02.18	01.98	03.95	03.60

TABLE 10

G-efficiency Values for Inscribed CCD

K	F	N	α_R	α_{AS}	α_{HS}	α_{GS}
2	2^2	11	87.27	83.52	83.08	83.30
3	2^3	17	87.81	85.20	84.62	84.92
4	2^4	27	95.24	92.50	91.84	92.18
5	2^5	45	83.04	88.60	87.13	88.92
6	2^{6-1}	47	96.85	93.82	92.94	93.39
7	2^{7-1}	81	81.06	85.37	85.52	85.46
8	2^{8-2}	83	96.58	97.35	96.93	97.14

harmonic axial distance is the most appropriate for $k = 7$ factors while the arithmetic axial distance is most appropriate for $k = 8$ factors.

4.6 MATLAB Programs for the VDGs

Two computer programs are written in the MATLAB software, R2014a, for plotting the variance dispersion graphs. The first program is for plotting the variance dispersion graphs in the spherical region while the second is for the cuboidal region. The two separate programs are prompted by the distinct nature of the design regions and the number of axial distances required in this study for each design region. The programs are developed using MATLAB commands and syntaxes required for the algorithmic/sequential computations of the prediction variances and corresponding radii. The two programs are built based on the exact closed forms of the variance dispersion graphs for the second-order central composite design given by Borkowski (1995) to ease the tedious computations required in the process of plotting the VDGs using the closed forms. The programs plot the variance dispersion graphs within fractions of a second irrespective of the number of graphs involved. Also, the programs accommodate the replication of the star component of the CCD considered in this study and are equally amenable to replication of the factorial portion of the CCD if required. The programs are presented in Appendices A.1 and A.2, respectively, for the spherical and cuboidal regions.

CHAPTER FIVE

SUMMARY AND CONCLUSION

5.1 Summary

The central composite design (CCD) is very popular among practitioners and experimenters who utilize response surface exploration. The location of the star points is very vital for the optimum use of the CCD and a handful of axial distances exist for various purposes. In this study, a set of three alternative axial distances are proposed for the CCD in each of the spherical and cuboidal design regions. The three sets of axial distances are the arithmetic, harmonic and geometric alphas which were derived as functions of the three Pythagorean means of the already existing axial distances. In order to evaluate the effects of the alternative sets of axial distances, the CCDs were evaluated and compared with the existing axial distances which include the spherical, practical and rotatable axial distances for the spherical region; cuboidal and practical axial distances for the cuboidal regions. Therefore, six variations of the CCD were evaluated in the spherical region and five variations were evaluated in the cuboidal region.

Two commonly used single value criteria for response surface design evaluation, the D- and G-efficiencies were employed in the evaluation of the variations of the central composite designs. It is common knowledge and has earlier been pointed out that in response surface methodology, single-value criteria, like the D- and G-efficiencies considered in this work, do not effectively reflect the prediction capabilities of a design in the design space of interest. Therefore, in addition to the D- and G-efficiencies, two commonly used graphical methods were also utilized in studying the prediction variance distributions of the variations of the CCD in the spherical and cuboidal regions. They are the variance dispersion graph and fraction of

design space graph which were used to monitor the stability of the prediction variances throughout the entire design region or where in the region has the best and worst prediction.

Replication of the star portion of the CCD was considered in the study with the aim of ascertaining the performances of the three alternative axial distances proposed in this study when there are partial replications of the CCD. The CCDs with the alternative axial distances were compared with the existing axial distances already mentioned here for the spherical and cuboidal regions. The performance evaluations of the star replicated CCDs were carried out using the graphical methods adopted for this study since earlier studies have shown that replication of the cube and star portions of the CCD does not improve the D- and G-efficiencies.

Furthermore, construction and evaluation of the inscribed central composite design was put in perspective. The four axial distances in this study which are functions of the rotatable axial distance were used in constructing the inscribed CCD with the aim of determining, through evaluation criteria, which of the axial distances is most appropriate for the construction. The D- and G-efficiency criteria were used to evaluate and compare the variations of the inscribed CCD which is only available in the spherical region.

From the results, this research has three major contributions as highlighted henceforth. Firstly, alternative axial distances, the arithmetic, harmonic and geometric alpha, were developed by exploiting the algebraic properties of the three Pythagorean means, arithmetic, harmonic and geometric means. The alternative axial distances were developed and made suitable for both the spherical and cuboidal design spaces. Furthermore, the alternative axial distances were adapted to accommodate the case of partial replication of the star portion of the CCD.

Secondly, six variants of the CCD involving the three alternative axial distances and the three existing axial distances for the spherical region from which the alternative ones were developed were obtained, evaluated and compared in the spherical region. Five variants of the CCD involving the three alternative axial distances developed for the cuboidal region and the two existing axial distances for the cuboidal region were also obtained, evaluated and compared in the cuboidal region. The evaluation and comparison of these variants of the CCD were made possible using two single value evaluation criteria and two graphical methods. In this way, the points of strengths and weaknesses of the alternative axial distances were highlighted.

Thirdly, the three alternative axial distances were used in the construction of inscribed central composite designs and the emanating designs evaluated using the D- and G-efficiency criteria. The results were compared with the traditional construction of the inscribed CCD using the rotatable axial distance and the benefits of using the three alternative axial distances in the construction of the inscribed CCD were highlighted.

Fourthly, the variance dispersion graph functions for second-order central composite design were automated as computer program which runs in MATLAB based in the FORTRAN programming language. The programs were developed for the spherical and cuboidal regions and were designed to accommodate the replication of the star portion of the CCD. If needed, the programs are also adaptable to the

5.2 Conclusion and recommendations

The analytical forms of the arithmetic, harmonic and geometric means were extensively exploited in the development of the arithmetic, harmonic and geometric alphas as formidable alternative axial distances for the central composite design. The statistical properties of these alternative axial distances were explored using the D- and G-efficiencies while the variance dispersion graph and fraction of design space graph were used to explore their prediction variance properties. It was observed that in the spherical region, the D-efficiency values of the arithmetic, harmonic and geometric axial distances are consistently better than those of the practical axial distance. The G-efficiency values of the three alternative axial distances in most cases remained the highest among the six variations of the central composite designs simultaneously evaluated in the spherical regions.

In the cuboidal region, the D-efficiency values of the arithmetic, harmonic and geometric axial distances are the highest among the five variations of the CCD evaluated for k = 2 to 8 factors. Also, the CCD with the three alternative axial distances have the highest G-efficiency values in the cuboidal region except for k = 5 and 8 where the CCD with cuboidal axial distance has the highest G-efficiency values. The D- and G-efficiency values of the practical axial distance mostly remained the worst for both the spherical and cuboidal regions.

The variance dispersion graphs in the spherical region shows that the variation of the CCD with arithmetic axial distance displayed the smallest and most stable scaled prediction variance throughout the entire design space. The variation of the CCD with cuboidal axial distance is the best within the $r \leq 0.5$ radius range in the cuboidal region. The instability beyond this radius range however, is a source of concern since predicting responses may be required throughout the entire design

region. The alternative axial distance, specifically, the harmonic alpha with the second smallest scaled prediction variances but with better stability throughout the design region is recommended for the cuboidal region. The arithmetic axial distance is also the best choice in the spherical region with the smallest and most stable scaled prediction variances as comparison with fraction of design space graphs also revealed. For the cuboidal region, the three alternative axial distances are the best with equal, smallest and most stable scaled prediction variances throughout the design space as shown using fraction of design space graphs.

The replication of the star portion of the CCD improved the prediction variance characteristics of the variations of the CCD in the spherical and cuboidal design regions. However, the variation of the CCD with arithmetic axial distance is the smallest and most stable scaled prediction variance characteristics in the spherical region as displayed in the VDG and FDSG. In the cuboidal region, any of the arithmetic, harmonic and geometric axial distances which produced the same smallest scaled prediction variance values is recommended for predicting responses. Furthermore, the harmonic axial distance is recommended for the construction of the inscribed central composite design.

In general and from the foregoing, the alternative axial distances, the arithmetic, harmonic and geometric axial distances, have yielded desirable results for the exploration of the response surfaces using the central composite design. The alternative axial distances are viable and formidable alternatives to the other existing axial distances for the central composite design in the spherical and cuboidal design regions.

5.3. Contributions to knowledge

The following are the contributions made in this research to knowledge:

a. the development of the arithmetic, harmonic and geometric axial distances for the spherical and cuboidal regions of the CCD using the concept of Pythagorean means.

b. the use of D-and G-efficiencies for comparing the alternative and the existing axial distance.

c. the use of graphical methods (Variance dispersion graph and fraction of design space graph) for comparison of the axial distances.

d. the use of computer algorithm to develop the variance dispersion graph.

REFERENCES

Anbari, F.T. & Lucas, J.M. (2008). Designing and running super-efficient experiments: Optimum blocking with one hard-to-change factor, *Journal of Quality Technology*, 40, 31 – 45.

Anderson, M. & Whitcomb, P. (2005). *RSM simplified: Optimizing Processes Using Response Surface Methods for Design of Experiment*, New York, Productivity Press.

Anderson-Cook, C.M, Borror, C.M. & Montgomery, D.C. (2009). Response surface design evaluation and comparison. *Journal of Statistical Planning and Inference,* 139, 629 – 641. Doi: 10.1016/j.jspi2008.04.004.

Atkinson, A.C. & Donev, A.N. (1992). *Optimum experimental designs*, New York, Oxford University Press.

Block, R.M. & Mee, R.W. (2001). *Some new second-order designs, Technical Report.* Department of Statistics, University of Tennessee,Tennessee.

Borkowski, J.J. (1995). Spherical prediction properties of central composite and box Behnken designs. *Technometrics,* 37 (4), 399 – 410.

Borkowski, J.J.& Valeroso, E.S. (2001). Comparison of design optimality criteria of reduced models for response surface designs in the hypercube. *Technometrics*, 43 (4), 468 – 477.

Borror, C.M., Montgomery, D.C. & Myers, R.H. (2002). Evaluation of statistical designs of experiments involving noise variables. *Journal of Quality Technology,* 34, 54 – 70.

Box, G.E.P. & Hunter, J.S. (1957). Multi-factor experimental designs for exploring response surfaces. *Annals of Mathematical Statistics,* 28, 195 – 241.

Box, G. E. P & Wilson, K. B. (1951). On the experimental attainment of optimum conditions. *Journal of the Royal Statistical Society,* Series B, 13, 1 – 45.

Chigbu, P. E., Ukaegbu, E. C. & Nwanya, J.C. (2009). On comparing the prediction variances of some central composite designs in spherical region: A review, *Statistica*, 4, 285-298.

Chigbu, P. E. & Ohaegbulem, U. O. (2011). On the preference of replicating factorial runs to axial runs in restricted second-order designs, *Journal of Applied Sciences*, 11 (22), 3732 – 3737.

Draper, N. R. (1982). Centre points in second-order response surface designs. *Technometrics,* 24 (2), 127 – 133.

Dykstra, O.Jr. (1959). Partial duplication of factorial experiments, *Technometrics*, 1 (1), 63 – 75.

Dykstra, O. Jr. (1960). Partial duplication of response surface designs, *Technometrics*, 2 (2), 185 – 195.

Dya'uddeen, B. H., Abdul, A. R. & Daud, W. M. A. W. (2012). On the limitation of Fenton oxidation operational parameters: A review, *International Journal of Chemical Reactor Engineering*, 10, 1 – 12.

Giovannitti-Jensen, A. & Myers, R. H. (1989). Graphical assessment of the prediction capability of response surface designs, *Technometrics*, 31 (2), 159 – 171.

Goldfarb, H. B., Borror, C. M., Montgomery, D. C. & Anderson-Cook, C.M. (2004). Three dimensional variance dispersion graphs for mixture-process experiments. *Journal of Quality Technology*, 36, 109 – 124.

Goos, P. (2009). Discussion of "Response surface design evaluation and comparison", *Journal of Statistical Planning & Inference*, 139, 657–659. DOI: 10.1016/j.jspi.2008.04.012.

Khuri, A. I. & Mukhopadhyay, S. (2010). Response surface methodology. *Wildlife Information Rescue in Education Service Computational Statistics*, 2, 128 – 149.

Jang, D. H. &Anderson-Cook, C.M. (2011). Fraction of design space plots for evaluating ridge estimators in mixture experiments. *Quality and Reliability Engineering International*, 27, 27 – 34.

Li, J., Liang, L., Borror, C.M., Anderson-Cook, C.M. & Montgomery, D.C. (2009). Graphical summaries to compare prediction variance performance for variations of the central composite design for 6 to 10 factors. *Quality Technology and Quantitative Management*, 6 (4), 433 – 449.

Liang, L., Anderson-Cook, C.M. & Robinson, T.J. (2006). Fraction of design space plots for split-plot designs, *Quality and Reliability Engineering International*, 22, 275 – 289.

Lucas, J. M. (2009). Discussion of "response surface design evaluation and comparison" by Christine Anderson-Cook, Connie Borror and Douglas Montgomery, *Journal of Statistical Planning and Inference*, 139, 660 – 661.

Mahsa, A., Morteza, B., Sirous, N. & Abdolhoscin, N. (2012). A central composite design for the optimization of the removal of the Azo-Dye methyl orange from waste water using the Fenton reaction, *Journal of Serbian Chemical Society*, 77 (2), 235 – 246.

Montgomery, D.C. (2013). *Design and analysis of experiments*, 8th Edition, New York, John Wiley and Sons Incorporation.

Myers, R. H., Montgomery, D. C. & Anderson-Cook, C. M. (2009). *Response surface methodology: process and product Optimization using designed experiments*, 3rd Edition, New York, Wiley and Sons Incorporation.

Nwobi, F. N., Okoroafor, A. C. & Onukogu I. B. (2001). Restricted second-order designs in one and two balls, *Statistica,* 61(1), 103 – 112.

Onukogu, I. B. (1997). *Foundations of optimum exploration of response surfaces.* Nsukka, Ephrata Press.

Ozol-Godfrey, A., Anderson-Cook, C. M. & Montgomery, D. C. (2005). Fraction of design space plots for examining model robustness. *Journal of Quality Technology,* 37, 223 – 235.

Ozol-Godfrey, A., Anderson-Cook, C. M. & Robinson, T. J. (2008). Fraction of design space plots for generalized linear models, *Journal of Statistical Planning and Inference,* 138, 223 – 235.

Park, Y. J., Richardson, D. E., Montgomery, D. C., Ozol-Godfrey, A., Borror, C. M & Anderson-Cook, C. M. (2005). Prediction variance properties of second-order designs for cuboidal regions. *Journal of Quality Technology,* 37, 253 – 266.

Piepel, G. F. (2009). Discussion of "Response surface design evaluation & comparison" by C. M. Anderson-Cook, C. M. Borror & D. C. Montgomery, *Journal of Statistical Planning and Inference*, 139, 653-656. DOI: 10.1016/j.jspi.2008.04.008.

Rozum, M. A. & Myers, R. H. (1991). Variance dispersion graphs for cuboidal regions. Paper presented at *Joint Statistical Meetings, American Statistical Association,* Atlanta, Georgia.

Trinca, L. A. & Gilmour, S. G. (1998). Variance dispersion graphs for comparing blocked response designs. *Journal of Quality Technology,* 30, 349 – 364.

Ukaegbu, E. C. (2017). Evaluation of prediction capabilities of partially replicated variations of some central composite design. *A PhD Thesis* submitted to the department of statistics, University of Nigeria, Nsukka.

Ukaegbu, E. C. & Chigbu, P. E. (2015a). Characterization of prediction variance properties of rotatable central composite designs for 3 to 10 factors. *International Journal of Computational & Theoretical Statistics,* 2 (2), 87 – 97.

Ukaegbu, E. C. & Chigbu, P. E. (2015b). Graphical evaluation of the prediction capabilities of partially replicated orthogonal central composite designs, *Quality and Reliability Engineering International*, 31, 707 – 717. DOI: 10.1002/qre.1630.

Ukaegbu, E. C. & Chigbu, P. E. (2017). Evaluation of orthogonally blocked central composite designs with partial replications, *Sankhya B,* DOI 10.1007/s13571-016-0120-z.

Vinning, G. G. (1988). An algorithm for graphical assessment of experimental designs, *Technical Report,* Department of Statistics,Virginia Polytechnic Institute and State University.

Vinning, G. G. (1993). A Computer program for generating variance dispersion graphs, *Journal of Quality Technology,* 25, 45 – 58.

Wong, W. K. (1993). Comparing robust properties of A, D, E and G-optimal designs, *Computational Statistics and Data Analysis,* 18, 441-448.

Zahran, A., Anderson-Cook, C. M. & Myers, R. H. (2003). Fraction of design space to access prediction capability of response surface designs, *Journal of Quality Technology*, 35 (4), 377 – 386.

Appendix A.1: MATLAB Program for Plotting the VDGs in Spherical Region

```
Define k, n, f and q (q =replication of star);
>> a1=spherical alpha value;
>> a2=arithmetic alpha value;
>> a3=rotatable alpha value;
>> a4=practical alpha value;
>> a5=harmonic alpha value;
>> a6=geometric alpha value
>> F1=f+(2*q*a1^2);
>> F2=f+(2*q*a2^2);
>> F3=f+(2*q*a3^2);
>> F4=f+(2*q*a4^2);
>> F5=f+(2*q*a5^2);
>> F6=f+(2*q*a6^2);
>> T1=(2*n*q*a1^4)+(k*n*f)-(k*F1^2);
>> T2=(2*n*q*a2^4)+(k*n*f)-(k*F2^2);
>> T3=(2*n*q*a3^4)+(k*n*f)-(k*F3^2);
>> T4=(2*n*q*a4^4)+(k*n*f)-(k*F4^2);
>> T5=(2*n*q*a5^4)+(k*n*f)-(k*F5^2);
>> T6=(2*n*q*a6^4)+(k*n*f)-(k*F6^2);
>> A11=((k*f)+(2*q*a1^4))/T1;
>> A12=((k*f)+(2*q*a2^4))/T2;
>> A13=((k*f)+(2*q*a3^4))/T3;
>> A14=((k*f)+(2*q*a4^4))/T4;
>> A15=((k*f)+(2*q*a5^4))/T5;
>> A16=((k*f)+(2*q*a6^4))/T6;
>> A21=-(F1/T1);
>> A22=-(F2/T2);
>> A23=-(F3/T3);
>> A24=-(F4/T4);
>> A25=-(F5/T5);
>> A26=-(F6/T6) ;
>> A31=((n*f)-F1^2)/T1;
>> A32=((n*f)-F2^2)/T2;
>> A33=((n*f)-F3^2)/T3;
>> A34=((n*f)-F4^2)/T4;
>> A35=((n*f)-F5^2)/T5;
>> A36=((n*f)-F6^2)/T6;
>> B1=-(2*A21)+(1/F1);
>> B2=-(2*A22)+(1/F2);
>> B3=-(2*A23)+(1/F3);
>> B4=-(2*A24)+(1/F4);
>> B5=-(2*A25)+(1/F5);
>> B6=-(2*A26)+(1/F6);
>> C1=(1/2)*((1/f)-(A31/(q*a1^4)));
>> C2=(1/2)*((1/f)-(A32/(q*a2^4)));
>> C3=(1/2)*((1/f)-(A33/(q*a3^4)));
>> C4=(1/2)*((1/f)-(A34/(q*a4^4)));
>> C5=(1/2)*((1/f)-(A35/(q*a5^4)));
```

```
>> C6=(1/2)*((1/f)-(A36/(q*a6^4)));
>> D1=(1/2)*(1/(q*a1^4)-(1/f));
>> D2=(1/2)*(1/(q*a2^4)-(1/f));
>> D3=(1/2)*(1/(q*a3^4)-(1/f));
>> D4=(1/2)*(1/(q*a4^4)-(1/f));
>> D5=(1/2)*(1/(q*a5^4)-(1/f));
>> D6=(1/2)*(1/(q*a6^4)-(1/f));
>> r=0:0.1:2.0;
>> V1=n*(A11+(B1*r.^2)+(C1-(D1/k))*r.^4);
>> V2=n*(A12+(B2*r.^2)+(C2-(D2/k))*r.^4);
>> V3=n*(A13+(B3*r.^2)+(C3-(D3/k))*r.^4);
>> V4=n*(A14+(B4*r.^2)+(C4-(D4/k))*r.^4);
>> V5=n*(A15+(B5*r.^2)+(C5-(D5/k))*r.^4);
>> V6=n*(A16+(B6*r.^2)+(C6-(D6/k))*r.^4);
plot(r,V1);
>> hold on
>> plot(r,V2);
>> plot(r,V3);
>> plot(r,V4);
>> plot(r,V5);
>> plot(r,V6);
>> hold off
```

Appendix A.2: MATLAB Program for Plotting the VDGs in Cuboidal Region

```
Define k, n, f and q (q =replication of star);
>> a1=cuboidal alpha value;
>> a2=practical alpha value;
>> a3=arithmetic alpha value;
>> a4=harmonic alpha value;
>> a5=geometric alpha value;
>> F1=f+(2*q*a1^2);
>> F2=f+(2*q*a2^2);
>> F3=f+(2*q*a3^2);
>> F4=f+(2*q*a4^2);
>> F5=f+(2*q*a5^2);
>> T1=(2*n*q*a1^4)+(k*n*f)-(k*F1^2);
>> T2=(2*n*q*a2^4)+(k*n*f)-(k*F2^2);
>> T3=(2*n*q*a3^4)+(k*n*f)-(k*F3^2);
>> T4=(2*n*q*a4^4)+(k*n*f)-(k*F4^2);
>> T5=(2*n*q*a5^4)+(k*n*f)-(k*F5^2);
>> A11=((k*f)+(2*q*a1^4))/T1;
>> A12=((k*f)+(2*q*a2^4))/T2;
>> A13=((k*f)+(2*q*a3^4))/T3;
>> A14=((k*f)+(2*q*a4^4))/T4;
>> A15=((k*f)+(2*q*a5^4))/T5;
>> A21=-(F1/T1);
>> A22=-(F2/T2);
>> A23=-(F3/T3);
>> A24=-(F4/T4);
>> A25=-(F5/T5);
>> A31=((n*f)-F1^2)/T1;
>> A32=((n*f)-F2^2)/T2;
>> A33=((n*f)-F3^2)/T3;
>> A34=((n*f)-F4^2)/T4;
>> A35=((n*f)-F5^2)/T5;
>> B1=-(2*A21)+(1/F1);
>> B2=-(2*A22)+(1/F2);
>> B3=-(2*A23)+(1/F3);
>> B4=-(2*A24)+(1/F4);
>> B5=-(2*A25)+(1/F5);
>> C1=(1/2)*((1/f)-(A31/(q*a1^4)));
>> C2=(1/2)*((1/f)-(A32/(q*a2^4)));
>> C3=(1/2)*((1/f)-(A33/(q*a3^4)));
>> C4=(1/2)*((1/f)-(A34/(q*a4^4)));
>> C5=(1/2)*((1/f)-(A35/(q*a5^4)));
>> D1=(1/2)*(1/(q*a1^4)-(1/f));
>> D2=(1/2)*(1/(q*a2^4)-(1/f));
>> D3=(1/2)*(1/(q*a3^4)-(1/f));
>> D4=(1/2)*(1/(q*a4^4)-(1/f));
>> D5=(1/2)*(1/(q*a5^4)-(1/f));
>> r=0:0.1:1.0;
>> V1=n*(A11+(B1*r.^2)+(C1-(D1/k))*r.^4);
```

```
>> V2=n*(A12+(B2*r.^2)+(C2-(D2/k))*r.^4);
>> V3=n*(A13+(B3*r.^2)+(C3-(D3/k))*r.^4);
>> V4=n*(A14+(B4*r.^2)+(C4-(D4/k))*r.^4);
>> V5=n*(A15+(B5*r.^2)+(C5-(D5/k))*r.^4);
plot(r,V1);
>> hold on
>> plot(r,V2);
>> plot(r,V3);
>> plot(r,V4);
>> plot(r,V5);
>> hold off
```

Appendix B.1: Extended Design Matrix for Four-Factor CCD with Spherical Alpha

1	X1	X2	X3	X4	X1^2	X2^2	X3^2	X4^2	X1*X2	X1*X3	X1*X4	X2*X3	X2*X4	X3*X4
1	-1	-1	-1	-1	1	1	1	1	1	1	1	1	1	1
1	1	-1	-1	-1	1	1	1	1	-1	-1	-1	1	1	1
1	-1	1	-1	-1	1	1	1	1	-1	1	1	-1	-1	1
1	1	1	-1	-1	1	1	1	1	1	-1	-1	-1	-1	1
1	-1	-1	1	-1	1	1	1	1	1	-1	1	-1	1	-1
1	1	-1	1	-1	1	1	1	1	-1	1	-1	-1	1	-1
1	-1	1	1	-1	1	1	1	1	-1	-1	1	1	-1	-1
1	1	1	1	-1	1	1	1	1	1	1	-1	1	-1	-1
1	-1	-1	-1	1	1	1	1	1	1	1	-1	1	-1	-1
1	1	-1	-1	1	1	1	1	1	-1	-1	1	1	-1	-1
1	-1	1	-1	1	1	1	1	1	-1	1	-1	-1	1	-1
1	1	1	-1	1	1	1	1	1	1	-1	1	-1	1	-1
1	-1	-1	1	1	1	1	1	1	1	-1	-1	-1	-1	1
1	1	-1	1	1	1	1	1	1	-1	1	1	-1	-1	1
1	-1	1	1	1	1	1	1	1	-1	-1	-1	1	1	1
1	1	1	1	1	1	1	1	1	1	1	1	1	1	1
1	-2	0	0	0	4	0	0	0	0	0	0	0	0	0
1	2	0	0	0	4	0	0	0	0	0	0	0	0	0
1	0	-2	0	0	0	4	0	0	0	0	0	0	0	0
1	0	2	0	0	0	4	0	0	0	0	0	0	0	0
1	0	0	-2	0	0	0	4	0	0	0	0	0	0	0
1	0	0	2	0	0	0	4	0	0	0	0	0	0	0
1	0	0	0	-2	0	0	0	4	0	0	0	0	0	0
1	0	0	0	2	0	0	0	4	0	0	0	0	0	0
1	0	0	0	0	0	0	0	0	0	0	0	0	0	0
1	0	0	0	0	0	0	0	0	0	0	0	0	0	0
1	0	0	0	0	0	0	0	0	0	0	0	0	0	0

Appendix B.2: Extended Design Matrix for Four-Factor CCD with Practical Alpha

1	X1	X2	X3	X4	X1^2	X2^2	X3^2	X4^2	X1*X2	X1*X3	X1*X4	X2*X3	X2*X4	X3*X4
1	-1	-1	-1	-1	1	1	1	1	1	1	1	1	1	1
1	1	-1	-1	-1	1	1	1	1	-1	-1	-1	1	1	1
1	-1	1	-1	-1	1	1	1	1	-1	1	1	-1	-1	1
1	1	1	-1	-1	1	1	1	1	1	-1	-1	-1	-1	1
1	-1	-1	1	-1	1	1	1	1	1	-1	1	-1	1	-1
1	1	-1	1	-1	1	1	1	1	-1	1	-1	-1	1	-1
1	-1	1	1	-1	1	1	1	1	-1	-1	1	1	-1	-1
1	1	1	1	-1	1	1	1	1	1	1	-1	1	-1	-1
1	-1	-1	-1	1	1	1	1	1	1	1	-1	1	-1	-1
1	1	-1	-1	1	1	1	1	1	-1	-1	1	1	-1	-1
1	-1	1	-1	1	1	1	1	1	-1	1	-1	-1	1	-1
1	1	1	-1	1	1	1	1	1	1	-1	1	-1	1	-1
1	-1	-1	1	1	1	1	1	1	1	-1	-1	-1	-1	1
1	1	-1	1	1	1	1	1	1	-1	1	1	-1	-1	1
1	-1	1	1	1	1	1	1	1	-1	-1	-1	1	1	1
1	1	1	1	1	1	1	1	1	1	1	1	1	1	1
1	-1.414	0	0	0	2	0	0	0	0	0	0	0	0	0
1	1.4142	0	0	0	2	0	0	0	0	0	0	0	0	0
1	0	-1.414	0	0	0	2	0	0	0	0	0	0	0	0
1	0	1.4142	0	0	0	2	0	0	0	0	0	0	0	0
1	0	0	-1.414	0	0	0	2	0	0	0	0	0	0	0
1	0	0	1.4142	0	0	0	2	0	0	0	0	0	0	0
1	0	0	0	-1.414	0	0	0	2	0	0	0	0	0	0
1	0	0	0	1.4142	0	0	0	2	0	0	0	0	0	0
1	0	0	0	0	0	0	0	0	0	0	0	0	0	0
1	0	0	0	0	0	0	0	0	0	0	0	0	0	0
1	0	0	0	0	0	0	0	0	0	0	0	0	0	0

Appendix B.3: Extended Design Matrix for Four-Factor CCD with Rotatable Alpha

1	X1	X2	X3	X4	X1^2	X2^2	X3^2	X4^2	X1*X2	X1*X3	X1*X4	X2*X3	X2*X4	X3*X4
1	-1	-1	-1	-1	1	1	1	1	1	1	1	1	1	1
1	1	-1	-1	-1	1	1	1	1	-1	-1	-1	1	1	1
1	-1	1	-1	-1	1	1	1	1	-1	1	1	-1	-1	1
1	1	1	-1	-1	1	1	1	1	1	-1	-1	-1	-1	1
1	-1	-1	1	-1	1	1	1	1	1	-1	1	-1	1	-1
1	1	-1	1	-1	1	1	1	1	-1	1	-1	-1	1	-1
1	-1	1	1	-1	1	1	1	1	-1	-1	1	1	-1	-1
1	1	1	1	-1	1	1	1	1	1	1	-1	1	-1	-1
1	-1	-1	-1	1	1	1	1	1	1	1	-1	1	-1	-1
1	1	-1	-1	1	1	1	1	1	-1	-1	1	1	-1	-1
1	-1	1	-1	1	1	1	1	1	-1	1	-1	-1	1	-1
1	1	1	-1	1	1	1	1	1	1	-1	1	-1	1	-1
1	-1	-1	1	1	1	1	1	1	1	-1	-1	-1	-1	1
1	1	-1	1	1	1	1	1	1	-1	1	1	-1	-1	1
1	-1	1	1	1	1	1	1	1	-1	-1	-1	1	1	1
1	1	1	1	1	1	1	1	1	1	1	1	1	1	1
1	-2	0	0	0	4	0	0	0	0	0	0	0	0	0
1	2	0	0	0	4	0	0	0	0	0	0	0	0	0
1	0	-2	0	0	0	4	0	0	0	0	0	0	0	0
1	0	2	0	0	0	4	0	0	0	0	0	0	0	0
1	0	0	-2	0	0	0	4	0	0	0	0	0	0	0
1	0	0	2	0	0	0	4	0	0	0	0	0	0	0
1	0	0	0	-2	0	0	0	4	0	0	0	0	0	0
1	0	0	0	2	0	0	0	4	0	0	0	0	0	0
1	0	0	0	0	0	0	0	0	0	0	0	0	0	0
1	0	0	0	0	0	0	0	0	0	0	0	0	0	0
1	0	0	0	0	0	0	0	0	0	0	0	0	0	0

Appendix B.4: Extended Design Matrix for Four-Factor CCD with Arithmetic Alpha in Spherical Region

1	X1	X2	X3	X4	X1^2	X2^2	X3^2	X4^2	X1*X2	X1*X3	X1*X4	X2*X3	X2*X4	X3*X4
1	-1	-1	-1	-1	1	1	1	1	1	1	1	1	1	1
1	1	-1	-1	-1	1	1	1	1	-1	-1	-1	1	1	1
1	-1	1	-1	-1	1	1	1	1	-1	1	1	-1	-1	1
1	1	1	-1	-1	1	1	1	1	1	-1	-1	-1	-1	1
1	-1	-1	1	-1	1	1	1	1	1	-1	1	-1	1	-1
1	1	-1	1	-1	1	1	1	1	-1	1	-1	-1	1	-1
1	-1	1	1	-1	1	1	1	1	-1	-1	1	1	-1	-1
1	1	1	1	-1	1	1	1	1	1	1	-1	1	-1	-1
1	-1	-1	-1	1	1	1	1	1	1	1	-1	1	-1	-1
1	1	-1	-1	1	1	1	1	1	-1	-1	1	1	-1	-1
1	-1	1	-1	1	1	1	1	1	-1	1	-1	-1	1	-1
1	1	1	-1	1	1	1	1	1	1	-1	1	-1	1	-1
1	-1	-1	1	1	1	1	1	1	1	-1	-1	-1	-1	1
1	1	-1	1	1	1	1	1	1	-1	1	1	-1	-1	1
1	-1	1	1	1	1	1	1	1	-1	-1	-1	1	1	1
1	1	1	1	1	1	1	1	1	1	1	1	1	1	1
1	-1.805	0	0	0	3.2569	0	0	0	0	0	0	0	0	0
1	1.8047	0	0	0	3.2569	0	0	0	0	0	0	0	0	0
1	0	-1.805	0	0	0	3.2569	0	0	0	0	0	0	0	0
1	0	1.8047	0	0	0	3.2569	0	0	0	0	0	0	0	0
1	0	0	-1.805	0	0	0	3.2569	0	0	0	0	0	0	0
1	0	0	1.8047	0	0	0	3.2569	0	0	0	0	0	0	0
1	0	0	0	-1.805	0	0	0	3.2569	0	0	0	0	0	0
1	0	0	0	1.8047	0	0	0	3.2569	0	0	0	0	0	0
1	0	0	0	0	0	0	0	0	0	0	0	0	0	0
1	0	0	0	0	0	0	0	0	0	0	0	0	0	0
1	0	0	0	0	0	0	0	0	0	0	0	0	0	0

Appendix B.5: Extended Design Matrix for Four-Factor CCD with Harmonic Alpha in Spherical Region

1	X1	X2	X3	X4	X1^2	X2^2	X3^2	X4^2	X1*X2	X1*X3	X1*X4	X2*X3	X2*X4	X3*X4
1	-1	-1	-1	-1	1	1	1	1	1	1	1	1	1	1
1	1	-1	-1	-1	1	1	1	1	-1	-1	-1	1	1	1
1	-1	1	-1	-1	1	1	1	1	-1	1	1	-1	-1	1
1	1	1	-1	-1	1	1	1	1	1	-1	-1	-1	-1	1
1	-1	-1	1	-1	1	1	1	1	1	-1	1	-1	1	-1
1	1	-1	1	-1	1	1	1	1	-1	1	-1	-1	1	-1
1	-1	1	1	-1	1	1	1	1	-1	-1	1	1	-1	-1
1	1	1	1	-1	1	1	1	1	1	1	-1	1	-1	-1
1	-1	-1	-1	1	1	1	1	1	1	1	-1	1	-1	-1
1	1	-1	-1	1	1	1	1	1	-1	-1	1	1	-1	-1
1	-1	1	-1	1	1	1	1	1	-1	1	-1	-1	1	-1
1	1	1	-1	1	1	1	1	1	1	-1	1	-1	1	-1
1	-1	-1	1	1	1	1	1	1	1	-1	-1	-1	-1	1
1	1	-1	1	1	1	1	1	1	-1	1	1	-1	-1	1
1	-1	1	1	1	1	1	1	1	-1	-1	-1	1	1	1
1	1	1	1	1	1	1	1	1	1	1	1	1	1	1
1	-1.757	0	0	0	3.0885	0	0	0	0	0	0	0	0	0
1	1.7574	0	0	0	3.0885	0	0	0	0	0	0	0	0	0
1	0	-1.757	0	0	0	3.0885	0	0	0	0	0	0	0	0
1	0	1.7574	0	0	0	3.0885	0	0	0	0	0	0	0	0
1	0	0	-1.757	0	0	0	3.0885	0	0	0	0	0	0	0
1	0	0	1.7574	0	0	0	3.0885	0	0	0	0	0	0	0
1	0	0	0	-1.757	0	0	0	3.0885	0	0	0	0	0	0
1	0	0	0	1.7574	0	0	0	3.0885	0	0	0	0	0	0
1	0	0	0	0	0	0	0	0	0	0	0	0	0	0
1	0	0	0	0	0	0	0	0	0	0	0	0	0	0
1	0	0	0	0	0	0	0	0	0	0	0	0	0	0

Appendix B.6: Extended Design Matrix for Four-Factor CCD with Geometric Alpha in Spherical Region

1	X1	X2	X3	X4	X1^2	X2^2	X3^2	X4^2	X1*X2	X1*X3	X1*X4	X2*X3	X2*X4	X3*X4
1	-1	-1	-1	-1	1	1	1	1	1	1	1	1	1	1
1	1	-1	-1	-1	1	1	1	1	-1	-1	-1	1	1	1
1	-1	1	-1	-1	1	1	1	1	-1	1	1	-1	-1	1
1	1	1	-1	-1	1	1	1	1	1	-1	-1	-1	-1	1
1	-1	-1	1	-1	1	1	1	1	1	-1	1	-1	1	-1
1	1	-1	1	-1	1	1	1	1	-1	1	-1	-1	1	-1
1	-1	1	1	-1	1	1	1	1	-1	-1	1	1	-1	-1
1	1	1	1	-1	1	1	1	1	1	1	-1	1	-1	-1
1	-1	-1	-1	1	1	1	1	1	1	1	-1	1	-1	-1
1	1	-1	-1	1	1	1	1	1	-1	-1	1	1	-1	-1
1	-1	1	-1	1	1	1	1	1	-1	1	-1	-1	1	-1
1	1	1	-1	1	1	1	1	1	1	-1	1	-1	1	-1
1	-1	-1	1	1	1	1	1	1	1	-1	-1	-1	-1	1
1	1	-1	1	1	1	1	1	1	-1	1	1	-1	-1	1
1	-1	1	1	1	1	1	1	1	-1	-1	-1	1	1	1
1	1	1	1	1	1	1	1	1	1	1	1	1	1	1
1	-1.782	0	0	0	3.1748	0	0	0	0	0	0	0	0	0
1	1.7818	0	0	0	3.1748	0	0	0	0	0	0	0	0	0
1	0	-1.782	0	0	0	3.1748	0	0	0	0	0	0	0	0
1	0	1.7818	0	0	0	3.1748	0	0	0	0	0	0	0	0
1	0	0	-1.782	0	0	0	3.1748	0	0	0	0	0	0	0
1	0	0	1.7818	0	0	0	3.1748	0	0	0	0	0	0	0
1	0	0	0	-1.782	0	0	0	3.1748	0	0	0	0	0	0
1	0	0	0	1.7818	0	0	0	3.1748	0	0	0	0	0	0
1	0	0	0	0	0	0	0	0	0	0	0	0	0	0
1	0	0	0	0	0	0	0	0	0	0	0	0	0	0
1	0	0	0	0	0	0	0	0	0	0	0	0	0	0

Appendix B.7: Extended Design Matrix for Four-Factor CCD with Cuboidal Alpha

1	X1	X2	X3	X4	X1^2	X2^2	X3^2	X4^2	X1*X2	X1*X3	X1*X4	X2*X3	X2*X4	X3*X4
1	-1	-1	-1	-1	1	1	1	1	1	1	1	1	1	1
1	1	-1	-1	-1	1	1	1	1	-1	-1	-1	1	1	1
1	-1	1	-1	-1	1	1	1	1	-1	1	1	-1	-1	1
1	1	1	-1	-1	1	1	1	1	1	-1	-1	-1	-1	1
1	-1	-1	1	-1	1	1	1	1	1	-1	1	-1	1	-1
1	1	-1	1	-1	1	1	1	1	-1	1	-1	-1	1	-1
1	-1	1	1	-1	1	1	1	1	-1	-1	1	1	-1	-1
1	1	1	1	-1	1	1	1	1	1	1	-1	1	-1	-1
1	-1	-1	-1	1	1	1	1	1	1	1	-1	1	-1	-1
1	1	-1	-1	1	1	1	1	1	-1	-1	1	1	-1	-1
1	-1	1	-1	1	1	1	1	1	-1	1	-1	-1	1	-1
1	1	1	-1	1	1	1	1	1	1	-1	1	-1	1	-1
1	-1	-1	1	1	1	1	1	1	1	-1	-1	-1	-1	1
1	1	-1	1	1	1	1	1	1	-1	1	1	-1	-1	1
1	-1	1	1	1	1	1	1	1	-1	-1	-1	1	1	1
1	1	1	1	1	1	1	1	1	1	1	1	1	1	1
1	-1	0	0	0	1	0	0	0	0	0	0	0	0	0
1	1	0	0	0	1	0	0	0	0	0	0	0	0	0
1	0	-1	0	0	0	1	0	0	0	0	0	0	0	0
1	0	1	0	0	0	1	0	0	0	0	0	0	0	0
1	0	0	-1	0	0	0	1	0	0	0	0	0	0	0
1	0	0	1	0	0	0	1	0	0	0	0	0	0	0
1	0	0	0	-1	0	0	0	1	0	0	0	0	0	0
1	0	0	0	1	0	0	0	1	0	0	0	0	0	0
1	0	0	0	0	0	0	0	0	0	0	0	0	0	0
1	0	0	0	0	0	0	0	0	0	0	0	0	0	0
1	0	0	0	0	0	0	0	0	0	0	0	0	0	0

Appendix B.8: Extended Design Matrix for Four-Factor Inscribed CCD with Rotatable Alpha

1	X1	X2	X3	X4	X1^2	X2^2	X3^2	X4^2	X1*X2	X1*X3	X1*X4	X2*X3	X2*X4	X3*X4
1	-0.5	-0.5	-0.5	-0.5	0.25	0.25	0.25	0.25	0.25	0.25	0.25	0.25	0.25	0.25
1	0.5	-0.5	-0.5	-0.5	0.25	0.25	0.25	0.25	-0.25	-0.25	-0.25	0.25	0.25	0.25
1	-0.5	0.5	-0.5	-0.5	0.25	0.25	0.25	0.25	-0.25	0.25	0.25	-0.25	-0.25	0.25
1	0.5	0.5	-0.5	-0.5	0.25	0.25	0.25	0.25	0.25	-0.25	-0.25	-0.25	-0.25	0.25
1	-0.5	-0.5	0.5	-0.5	0.25	0.25	0.25	0.25	0.25	-0.25	0.25	-0.25	0.25	-0.25
1	0.5	-0.5	0.5	-0.5	0.25	0.25	0.25	0.25	-0.25	0.25	-0.25	-0.25	0.25	-0.25
1	-0.5	0.5	0.5	-0.5	0.25	0.25	0.25	0.25	-0.25	-0.25	0.25	0.25	-0.25	-0.25
1	0.5	0.5	0.5	-0.5	0.25	0.25	0.25	0.25	0.25	0.25	-0.25	0.25	-0.25	-0.25
1	-0.5	-0.5	-0.5	0.5	0.25	0.25	0.25	0.25	0.25	0.25	-0.25	0.25	-0.25	-0.25
1	0.5	-0.5	-0.5	0.5	0.25	0.25	0.25	0.25	-0.25	-0.25	0.25	0.25	-0.25	-0.25
1	-0.5	0.5	-0.5	0.5	0.25	0.25	0.25	0.25	-0.25	0.25	-0.25	-0.25	0.25	-0.25
1	0.5	0.5	-0.5	0.5	0.25	0.25	0.25	0.25	0.25	-0.25	0.25	-0.25	0.25	-0.25
1	-0.5	-0.5	0.5	0.5	0.25	0.25	0.25	0.25	0.25	-0.25	-0.25	-0.25	-0.25	0.25
1	0.5	-0.5	0.5	0.5	0.25	0.25	0.25	0.25	-0.25	0.25	0.25	-0.25	-0.25	0.25
1	-0.5	0.5	0.5	0.5	0.25	0.25	0.25	0.25	-0.25	-0.25	-0.25	0.25	0.25	0.25
1	0.5	0.5	0.5	0.5	0.25	0.25	0.25	0.25	0.25	0.25	0.25	0.25	0.25	0.25
1	-1	0	0	0	1	0	0	0	0	0	0	0	0	0
1	1	0	0	0	1	0	0	0	0	0	0	0	0	0
1	0	-1	0	0	0	1	0	0	0	0	0	0	0	0
1	0	1	0	0	0	1	0	0	0	0	0	0	0	0
1	0	0	-1	0	0	0	1	0	0	0	0	0	0	0
1	0	0	1	0	0	0	1	0	0	0	0	0	0	0
1	0	0	0	-1	0	0	0	1	0	0	0	0	0	0
1	0	0	0	1	0	0	0	1	0	0	0	0	0	0
1	0	0	0	0	0	0	0	0	0	0	0	0	0	0
1	0	0	0	0	0	0	0	0	0	0	0	0	0	0
1	0	0	0	0	0	0	0	0	0	0	0	0	0	0

Appendix B.9: Extended Design Matrix for Four-Factor Inscribed CCD with Arithmetic Alpha

1.00	X1	X2	X3	X4	XI^2	X2^2	X3^2	X4^2	X1*X2	X1*X3	X1*X4	X2*X3	X2*X4	X3*X4
1.00	-0.55	-0.55	-0.55	-0.55	0.31	0.31	0.31	0.31	0.31	0.31	0.31	0.31	0.31	0.31
1.00	0.55	-0.55	-0.55	-0.55	0.31	0.31	0.31	0.31	-0.31	-0.31	-0.31	0.31	0.31	0.31
1.00	-0.55	0.55	-0.55	-0.55	0.31	0.31	0.31	0.31	-0.31	0.31	0.31	-0.31	-0.31	0.31
1.00	0.55	0.55	-0.55	-0.55	0.31	0.31	0.31	0.31	0.31	-0.31	-0.31	-0.31	-0.31	0.31
1.00	-0.55	-0.55	0.55	-0.55	0.31	0.31	0.31	0.31	0.31	-0.31	0.31	-0.31	0.31	-0.31
1.00	0.55	-0.55	0.55	-0.55	0.31	0.31	0.31	0.31	-0.31	0.31	-0.31	-0.31	0.31	-0.31
1.00	-0.55	0.55	0.55	-0.55	0.31	0.31	0.31	0.31	-0.31	-0.31	0.31	0.31	-0.31	-0.31
1.00	0.55	0.55	0.55	-0.55	0.31	0.31	0.31	0.31	0.31	0.31	-0.31	0.31	-0.31	-0.31
1.00	-0.55	-0.55	-0.55	0.55	0.31	0.31	0.31	0.31	0.31	0.31	-0.31	0.31	-0.31	-0.31
1.00	0.55	-0.55	-0.55	0.55	0.31	0.31	0.31	0.31	-0.31	-0.31	0.31	0.31	-0.31	-0.31
1.00	-0.55	0.55	-0.55	0.55	0.31	0.31	0.31	0.31	-0.31	0.31	-0.31	-0.31	0.31	-0.31
1.00	0.55	0.55	-0.55	0.55	0.31	0.31	0.31	0.31	0.31	-0.31	0.31	-0.31	0.31	-0.31
1.00	-0.55	-0.55	0.55	0.55	0.31	0.31	0.31	0.31	0.31	-0.31	-0.31	-0.31	-0.31	0.31
1.00	0.55	-0.55	0.55	0.55	0.31	0.31	0.31	0.31	-0.31	0.31	0.31	-0.31	-0.31	0.31
1.00	-0.55	0.55	0.55	0.55	0.31	0.31	0.31	0.31	-0.31	-0.31	-0.31	0.31	0.31	0.31
1.00	0.55	0.55	0.55	0.55	0.31	0.31	0.31	0.31	0.31	0.31	0.31	0.31	0.31	0.31
1.00	-1.00	0.00	0.00	0.00	1.00	0.00	0.00	0.00	0.00	0.00	0.00	0.00	0.00	0.00
1.00	1.00	0.00	0.00	0.00	1.00	0.00	0.00	0.00	0.00	0.00	0.00	0.00	0.00	0.00
1.00	0.00	-1.00	0.00	0.00	0.00	1.00	0.00	0.00	0.00	0.00	0.00	0.00	0.00	0.00
1.00	0.00	1.00	0.00	0.00	0.00	1.00	0.00	0.00	0.00	0.00	0.00	0.00	0.00	0.00
1.00	0.00	0.00	-1.00	0.00	0.00	0.00	1.00	0.00	0.00	0.00	0.00	0.00	0.00	0.00
1.00	0.00	0.00	1.00	0.00	0.00	0.00	1.00	0.00	0.00	0.00	0.00	0.00	0.00	0.00
1.00	0.00	0.00	0.00	-1.00	0.00	0.00	0.00	1.00	0.00	0.00	0.00	0.00	0.00	0.00
1.00	0.00	0.00	0.00	1.00	0.00	0.00	0.00	1.00	0.00	0.00	0.00	0.00	0.00	0.00
1.00	0.00	0.00	0.00	0.00	0.00	0.00	0.00	0.00	0.00	0.00	0.00	0.00	0.00	0.00
1.00	0.00	0.00	0.00	0.00	0.00	0.00	0.00	0.00	0.00	0.00	0.00	0.00	0.00	0.00
1.00	0.00	0.00	0.00	0.00	0.00	0.00	0.00	0.00	0.00	0.00	0.00	0.00	0.00	0.00

Appendix B.10: Extended Design Matrix for Four-Factor Inscribed CCD with Harmonic Alpha

1.00	X1	X2	X3	X4	X1^2	X2^2	X3^2	X4^2	X1*X2	X1*X3	X1*X4	X2*X3	X2*X4	X3*X4
1.00	-0.57	-0.57	-0.57	-0.57	0.32	0.32	0.32	0.32	0.32	0.32	0.32	0.32	0.32	0.32
1.00	0.57	-0.57	-0.57	-0.57	0.32	0.32	0.32	0.32	-0.32	-0.32	-0.32	0.32	0.32	0.32
1.00	-0.57	0.57	-0.57	-0.57	0.32	0.32	0.32	0.32	-0.32	0.32	0.32	-0.32	-0.32	0.32
1.00	0.57	0.57	-0.57	-0.57	0.32	0.32	0.32	0.32	0.32	-0.32	-0.32	-0.32	-0.32	0.32
1.00	-0.57	-0.57	0.57	-0.57	0.32	0.32	0.32	0.32	0.32	-0.32	0.32	-0.32	0.32	-0.32
1.00	0.57	-0.57	0.57	-0.57	0.32	0.32	0.32	0.32	-0.32	0.32	-0.32	-0.32	0.32	-0.32
1.00	-0.57	0.57	0.57	-0.57	0.32	0.32	0.32	0.32	-0.32	-0.32	0.32	0.32	-0.32	-0.32
1.00	0.57	0.57	0.57	-0.57	0.32	0.32	0.32	0.32	0.32	0.32	-0.32	0.32	-0.32	-0.32
1.00	-0.57	-0.57	-0.57	0.57	0.32	0.32	0.32	0.32	0.32	0.32	-0.32	0.32	-0.32	-0.32
1.00	0.57	-0.57	-0.57	0.57	0.32	0.32	0.32	0.32	-0.32	-0.32	0.32	0.32	-0.32	-0.32
1.00	-0.57	0.57	-0.57	0.57	0.32	0.32	0.32	0.32	-0.32	0.32	-0.32	-0.32	0.32	-0.32
1.00	0.57	0.57	-0.57	0.57	0.32	0.32	0.32	0.32	0.32	-0.32	0.32	-0.32	0.32	-0.32
1.00	-0.57	-0.57	0.57	0.57	0.32	0.32	0.32	0.32	0.32	-0.32	-0.32	-0.32	-0.32	0.32
1.00	0.57	-0.57	0.57	0.57	0.32	0.32	0.32	0.32	-0.32	0.32	0.32	-0.32	-0.32	0.32
1.00	-0.57	0.57	0.57	0.57	0.32	0.32	0.32	0.32	-0.32	-0.32	-0.32	0.32	0.32	0.32
1.00	0.57	0.57	0.57	0.57	0.32	0.32	0.32	0.32	0.32	0.32	0.32	0.32	0.32	0.32
1.00	-1.00	0.00	0.00	0.00	1.00	0.00	0.00	0.00	0.00	0.00	0.00	0.00	0.00	0.00
1.00	1.00	0.00	0.00	0.00	1.00	0.00	0.00	0.00	0.00	0.00	0.00	0.00	0.00	0.00
1.00	0.00	-1.00	0.00	0.00	0.00	1.00	0.00	0.00	0.00	0.00	0.00	0.00	0.00	0.00
1.00	0.00	1.00	0.00	0.00	0.00	1.00	0.00	0.00	0.00	0.00	0.00	0.00	0.00	0.00
1.00	0.00	0.00	-1.00	0.00	0.00	0.00	1.00	0.00	0.00	0.00	0.00	0.00	0.00	0.00
1.00	0.00	0.00	1.00	0.00	0.00	0.00	1.00	0.00	0.00	0.00	0.00	0.00	0.00	0.00
1.00	0.00	0.00	0.00	-1.00	0.00	0.00	0.00	1.00	0.00	0.00	0.00	0.00	0.00	0.00
1.00	0.00	0.00	0.00	1.00	0.00	0.00	0.00	1.00	0.00	0.00	0.00	0.00	0.00	0.00
1.00	0.00	0.00	0.00	0.00	0.00	0.00	0.00	0.00	0.00	0.00	0.00	0.00	0.00	0.00
1.00	0.00	0.00	0.00	0.00	0.00	0.00	0.00	0.00	0.00	0.00	0.00	0.00	0.00	0.00
1.00	0.00	0.00	0.00	0.00	0.00	0.00	0.00	0.00	0.00	0.00	0.00	0.00	0.00	0.00

Appendix B.11: Extended Design Matrix for Four-Factor Inscribed CCD with Geometric Alpha

1.00	X1	X2	X3	X4	X1^2	X2^2	X3^2	X4^2	X1*X2	X1*X3	X1*X4	X2*X3	X2*X4	X3*X4
1.00	-0.56	-0.56	-0.56	-0.56	0.31	0.31	0.31	0.31	0.31	0.31	0.31	0.31	0.31	0.31
1.00	0.56	-0.56	-0.56	-0.56	0.31	0.31	0.31	0.31	-0.31	-0.31	-0.31	0.31	0.31	0.31
1.00	-0.56	0.56	-0.56	-0.56	0.31	0.31	0.31	0.31	-0.31	0.31	0.31	-0.31	-0.31	0.31
1.00	0.56	0.56	-0.56	-0.56	0.31	0.31	0.31	0.31	0.31	-0.31	-0.31	-0.31	-0.31	0.31
1.00	-0.56	-0.56	0.56	-0.56	0.31	0.31	0.31	0.31	0.31	-0.31	0.31	-0.31	0.31	-0.31
1.00	0.56	-0.56	0.56	-0.56	0.31	0.31	0.31	0.31	-0.31	0.31	-0.31	-0.31	0.31	-0.31
1.00	-0.56	0.56	0.56	-0.56	0.31	0.31	0.31	0.31	-0.31	-0.31	0.31	0.31	-0.31	-0.31
1.00	0.56	0.56	0.56	-0.56	0.31	0.31	0.31	0.31	0.31	0.31	-0.31	0.31	-0.31	-0.31
1.00	-0.56	-0.56	-0.56	0.56	0.31	0.31	0.31	0.31	0.31	0.31	-0.31	0.31	-0.31	-0.31
1.00	0.56	-0.56	-0.56	0.56	0.31	0.31	0.31	0.31	-0.31	-0.31	0.31	0.31	-0.31	-0.31
1.00	-0.56	0.56	-0.56	0.56	0.31	0.31	0.31	0.31	-0.31	0.31	-0.31	-0.31	0.31	-0.31
1.00	0.56	0.56	-0.56	0.56	0.31	0.31	0.31	0.31	0.31	-0.31	0.31	-0.31	0.31	-0.31
1.00	-0.56	-0.56	0.56	0.56	0.31	0.31	0.31	0.31	0.31	-0.31	-0.31	-0.31	-0.31	0.31
1.00	0.56	-0.56	0.56	0.56	0.31	0.31	0.31	0.31	-0.31	0.31	0.31	-0.31	-0.31	0.31
1.00	-0.56	0.56	0.56	0.56	0.31	0.31	0.31	0.31	-0.31	-0.31	-0.31	0.31	0.31	0.31
1.00	0.56	0.56	0.56	0.56	0.31	0.31	0.31	0.31	0.31	0.31	0.31	0.31	0.31	0.31
1.00	-1.00	0.00	0.00	0.00	1.00	0.00	0.00	0.00	0.00	0.00	0.00	0.00	0.00	0.00
1.00	1.00	0.00	0.00	0.00	1.00	0.00	0.00	0.00	0.00	0.00	0.00	0.00	0.00	0.00
1.00	0.00	-1.00	0.00	0.00	0.00	1.00	0.00	0.00	0.00	0.00	0.00	0.00	0.00	0.00
1.00	0.00	1.00	0.00	0.00	0.00	1.00	0.00	0.00	0.00	0.00	0.00	0.00	0.00	0.00
1.00	0.00	0.00	-1.00	0.00	0.00	0.00	1.00	0.00	0.00	0.00	0.00	0.00	0.00	0.00
1.00	0.00	0.00	1.00	0.00	0.00	0.00	1.00	0.00	0.00	0.00	0.00	0.00	0.00	0.00
1.00	0.00	0.00	0.00	-1.00	0.00	0.00	0.00	1.00	0.00	0.00	0.00	0.00	0.00	0.00
1.00	0.00	0.00	0.00	1.00	0.00	0.00	0.00	1.00	0.00	0.00	0.00	0.00	0.00	0.00
1.00	0.00	0.00	0.00	0.00	0.00	0.00	0.00	0.00	0.00	0.00	0.00	0.00	0.00	0.00
1.00	0.00	0.00	0.00	0.00	0.00	0.00	0.00	0.00	0.00	0.00	0.00	0.00	0.00	0.00
1.00	0.00	0.00	0.00	0.00	0.00	0.00	0.00	0.00	0.00	0.00	0.00	0.00	0.00	0.00

Appendix B.11: Extended Design Matrix for Four-Factor Star-Replicated CCD with Rotatable Alpha when $n_2 = 2$

1.00	X1	X2	X3	X4	X1^2	X2^2	X3^2	X4^2	X1*X2	X1*X3	X1*X4	X2*X3	X2*X4	X3*X4
1.00	-1.00	-1.00	-1.00	-1.00	1.00	1.00	1.00	1.00	1.00	1.00	1.00	1.00	1.00	1.00
1.00	1.00	-1.00	-1.00	-1.00	1.00	1.00	1.00	1.00	-1.00	-1.00	-1.00	1.00	1.00	1.00
1.00	-1.00	1.00	-1.00	-1.00	1.00	1.00	1.00	1.00	-1.00	1.00	1.00	-1.00	-1.00	1.00
1.00	1.00	1.00	-1.00	-1.00	1.00	1.00	1.00	1.00	1.00	-1.00	-1.00	-1.00	-1.00	1.00
1.00	-1.00	-1.00	1.00	-1.00	1.00	1.00	1.00	1.00	1.00	-1.00	1.00	-1.00	1.00	-1.00
1.00	1.00	-1.00	1.00	-1.00	1.00	1.00	1.00	1.00	-1.00	1.00	-1.00	-1.00	1.00	-1.00
1.00	-1.00	1.00	1.00	-1.00	1.00	1.00	1.00	1.00	-1.00	-1.00	1.00	1.00	-1.00	-1.00
1.00	1.00	1.00	1.00	-1.00	1.00	1.00	1.00	1.00	1.00	1.00	-1.00	1.00	-1.00	-1.00
1.00	-1.00	-1.00	-1.00	1.00	1.00	1.00	1.00	1.00	1.00	1.00	-1.00	1.00	-1.00	-1.00
1.00	1.00	-1.00	-1.00	1.00	1.00	1.00	1.00	1.00	-1.00	-1.00	1.00	1.00	-1.00	-1.00
1.00	-1.00	1.00	-1.00	1.00	1.00	1.00	1.00	1.00	-1.00	1.00	-1.00	-1.00	1.00	-1.00
1.00	1.00	1.00	-1.00	1.00	1.00	1.00	1.00	1.00	1.00	-1.00	1.00	-1.00	1.00	-1.00
1.00	-1.00	-1.00	1.00	1.00	1.00	1.00	1.00	1.00	1.00	-1.00	-1.00	-1.00	-1.00	1.00
1.00	1.00	-1.00	1.00	1.00	1.00	1.00	1.00	1.00	-1.00	1.00	1.00	-1.00	-1.00	1.00
1.00	-1.00	1.00	1.00	1.00	1.00	1.00	1.00	1.00	-1.00	-1.00	-1.00	1.00	1.00	1.00
1.00	1.00	1.00	1.00	1.00	1.00	1.00	1.00	1.00	1.00	1.00	1.00	1.00	1.00	1.00
1.00	-1.68	0.00	0.00	0.00	2.83	0.00	0.00	0.00	0.00	0.00	0.00	0.00	0.00	0.00
1.00	-1.68	0.00	0.00	0.00	2.83	0.00	0.00	0.00	0.00	0.00	0.00	0.00	0.00	0.00
1.00	1.68	0.00	0.00	0.00	2.83	0.00	0.00	0.00	0.00	0.00	0.00	0.00	0.00	0.00
1.00	1.68	0.00	0.00	0.00	2.83	0.00	0.00	0.00	0.00	0.00	0.00	0.00	0.00	0.00
1.00	0.00	-1.68	0.00	0.00	0.00	2.83	0.00	0.00	0.00	0.00	0.00	0.00	0.00	0.00
1.00	0.00	-1.68	0.00	0.00	0.00	2.83	0.00	0.00	0.00	0.00	0.00	0.00	0.00	0.00
1.00	0.00	1.68	0.00	0.00	0.00	2.83	0.00	0.00	0.00	0.00	0.00	0.00	0.00	0.00
1.00	0.00	1.68	0.00	0.00	0.00	2.83	0.00	0.00	0.00	0.00	0.00	0.00	0.00	0.00
1.00	0.00	0.00	-1.68	0.00	0.00	0.00	2.83	0.00	0.00	0.00	0.00	0.00	0.00	0.00
1.00	0.00	0.00	-1.68	0.00	0.00	0.00	2.83	0.00	0.00	0.00	0.00	0.00	0.00	0.00
1.00	0.00	0.00	1.68	0.00	0.00	0.00	2.83	0.00	0.00	0.00	0.00	0.00	0.00	0.00
1.00	0.00	0.00	1.68	0.00	0.00	0.00	2.83	0.00	0.00	0.00	0.00	0.00	0.00	0.00
1.00	0.00	0.00	0.00	-1.68	0.00	0.00	0.00	2.83	0.00	0.00	0.00	0.00	0.00	0.00
1.00	0.00	0.00	0.00	-1.68	0.00	0.00	0.00	2.83	0.00	0.00	0.00	0.00	0.00	0.00
1.00	0.00	0.00	0.00	1.68	0.00	0.00	0.00	2.83	0.00	0.00	0.00	0.00	0.00	0.00
1.00	0.00	0.00	0.00	1.68	0.00	0.00	0.00	2.83	0.00	0.00	0.00	0.00	0.00	0.00
1.00	0.00	0.00	0.00	0.00	0.00	0.00	0.00	0.00	0.00	0.00	0.00	0.00	0.00	0.00
1.00	0.00	0.00	0.00	0.00	0.00	0.00	0.00	0.00	0.00	0.00	0.00	0.00	0.00	0.00
1.00	0.00	0.00	0.00	0.00	0.00	0.00	0.00	0.00	0.00	0.00	0.00	0.00	0.00	0.00

Appendix B.12: Extended Design Matrix for Four-Factor Star-Replicated CCD with Rotatable Alpha when $n_2 = 3$

1.00	X1	X2	X3	X4	X1^2	X2^2	X3^2	X4^2	X1*X2	X1*X3	X1*X4	X2*X3	X2*X4	X3*X4
1.00	-1.00	-1.00	-1.00	-1.00	1.00	1.00	1.00	1.00	1.00	1.00	1.00	1.00	1.00	1.00
1.00	1.00	-1.00	-1.00	-1.00	1.00	1.00	1.00	1.00	-1.00	-1.00	-1.00	1.00	1.00	1.00
1.00	-1.00	1.00	-1.00	-1.00	1.00	1.00	1.00	1.00	-1.00	1.00	1.00	-1.00	-1.00	1.00
1.00	1.00	1.00	-1.00	-1.00	1.00	1.00	1.00	1.00	1.00	-1.00	-1.00	-1.00	-1.00	1.00
1.00	-1.00	-1.00	1.00	-1.00	1.00	1.00	1.00	1.00	1.00	-1.00	1.00	-1.00	1.00	-1.00
1.00	1.00	-1.00	1.00	-1.00	1.00	1.00	1.00	1.00	-1.00	1.00	-1.00	-1.00	1.00	-1.00
1.00	-1.00	1.00	1.00	-1.00	1.00	1.00	1.00	1.00	-1.00	-1.00	1.00	1.00	-1.00	-1.00
1.00	1.00	1.00	1.00	-1.00	1.00	1.00	1.00	1.00	1.00	1.00	-1.00	1.00	-1.00	-1.00
1.00	-1.00	-1.00	-1.00	1.00	1.00	1.00	1.00	1.00	1.00	1.00	-1.00	1.00	-1.00	-1.00
1.00	1.00	-1.00	-1.00	1.00	1.00	1.00	1.00	1.00	-1.00	-1.00	1.00	1.00	-1.00	-1.00
1.00	-1.00	1.00	-1.00	1.00	1.00	1.00	1.00	1.00	-1.00	1.00	-1.00	-1.00	1.00	-1.00
1.00	1.00	1.00	-1.00	1.00	1.00	1.00	1.00	1.00	1.00	-1.00	1.00	-1.00	1.00	-1.00
1.00	-1.00	-1.00	1.00	1.00	1.00	1.00	1.00	1.00	1.00	-1.00	-1.00	-1.00	-1.00	1.00
1.00	1.00	-1.00	1.00	1.00	1.00	1.00	1.00	1.00	-1.00	1.00	1.00	-1.00	-1.00	1.00
1.00	-1.00	1.00	1.00	1.00	1.00	1.00	1.00	1.00	-1.00	-1.00	-1.00	1.00	1.00	1.00
1.00	1.00	1.00	1.00	1.00	1.00	1.00	1.00	1.00	1.00	1.00	1.00	1.00	1.00	1.00
1.00	-1.41	0.00	0.00	0.00	2.00	0.00	0.00	0.00	0.00	0.00	0.00	0.00	0.00	0.00
1.00	-1.41	0.00	0.00	0.00	2.00	0.00	0.00	0.00	0.00	0.00	0.00	0.00	0.00	0.00
1.00	-1.41	0.00	0.00	0.00	2.00	0.00	0.00	0.00	0.00	0.00	0.00	0.00	0.00	0.00
1.00	1.41	0.00	0.00	0.00	2.00	0.00	0.00	0.00	0.00	0.00	0.00	0.00	0.00	0.00
1.00	1.41	0.00	0.00	0.00	2.00	0.00	0.00	0.00	0.00	0.00	0.00	0.00	0.00	0.00
1.00	1.41	0.00	0.00	0.00	2.00	0.00	0.00	0.00	0.00	0.00	0.00	0.00	0.00	0.00
1.00	0.00	-1.41	0.00	0.00	0.00	2.00	0.00	0.00	0.00	0.00	0.00	0.00	0.00	0.00
1.00	0.00	-1.41	0.00	0.00	0.00	2.00	0.00	0.00	0.00	0.00	0.00	0.00	0.00	0.00
1.00	0.00	-1.41	0.00	0.00	0.00	2.00	0.00	0.00	0.00	0.00	0.00	0.00	0.00	0.00
1.00	0.00	1.41	0.00	0.00	0.00	2.00	0.00	0.00	0.00	0.00	0.00	0.00	0.00	0.00
1.00	0.00	1.41	0.00	0.00	0.00	2.00	0.00	0.00	0.00	0.00	0.00	0.00	0.00	0.00
1.00	0.00	1.41	0.00	0.00	0.00	2.00	0.00	0.00	0.00	0.00	0.00	0.00	0.00	0.00
1.00	0.00	0.00	-1.41	0.00	0.00	0.00	2.00	0.00	0.00	0.00	0.00	0.00	0.00	0.00
1.00	0.00	0.00	-1.41	0.00	0.00	0.00	2.00	0.00	0.00	0.00	0.00	0.00	0.00	0.00
1.00	0.00	0.00	-1.41	0.00	0.00	0.00	2.00	0.00	0.00	0.00	0.00	0.00	0.00	0.00
1.00	0.00	0.00	1.41	0.00	0.00	0.00	2.00	0.00	0.00	0.00	0.00	0.00	0.00	0.00
1.00	0.00	0.00	1.41	0.00	0.00	0.00	2.00	0.00	0.00	0.00	0.00	0.00	0.00	0.00
1.00	0.00	0.00	1.41	0.00	0.00	0.00	2.00	0.00	0.00	0.00	0.00	0.00	0.00	0.00
1.00	0.00	0.00	0.00	-1.41	0.00	0.00	0.00	2.00	0.00	0.00	0.00	0.00	0.00	0.00
1.00	0.00	0.00	0.00	-1.41	0.00	0.00	0.00	2.00	0.00	0.00	0.00	0.00	0.00	0.00
1.00	0.00	0.00	0.00	-1.41	0.00	0.00	0.00	2.00	0.00	0.00	0.00	0.00	0.00	0.00
1.00	0.00	0.00	0.00	1.41	0.00	0.00	0.00	2.00	0.00	0.00	0.00	0.00	0.00	0.00
1.00	0.00	0.00	0.00	1.41	0.00	0.00	0.00	2.00	0.00	0.00	0.00	0.00	0.00	0.00
1.00	0.00	0.00	0.00	1.41	0.00	0.00	0.00	2.00	0.00	0.00	0.00	0.00	0.00	0.00
1.00	0.00	0.00	0.00	0.00	0.00	0.00	0.00	0.00	0.00	0.00	0.00	0.00	0.00	0.00
1.00	0.00	0.00	0.00	0.00	0.00	0.00	0.00	0.00	0.00	0.00	0.00	0.00	0.00	0.00
1.00	0.00	0.00	0.00	0.00	0.00	0.00	0.00	0.00	0.00	0.00	0.00	0.00	0.00	0.00

LIST OF ABBREVIATIONS

CCD	-	Central Composite Design
VDG	-	Variance Dispersion Graph
FDSG	-	Fraction of Design Space Graph
RSM	-	Response Surface Methodology
UPV	-	Un-scaled Prediction Variance
PV	-	Prediction Variance
SCD	-	Small Composite Design
MinRes(V)D	-	Minimum Resolution (V) Design
VIF	-	Variance Inflation Factor

FLY LEAF

CERTIFICATION

This is to certify that this thesis titled "Alternative Axial Distances for Spherical and Cuboidal Regions of Central Composite Designs and their Properties" and carried out by Onyishi, Linus Ifeanyi with Reg. Number MTH/Ph.D./08/001 has been examined and found worthy of the award of the degree of Ph.D degree in Statistics.

1. EXTERNAL EXAMINER

   Name: Prof. E.C. Nduka — Signature: .....

   Status: Professor — Date: 17/04/19

2. CHIEF SUPERVISOR

   Name: Prof. M.E. Nja — Signature: .....

   Status: Professor — Date: 17/04/19

3. 2ND SUPERVISOR

   Name: Prof. E.O. Effanga — Signature: .....

   Status: Professor — Date: 17/04/19

4. HEAD OF DEPARTMENT

   Name: Prof. S.S. Akpan — Signature: .....

   Status: Professor — Date: 17/04/19

5. GRADUATE SCHOOL REPRESENTATIVE

   Name: Prof. Imo E. Umoinyang — Signature: .....

   Status: Professor — Date: 17/4/19

DECLARATION

I, ONYISHI, LINUS IFEANYI with Registration number, MTH/Ph.D/08/001, hereby declare that this thesis on Alternative Axial Distances for Spherical and Cuboidal Regions of Central Composite Designs and their Properties is original, and has been written by me. It is a record of my research and has not been presented before in any previous publication.

Name ONYISHI LINUS IFEANYI Signature

(Student/Candidate)

Date 17/04/2019

ACKNOWLEDGMENT

I am first and foremost grateful to God Almighty who gave me the good health of mind and body to bring this thesis to completion. I am very much grateful to my Chief Supervisor, Prof M.E. Nja for his commitment and scholarly contributions to this thesis. His constructive criticism and wealth of knowledge provided the necessary compass for the actualization of this work.

I am also very grateful to my second supervisor, Prof. E.O. Effanga whose contributions went a long way to put this work to shape. He also allotted ample time to read and correct, where necessary, this thesis as the need arose. My profound gratitude also goes to the Head of Department of Statistics, Prof. S. S. Akpan for his unflinching support for the progress of this thesis, both in season and out of season. He was always there for both academic and moral support that led to the outcome of this thesis.

I am equally profoundly grateful to Prof. C. E. Onwukwe, Prof. I. E. Enang and Dr. T. O. Ugbe for their special contributions to the progress and the outcome of this research. Their whole-hearted and unalloyed views and suggestions, in no little measure, contributed to the present shape and standard of this thesis. The contributions of Mr. O.I. Ojo and Mr. I. E. Egong are equally appreciable, I am grateful to them too. My gratitude also goes to Dr. J. A. Ugboh of the Department of Mathematics.

To my colleagues and friends from other Universities and educational Institutions, I also owe a lot of thanks. Some of them include Dr. F. C. Eze and Dr. E. Umeh of Nnamdi Azikiwe University, Awka; Dr. E.C. Ukaegbu and Prof. F. I.Ugwuowo of the University of Nigeria, Nsukka. I am also grateful to other contributors too many to mention.

This acknowledgment cannot be complete without extending my appreciation to my employer, the management of Federal Polytechnic, Nasarawa, Nasarawa State, through whom the Education Trust Fund (ETF) sponsored this research. In the same vein, I am grateful to my immediate boss in the Department of Mathematics and Statistics, Federal Polytechnic, Nasarawa, Dr. Y.B. Usman, for this concern over my research.

My special gratitude goes to my darling wife, Ifeyinwa and my Children, for their patience throughout the period of my study. I am very grateful to my brothers and sisters for their contributions. It is equally worthwhile to express my gratitude to my in-laws, especially Rev. Fr. Romanus Ezeuwgu for his financial and moral support. I will not fail to appreciate the effort of Mrs. Peace Bassey (computer operator) who also contributed to the success of this thesis.

ABSTRACT

In this study, three axial distances are proposed as alternatives to the existing axial distances of the Central Composite Design(CCD) in spherical and cuboidal design regions with the aim of providing formidable alternatives to the existing axial distances of the CCD whose prediction properties are less extreme and more stable in the spherical and cuboidal design regions. The three alternative axial distances, namelythe arithmetic, harmonic and geometric axial distances, each, for spherical and cuboidal regions, were developed algebraically based on the concepts of the three Pythagorean means. The strengths and weaknesses of the alternative axial distances were validated by comparing their performances with the existing axial distances in the spherical and cuboidal regions. The D- and G-efficiencies are used for comparison while the two graphical methods adopted are the variance dispersion graph (VDG) and fraction of design space graph (FDSG). Furthermore, effect of partial replications of the star portion of the CCD on the alternative axial distances were evaluated by comparing the performances of the replicated variations of the CCD in the spherical and cuboidal regions. Also, the alternative axial distances were utilized in the construction of the inscribed CCD in order to determine their benefits in improving the performances of the inscribed CCD. The results show that the three alternative axial distances provide D-efficiency values that are consistently better than that of the practical axial distance and often compete favourably with those of the spherical and rotatable axial distances in the spherical region. The G-efficiency values of the alternative axial distances are better for most of the sets of factors considered. In the cuboidal region, the three alternative axial distances are consistently better in terms of the D- and G-efficiencies. The stability and prediction capabilities of the CCD with arithmetic axial distance remain the best in the spherical region and the second best in

the cubloidal region. However, the case of the cuboidal region improved with the replication of the star portion as the three alternative axial distances became the best and the most stable in terms of scaled prediction variances. The alternative axial distancesalso improved the performances of the inscribed CCD when used to construct the design. Two computer programs were developed in MATLAB software which constructs the variance dispersion graphs of competing designs in very little time of less than a second. It is therefore concluded that the alternative axial distances developed in this study have yielded desirable results for the exploration of the response surfaces using the central composite design. It is strongly recommended that the central composite design with arithmetic axial distance would be the experimenter's choice should the D-efficiency be the criterion for response surface exploration.

(Word counts: 441)

TABLE OF CONTENTS

LIST OF TABLES

LIST OF FIGURES